Premier Flight Systems

Presents the

PFS-1000 Jet Family

In response to the 2016-2017 AIAA Foundation Undergraduate Team Aircraft Design Competition

Presented by California State Polytechnic University Pomona
Aerospace Engineering Department
Aircraft Design 2016 - 2017

California State Polytechnic University, Pomona

Premier Flight Systems WBS

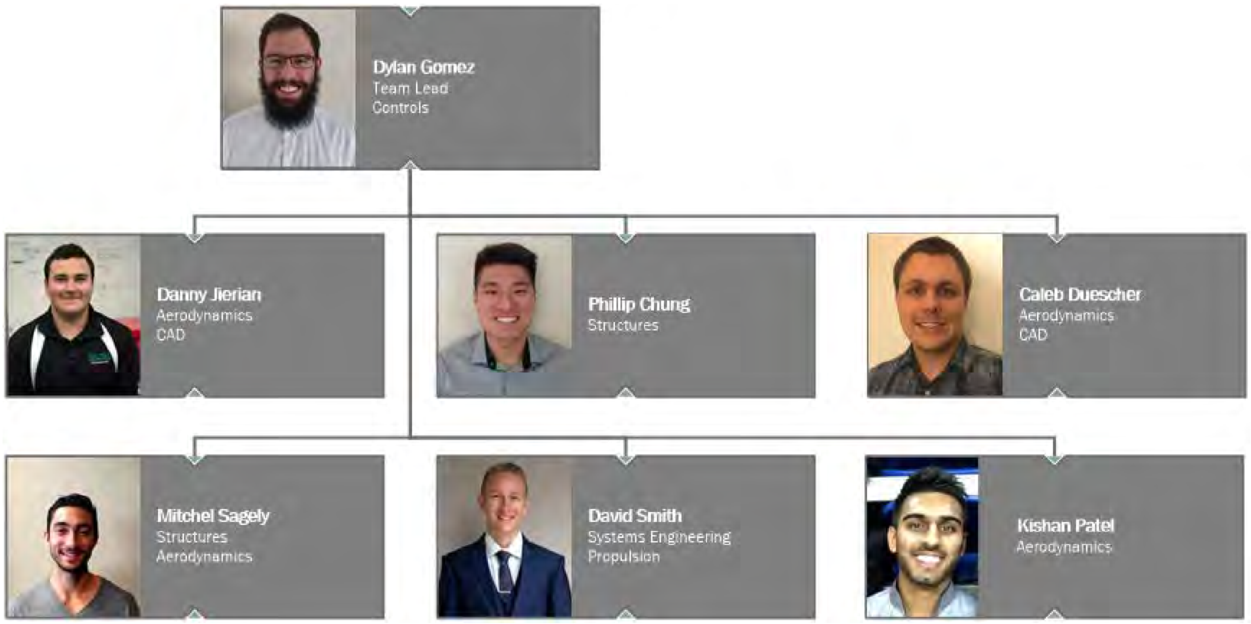

Premier Flight Systems Team AIAA Member Numbers

Name	Signature	AIAA Member Number	Email
Chung, Phillip		819303	PhillipChung@cpp.edu
Duescher, Caleb		760812	CalebDuescher@gmail.com
Gomez, Dylan		820062	gogogomez211@gmail.com
Jierian, Danny		819308	DanJierian@gmail.com
Patel, Kishan		796605	kjpatel@cpp.edu
Sagely, Mitchell		820063	MitchSagely@yahoo.com
Smith, David		819376	DavidSmith@cpp.edu

Table of Contents

Premier Flight Systems WBS 2
Premier Flight Systems Team AIAA Member Numbers 2
Table of Contents 3
Executive Summary 5
List of Figures 8
List of Tables 10
List of Symbols & Abbreviations 11
1.0 Design Requirements 14
2.0 Mission Profile 15
3.0 Configuration Overview 16
3.1 Final Design 16
3.1.1 Design Concepts 17
3.1.2 Three-View Drawings 12
3.2 Alternative Concepts 15
3.2.1 Innovative and Conventional Design 15
3.2.2 Comparison and Down Select 17
4.0 Initial Sizing 18
5.0 Wing Selection 19
5.1 Computational Fluid Dynamics 21
5.2 Wing Planform 22
5.3 Airfoil 23
5.4 High Lift Devices 25
6.0 Aerodynamic Performance 27
6.1 Drag (Parasite, Induced, Compressibility) 27
6.2 L/D and Other Performances 28
7.0 Stability and Control 29
7.1 Vertical Tail 29
7.2 Horizontal Tail 30
8.0 Propulsion System 33
9.0 Aircraft Performance 36
9.1 Payload Range Calculations 36

9.2 Take-off/ Landing Performance ... 37
9.3 Operational Envelope ... 39
9.4 Rate of Climb ... 41
10.0 Weights ... 42
10.1 Weight Breakdown ... 42
10.2 CG Travel ... 43
11.0 Material Selection ... 47
12.0 Structural Analysis ... 47
12.1 V-n Diagram ... 47
12.2 Wing ... 49
12.3 Fuselage ... 53
13.0 Landing Gear ... 58
14.0 Fuselage Configurations ... 59
14.1 Cabin Interior Layout ... 59
14.3 TV's and Power ... 62
15.0 Subsystems ... 64
15.1 Fuel ... 64
15.2 Hydraulics ... 66
15.3 Auxiliary Power Unit ... 67
15.4 Electrical Subsystem ... 68
15.5 Environmental Control Systems (ECS) ... 69
16.0 Commonality Analysis ... 70
17.0 Manufacturing ... 72
18.0 Maintainability ... 74
19.0 Reliability ... 75
20.0 Costs ... 76
20.1 PFS-1000 Program Costs ... 76
20.2 Direct Operating Costs ... 79
21.0 Conclusion ... 81
Appendix A: Compliance Matrix ... 82
Appendix B: Reference List ... 83

Executive Summary

Premier Flight Systems presents the PFS-1000 family of light business jets to fulfill the RFP created by the American Institute of Aeronautics and Astronautics. The PFS-1000 family was created to meet the market demand for a new modern business jet with competitive price and performance. The RFP states that the aircraft shall have two models, 6 and 8 passenger, with a build commonality of at least 70%; the design created by Premier Flight Systems has a commonality of 94.3%. The result of high commonality between the 6 and 8 passenger is a competitive purchase price of $9.2 and $9.8 million for the respective model. Also requested is that the aircraft shall have a max cruise of Mach 0.85 at 35,000 ft with a service ceiling of 45,000ft. Figure 1 below shows the cruise capabilities of the 8 passenger model. Another flight characteristic required is a flight range of 2,500 nmi. Figure 2 shows that the PFS-1000 8 passenger meets the requirement. Other qualities that the RFP requires are: climb rate of 3,500 ft/min, balanced field length of 4,000 ft, landing field length of 3,600 ft, FAR 23/25 compliance, and baggage requirements for the 6 and 8 passenger, all of which the PFS-1000 family meets.

The PFS-1000 light business jet family’s key design feature is the interior virtual skyline to replace the passenger windows. The virtual skyline is a customizable AMOLED display that runs along the length of the cabin. The virtual skyline can display a stream of the exterior or video of any scenery (in case of fear of flying). Implementation of the virtual skyline creates a unique memorable flight experience while also saving 30% of the fuselage weight since the displays are very thin and light. Figure 3 shows a rendition of the cabin interior with the virtual skyline installed. Reduced fuselage weight and L/D max of 17.9 (6 passenger) and 17.4 (8 passenger) give the 6 and 8 passenger models an hourly operating cost of $1,788 and $2,171 respectively. Table 1 shows the purchase prices and operating prices of the PSF-1000 family and some similar competitors. Given the performance stated, the PFS-1000 family successfully meets all requirements stated in the RFP and will be a strong competitor in the light business jet market.

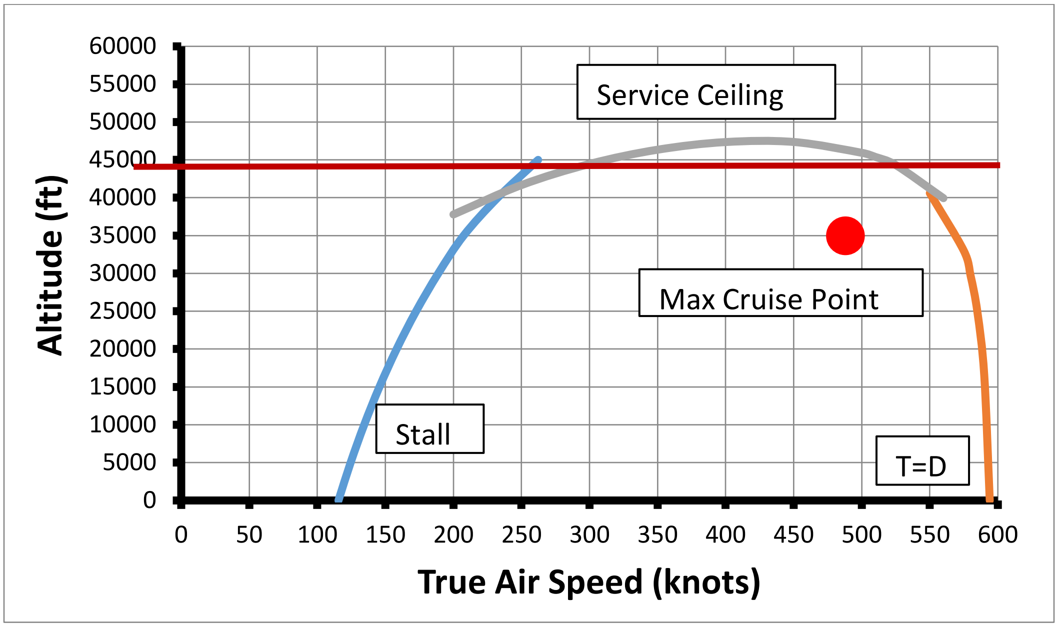

Figure 1: 8 Passenger Operational Envelope

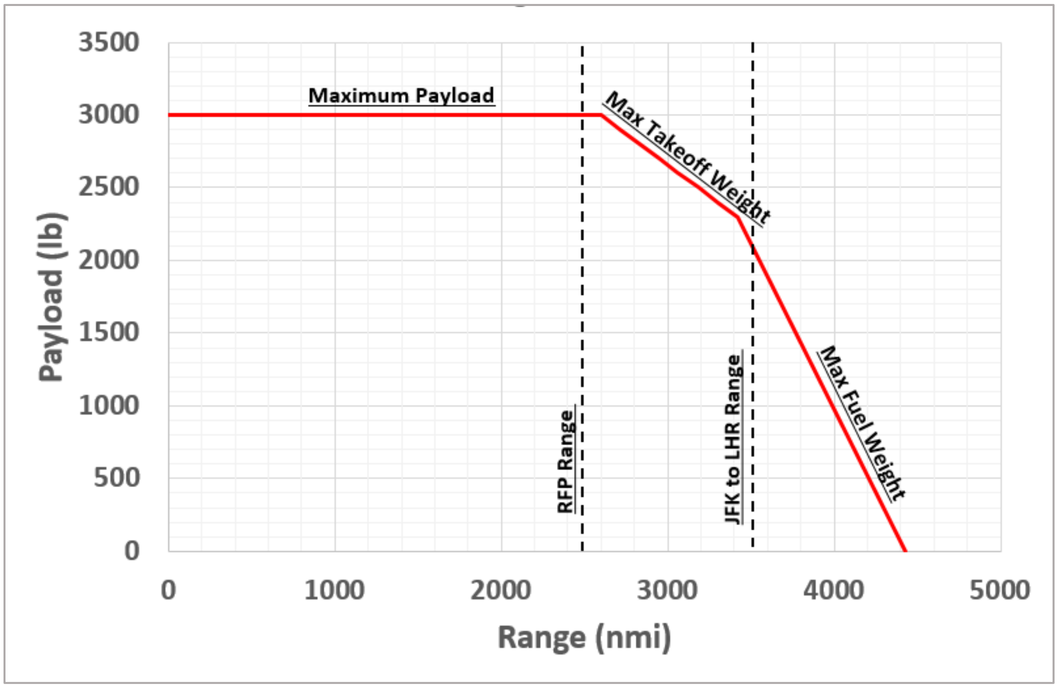

Figure 2: 8 Passenger Payload Range Curve

Figure 3: Virtual Skyline Render

Table 1: Performance and Cost

Aircraft	Passengers	Range (nmi)	Max Cruise (Kts)	Unit Cost (Millions)	Hourly Operating Cost
PFS-1000 (6-PAX)	6	2,500	489	$9.2	$1,787.70
PFS-1000 (8-PAX)	8	2,500	489	$9.6	$2,170.60
Cessna Citation CJ4	7	2,165	454	$8.995	$1,970.20
Embraer Phenom 300	7	2,268	444	$8.995	$1,757.50
SyberJet SJ30	5	2,500	486	$8.31	$1,607.80

List of Figures

Figure 2.0- 1: Typical Mission Profile 15
Figure 3.1-1 Isometric View of 6-Passenger Aircraft 16
Figure 3.1-2 Isometric View of 8-Passenger Aircraft 17
Figure 3.2.1-1 Pre-Downselect Innovative Design Isometric View 16
Figure 3.2.1-2 Pre-Downselect Conventional Design Isometric View 16
Figure 4.0- 1: Design Constraint Diagram 18
Figure 5.0-1: Effect of Leading Edge Sweep and Aspect Ratio on Range 20
Figure 5.0-2: Effect of Leading Edge Sweep and Aspect Ratio on Wing Weight 20
Figure 5.1-1: CFD Validation Curve 21
Figure 5.2-1: PFS-1000 Wing Planform (dimensions are in inches) 23
Figure 5.3-1: C_l / C_d vs. C_d Airfoil Comparison 24
Figure 5.3-2: C_l vs. α Airfoil Comparison 24
Figure 5.3-3: C_l vs. C_d Airfoil Comparison 25
Figure 5.3-4: NACA65-412 Airfoil Shape 25
Figure 5.3-1: Lift Coefficient Comparison for Flapped and Non-Flapped Wing 26
Figure 6.2-1: Drag Polar for PFS-1000 Family 28
Figure 7.1-1: Vertical Tail Side View 30
Figure 7.2-1: Notch Diagram for 6 Passenger Horizontal Tail 31
Figure 7.2-2: Horizontal Tail Top View 32
Figure 8.0-1: Comparing Engine Thrusts 33
Figure 8.0-2: Comparing Engine TSFC 34
Figure 8.0-3: FJ44-3A Engine 34
Figure 8.0-4: FJ44-3A TSFC vs. Mach @ Altitude 35
Figure 9.1-1: 6-Passenger Payload Range Curve 36
Figure 9.1-2: 8-Passenger Payload Range Curve 37
Figure 9.2-1: Balanced Field Length for 6 Passenger 38
Figure 9.2-2: Balanced Field Length for 8-Passenger 38
Figure 9.3-1: Operational Envelope for 6-Passenger 40
Figure 9.3-2: Operational Envelope for 8-Passenger 40
Figure 10.1-1 Weight Percentage Breakdown: 6 Passenger 43

Figure 10.1-2 Weight Percentage Breakdown: 8 Passenger 43
Figure 10.2-1 Center of Gravity Location: 6-Passenger 44
Figure 10.2-2 Center of Gravity Location:8-Passenger 45
Figure 10.2-3 Center of Gravity Travel: 6 Passenger 45
Figure 10.2-4 Center of Gravity Travel: 8 Passenger 46
Figure 12.1-1 V-n Diagram for 6-Passenger Model 47
Figure 12.1-2 V-n Diagram for 8-Passenger Model 48
Figure 12.2-1: Various Lift Distribution 49
Figure 12.2-2: Average Lift Distribution 50
Figure 12.2-3: Spanwise Shear Loading of Wing 51
Figure 12.2-4: Bending Moment of Wing 51
Figure 12.2-5: Internal Structure of Wing 53
Figure 12.3-1: Internal Structure of Fuselage 54
Figure 12.3-2: Breakdown of Fuselage for Analysis – Skin Panel, Stiffener, Frame 55
Figure 12.3-3: Fuselage with Windows 55
Figure 12.3-4: Fuselage without Windows 56
Figure 13.0-1 Landing Gear Placement and Tip-Back Angle 58
Figure 14.0-1 Fuselage layout and aisle view 59
Figure 14.1-1: 6 Passenger Interior 60
Figure 14.1-2: Dimensioned 6-Passenger Layout 61
Figure 14.2-3: 8 Passenger Interior 61
Figure 14.1-4: Dimensioned 8-Passenger Layout 62
Figure 15.1-1 Fuel Tanks: 6 Passenger 65
Figure 15.1-2 Fuel Tanks: 8 Passenger 65
Figure 15.2-1 Hydraulic System 6-Passenger 66
Figure 15.2-1 Hydraulic System 8-Passenger 67
Figure 15.4-1: Electrical Schematic: 6 Passenger 68
Figure 15.4-2: Electrical Schematic: 8 Passenger 69
Figure 17.0-1: Manufacturing Process Flow 72
Figure 18.0-1: MSG-3 Visual Representation 74
Figure 20.1-1: 6-Passenger R, D, T, & E Costs 76

Figure 20.1-2: Program Costs (8 Passenger) 77
Figure 20.1-3: PFS-1000 Program Breakeven Point 78
Figure 20.2-1: 6 Passenger Jet Direct Operating Costs 79
Figure 20.2-2: 8 Passenger Direct Operating Costs 80

List of Tables

Table 3.2.2-1 Conventional and Innovative Down Select Considerations 17
Table 5.2-1: Wing Parameters 23
Table 6.1-1: Drag Coefficient Values for M=0.85 @ 35,000 ft 27
Table 7.1-1: Vertical Tail Parameters 29
Table 7.2-1: Horizontal Tail Parameters 31
Table 9.2-1: Landing and Takeoff Distances 39
Table 10.1-1 Weights: 6 and 8 Passenger 42
Table 12.2-1: Spar Dimensions 52
Table 12.3-1: Fuselage Structure Component Characteristics 54
Table 12.3-2: 6-seater Total Weight Savings 56
Table 12.3-3: 8-seater Total Weight Savings 56
Table 14.3: Virtual Skyline Equipment 63
Table 15.1-1 Fuel Sizing for 6 and 8 Passenger 64
Table 16.0-1 Commonality Analysis 71
Table 20.1-1: Business Jet DOC Comparison 78
Table A-1: Compliance Matrix 82

List of Symbols & Abbreviations

α	Angle of Attack
ac	Aerodynamic Center
AR	Aspect Ratio
AIAA	American Institute of Aeronautics and Astronautics
APU	Auxiliary Power Unit
b	Wing Span
c	Root Chord
CG	Center of Gravity
C_d	Drag Coefficient
C_{Do}	Zero Lift Drag Coefficient
C_{DC}	Compressibility Drag Coefficient
C_{Di}	Induced Drag Coefficient
C_{DP}	Parasite Drag Coefficient
C_l	Lift Coefficient
C_f	Flap Root Chord
C_{HT}	Horizontal Tail Coefficient
C_{VT}	Vertical Tail Coefficient
CFD	Computational Fluid Dynamics
CG	Center of Gravity
D	Drag
D.O.C.	Direct Operating Costs
ECS	Environmental Control System
EIS	Entry into Service
FAA	Federal Aviation Administration
FAR	Federal Aviation Regulation
Fpm	Feet per Minute

GSE	Ground Support Equipment
ISA	International Standard Atmosphere
k	Drag Constant
kt	knots
Ksi	Kilo pounds per square inch
LCD	Liquid Crystal Display
L/D	Lift to Drag Ratio
LE	Leading Edge
M	Mach Number
MAC	Mean Aerodynamic Chord
M_{dd}	Mach Drag Divergence Number
MTOW	Max Takeoff Weight
n	Load Factor
NACA	National Advisory Committee for Aeronautics
NASA	National Aeronautics and Space Administration
Nmi	Nautical Mile
OLED	Organic Light-Emitting Diode
PAX	Passenger
PFS	Premier Flight Systems
np	Neutral Point
QC	Quality Control
RFP	Request for Proposal
Re	Reynolds Number
S	Wing Planform Area
SSL	Standard Sea Level
S_{HT}	Horizontal Tail Area
S_{VT}	Vertical Tail Area

T	Thrust
t/c	Thickness Ratio (Wing)
TE	Trailing Edge
TSFC	Thrust Specific Fuel Consumption
T/W	Thrust to Weight Ratio
W	Weight
W/S	Wing Loading
V	Velocity

1.0 Design Requirements

Per the RFP, the aircraft family should share at least 70% commonality by the structural weight between the 6 and the 8-passenger aircraft. Both the 6 and 8-passenger aircraft must be able to fly at least 2,500 nmi with a 100 nmi alternate. Both configurations of this aircraft family must be able to fly a max speed of Mach 0.85 at an altitude of 35,000 feet. The aircraft family must be able to reach this cruise altitude by climbing at a max rate of 3,500 feet per min.

The 6-passenger configuration requires: 6 passenger capacity, minimum 1 pilot, luggage capacity of 500 lb and 30 cubic feet. The 8-passenger configuration requires: 8 passenger capacity, 2 pilots, luggage capacity of 1000 lb and 60 cubic feet. Both aircraft in this family must have a maximum sea level takeoff balanced field length of 4,000 ft at MTOW and a maximum landing field length of 3,600 feet at typical landing weight.

2.0 Mission Profile

In the RFP the required payload weights are designated for both the 6 and 8-passenger configurations in this light business jet family and both must be able to complete the same mission profile with the respective design weights of 500 lb/ 30 cubic feet and 1000 lb/ 60 cubic feet. The RFP states that both configurations must be able to fly at a max speed of Mach 0.85 at an altitude of 35,000 ft. Cruising at this altitude both, configurations must be able to fly at least 2,500 nmi with a 100 nmi alternate. The typical mission profile can be seen below in Figure 2.0-1.

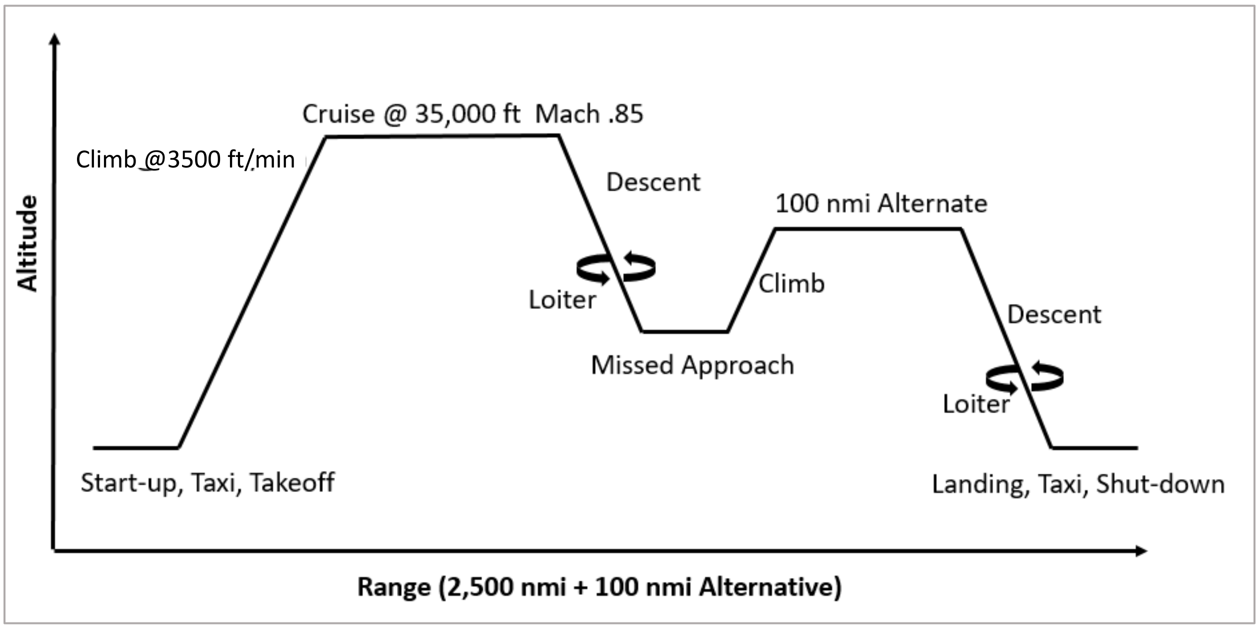

Figure 2.0- 1: Typical Mission Profile

3.0 Configuration Overview

3.1 Final Design

The PFS-1000 family of aircraft consists of a 6 and 8 passenger variant. The 6-passenger variant has two rows of opposing seats, with a back row facing forward. The 8-passenger variant has two blocks of opposing seats, with the middle rows facing back to back. These configurations offer the most compact design without compromising comfort. Both planes share the majority of the components that make up the aircraft. Because the fuselage is designed to be made of a series of plugs, the only difference between the 6 and the 8-passenger variants is a plug section of the fuselage. This means that the engines, wings, tails and any other critical components are the same for both aircraft. Both aircraft feature the windowless design that uses cameras and televisions to show an outside view of an aircraft. This improves aircraft performance, decreases weight, and offers a unique perspective for passengers who get to see their surroundings from a brand-new point of view.

Figure 3.1-1 Isometric View of 6-Passenger Aircraft

Figure 3.1-2 Isometric View of 8-Passenger Aircraft

3.1.1 Design Concepts

The primary goal was to fulfil the provided requirements. Any additional components that provided benefit but weren't strictly required by the RFP had to be fully justified before being added into the configuration. The primary purpose of traveling in a business jet is productivity. Whether this be in the form of faster travel, added privacy, or luxurious transport, a business jet must accommodate the modern traveler. The requirements suggest high airport accessibility, short travel times, and a cross-country range.

While the modern traveler soars above the population, they do not want to be disconnected from those below. A key feature of all new business jets must be constant, reliable communication during fight. This is achievable through onboard communications for all devices both Wi-Fi and cellular.

Any savings found should be passed onto the customer. Not very often does a decrease in cost provide an additional feature. The PFS-1000 family of jets would like to introduce a windowless design concept that displays the surrounding world on seamless screens along the fuselage interior. These screens add a new dimension to travel, showing to the traveler the outside world as it is or as they would like it to be. They are fully customizable in landscape selection from sunny beaches to star filled skies. A nervous flyer is no longer as they convert the stormy horizon to a peaceful countryside.

Imagination is the only limit and affordability is the name of the game. The windowless design concept is proven later in this proposal to decrease fuselage weight and therefore provide a fuel savings which reduces cost. Within a short three years, the first PFS-1000 business jet will be available for flight. With this in mind, design concepts had to be proven effective and durable in a short period of time. Designs using composite materials had to be abandoned due to long certification lead times. The added benefit is once again a decrease in cost to the customer. While the costs decrease yearly, composite manufacturing is still more expensive than traditional fabrication methods. Using time-tested technologies, the PFS-1000 family of aircraft will be readily available and of superior reliability.

3.1.2 Three-View Drawings

6 Passenger
Variant

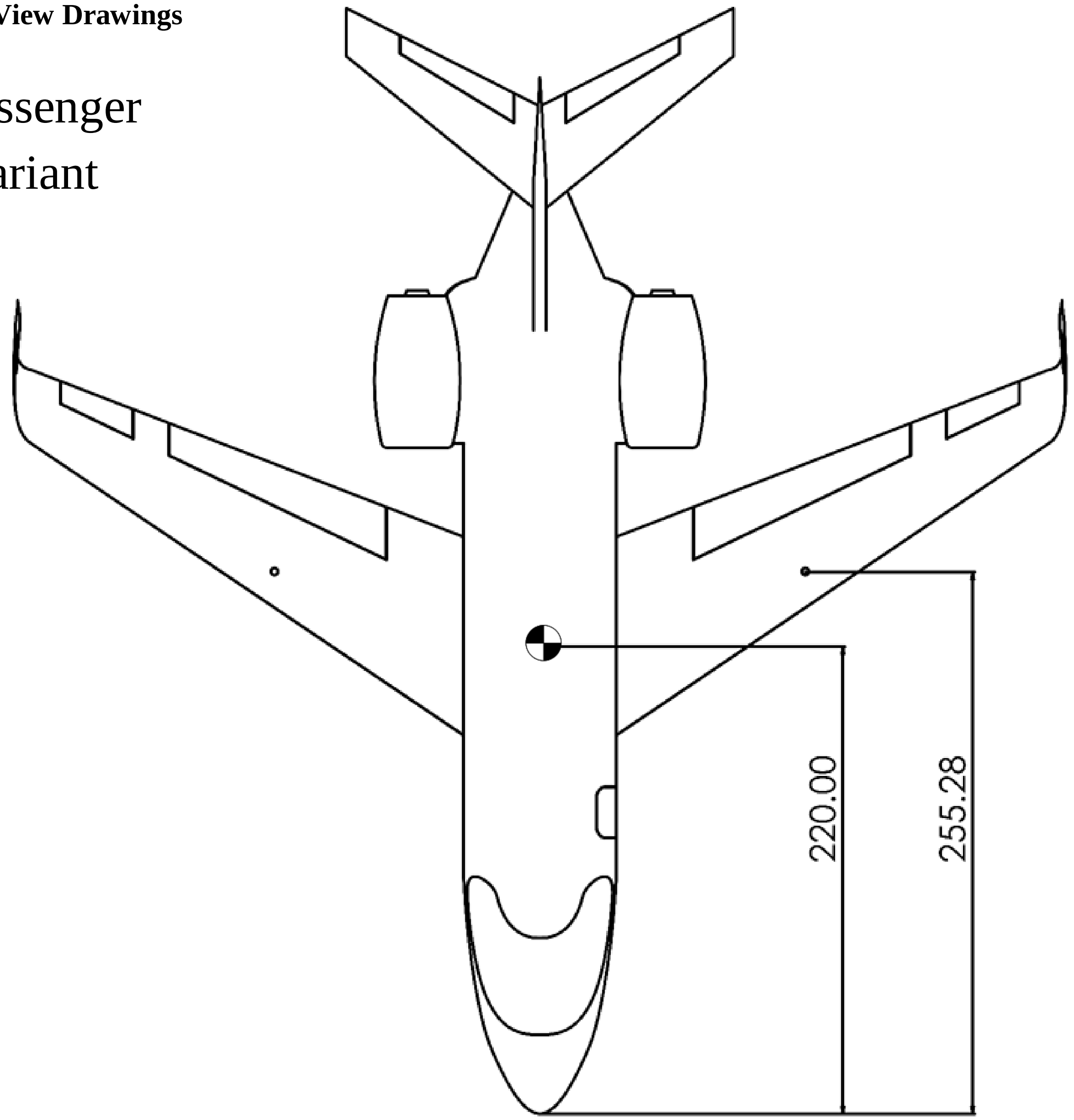

Characteristics Summary	
Aircraft Length	43.06 ft
Aircraft Height	13.33 ft
Wing Area	165.2 ft^2
Wing Sweep	34°
Engine	FJ44-3A
Gross Takeoff Weight	10,799 lb

*All dimensions are in inches

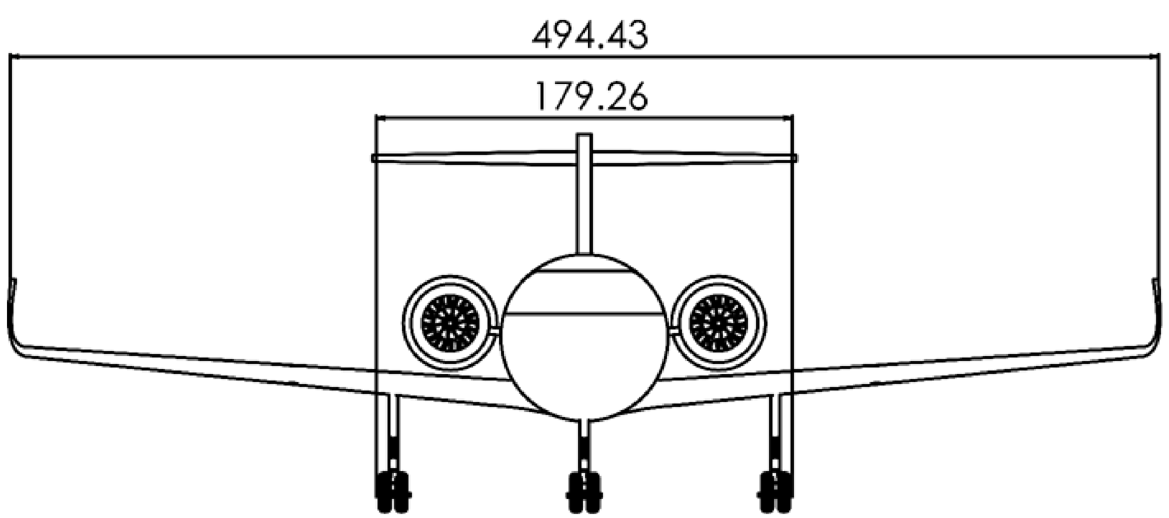

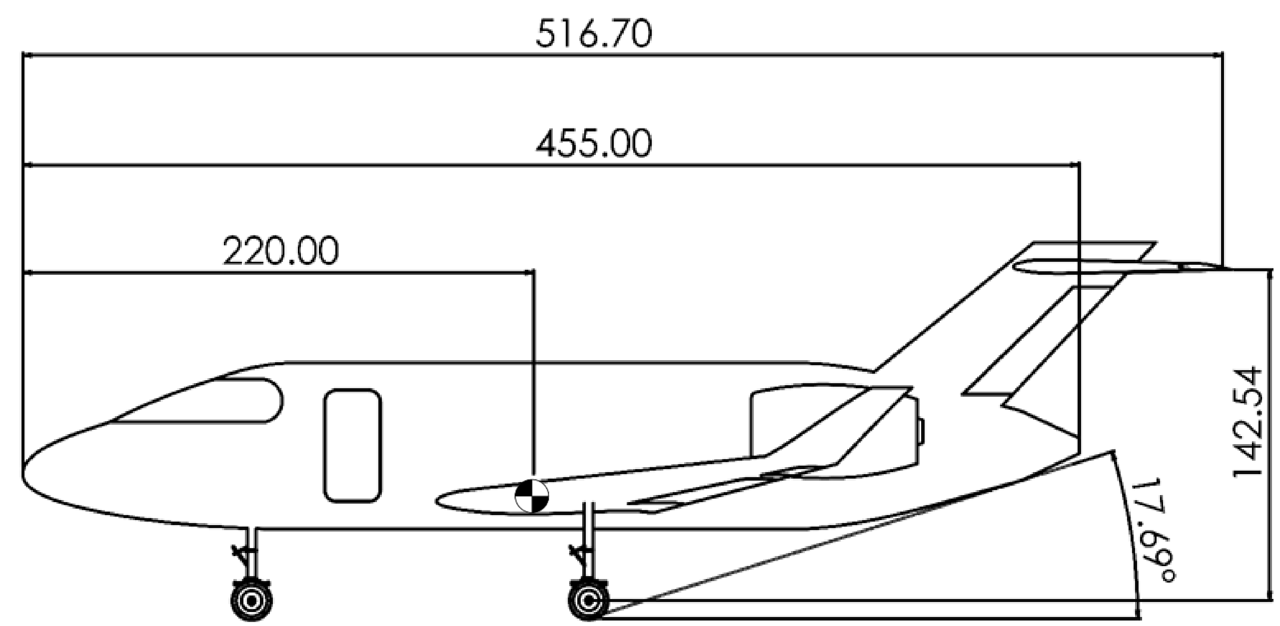

8 Passenger Variant

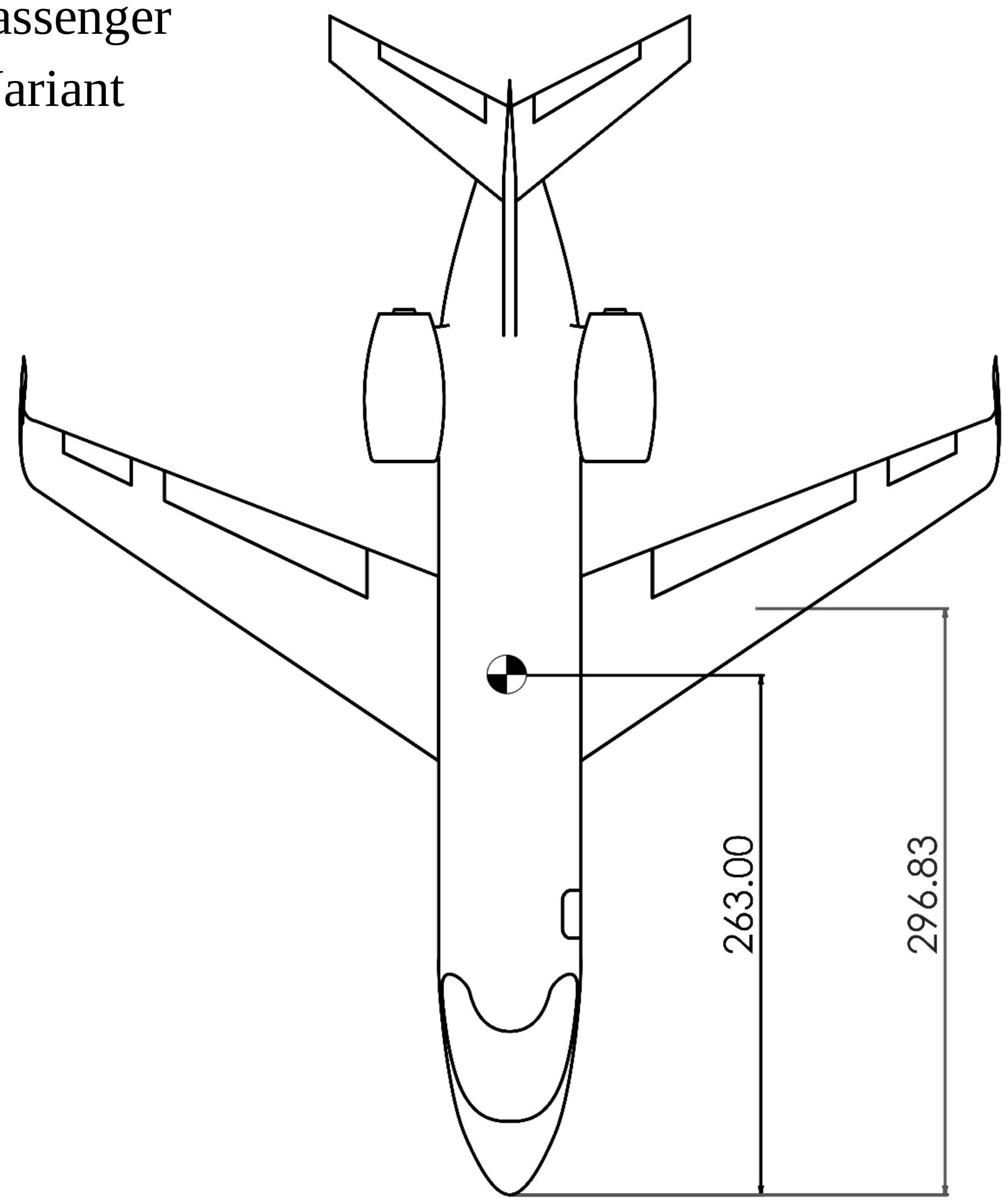

Characteristics Summary	
Aircraft Length	49.74ft
Aircraft Height	14.08 ft
Wing Area	165.2 ft^2
Wing Sweep	34°
Engine	FJ44-3A
Gross Takeoff Weight	11,959 lb

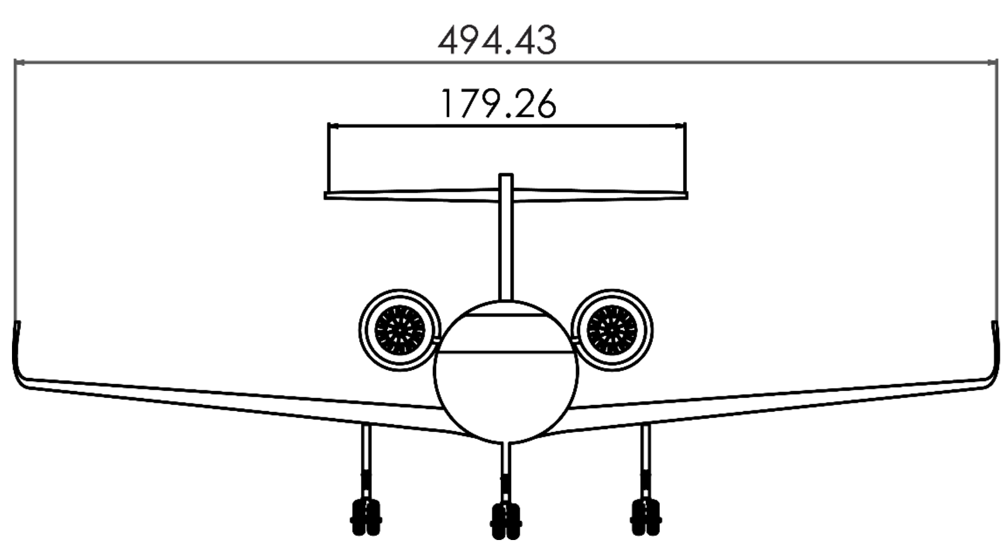

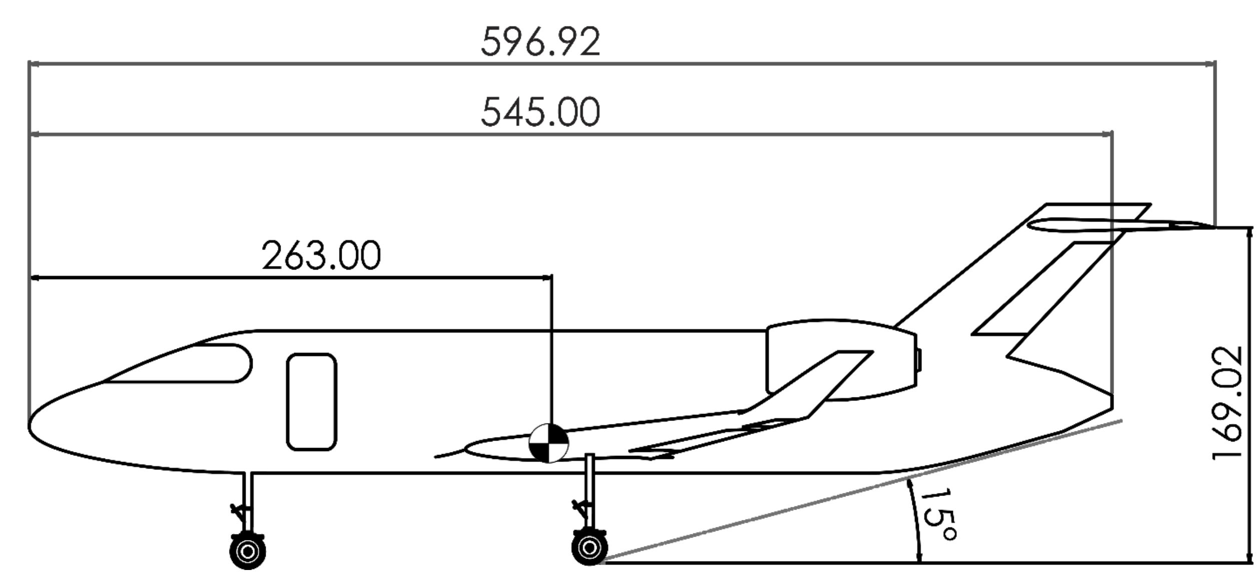

3.2 Alternative Concepts

Two designs (one conventional and one innovative) were created in the initial conceptual design phase with the intent of comparing the two and selecting the superior design. The innovative design allowed for research and analysis of new and emerging technologies and aircraft design concepts. A conventional design was created to improve on the industry standard design and to allow for a fallback design in case the innovative design could not meet the RFP requirements.

3.2.1 Innovative and Conventional Design

The philosophy behind the innovative design was to improve upon the standard industry design with currently available technologies that had yet to be implemented. The innovative design included structure made of 50% composite material. Composites were implemented into the design to reduce structural weight and to reduce operational cost by reducing fuel consumption. A key feature implemented in the innovative design was to supplement passenger windows with a virtual skyline. This would be an image shown on screens that run along the interior walls. The rationale behind this design was to reduce fuselage weight by eliminating heavy support structure for windows. The screens would provide a live feed of the external environment or could be altered to display any scenery the passenger desires. The display provides a larger viewing area than a window is capable of providing. With current production quality of high definition screens, high image quality, energy efficiency, and added weight are accounted for. Section 12.3 dives into the details of weight savings. Having a large, customizable screen to display the environment creates a more memorable and exciting flight experience for the passenger. The isometric views of the innovative and conventional designs are shown in Figure 3.2.1-1 and Figure 3.2.1-2 respectively.

Figure 3.2.1-1 Pre-Downselect Innovative Design Isometric View

Figure 3.2.1-2 Pre-Downselect Conventional Design Isometric View

Since the innovative design incorporated only structural changes on the fuselage, the remaining aircraft components such as the wing, tail, engine, landing gear, etc. remain unchanged when compared to the conventional design.

3.2.2 Comparison and Down Select

As the design process progressed, both the innovative and conventional designs were able to meet the RFP requirements. As seen in Table 3.2.2-1, the price of the conventional design was considerably higher than the innovative.

Table 3.2.2-1 Conventional and Innovative Down Select Considerations

	Conventional Design		Innovative Design	
	6 Passenger	8 Passenger	6 Passenger	8 Passenger
Aircraft Price	$ 10 Million	$ 12 Million	$15 Million	$18 Million
Direct Operating Cost	$34.92/Seat-Mile	$28.94/Seat-Mile	$34.49/Seat-Mile	$28.52/Seat-Mile
Range	2555 nmi	2684 nmi	2614 nmi	2741 nmi
Takeoff Weight	11,090 lb	12,293 lb	10,724 lb	11,858 lb

The driving cost hike was the use of composite materials. Ultimately, both the innovative and conventional designs were combined to eliminate composites and incorporate the windowless design. Beyond cost, eliminating composites supported the timeline to meet the EIS date of 2020. Sufficient time does not exist to certify composite structures into the design of the aircraft (AC 20-107B - Composite Aircraft Structure Document Information). The down select resulted in a windowless design without composite structure and high commonality between the 6-passenger and 8-passenger configurations.

4.0 Initial Sizing

The constraint diagram below in Figure 1.0-1, was constructed using the design requirements specified above and by the RFP. Once the constraint diagram was constructed is was used for the initial sizing of the business jets, as well as to visual which requirements are the most constraining. From the constraint diagram, it can be seen that the take-off and climb rate are the most restricting requirements. The initial sizing points chosen for the business jets is thrust to weight ratio of 0.49 and a wing loading of 57.0 for the 6-passenger, as well as a thrust to weight ratio of 0.38 and a wing loading of 73 for the 8-passenger.

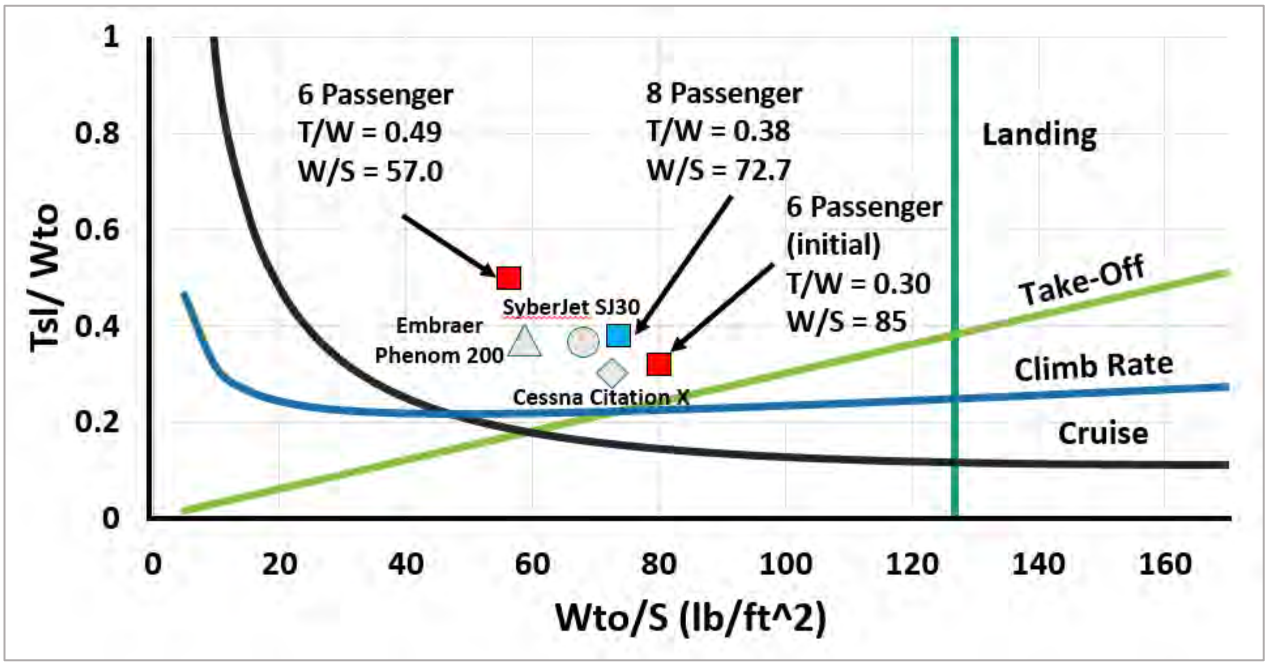

Figure 4.0- 1: Design Constraint Diagram

5.0 Wing Selection

The wing design process began once an initial design point was selected for both aircraft. To maintain commonality and reduce production cost, the wing designed for the 8-passenger aircraft was also used for the 6-passenger aircraft. The PFS-1000 family was designed to have the lowest wing weight that could fulfill the range requirement. Placing the wing on the bottom of the fuselage was the most convenient to maximize interior space.

The important parameters needed to initiate the wing design were wing loading and maximum takeoff weight which were determined by the constraint diagram in Section 4.0. The optimum aspect ratio was determined by performing two trade studies: 1) The effect of leading edge sweep and aspect ratio on range and 2) The effect of leading edge sweep and aspect ratio on wing weight, which are shown in Figure 5.0-1 and Figure 5.0-2 respectively. The trade studies included aspect ratios ranging from 4 to 12 and leading edge sweep ranging from 26 to 40 degrees. The minimum leading edge sweep angle was determined based on the Mach drag divergence, M_{dd}. The M_{dd} is the Mach number at which the aerodynamic drag on an airfoil increases significantly as the Mach number increases. To keep the drag low, the minimum sweep needed was calculated using the Korn Equation to be 33.9 degrees. To fulfill that constraint, a leading edge sweep angle of 34 degrees was selected to maintain the smallest possible sweep. To find the optimum aspect ratio, initially an AR of 7 was chosen since it met the range constraint and it gave room for error which can be seen by the red dot in Figure 5.0-1. The Breguet Range equation was used to calculate the range for the aspect ratios. The initial AR of 7 was used for the second trade study in Figure 5.0-2 to observe the weight of the wing. The equation used to find the wing weight came from Reference [5]. The weight is the total weight for both wings combined. Comparing the two trade studies showed that increasing the aspect ratio would increase the range and wing weight. Decreasing the aspect ratio would decrease the range and wing weight, but would move it closer to the range constraint. A margin of error was added and therefore an aspect ratio of 7 was chosen.

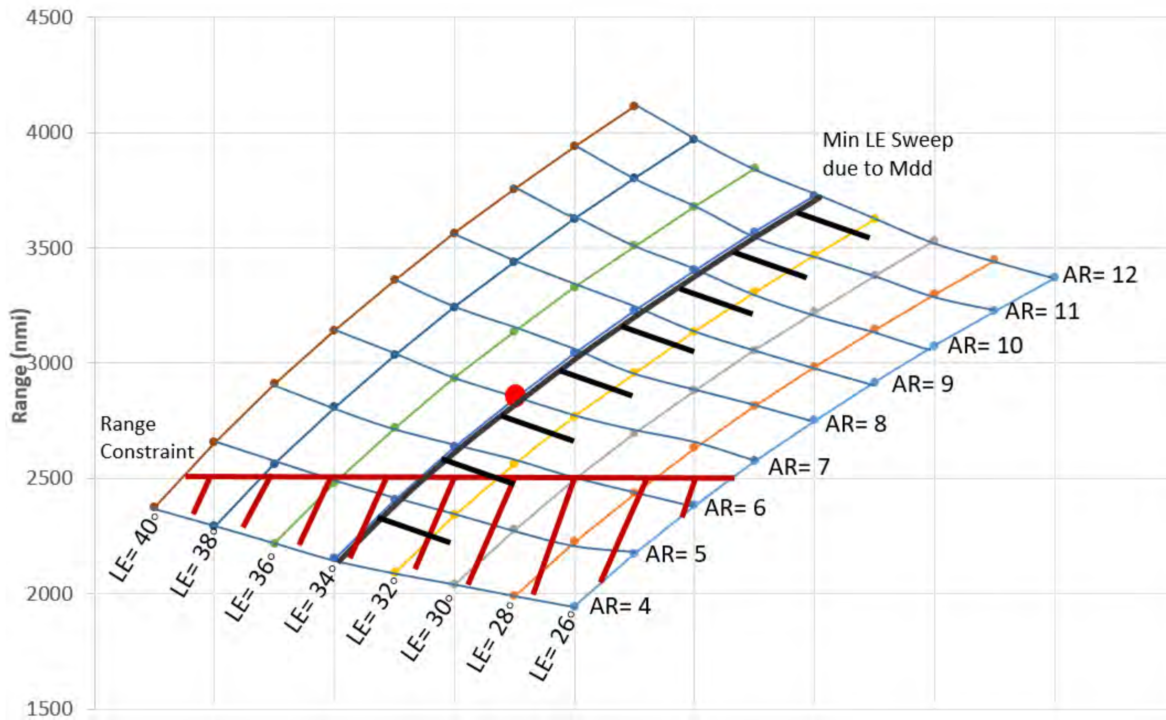

Figure 5.0-1: Effect of Leading Edge Sweep and Aspect Ratio on Range

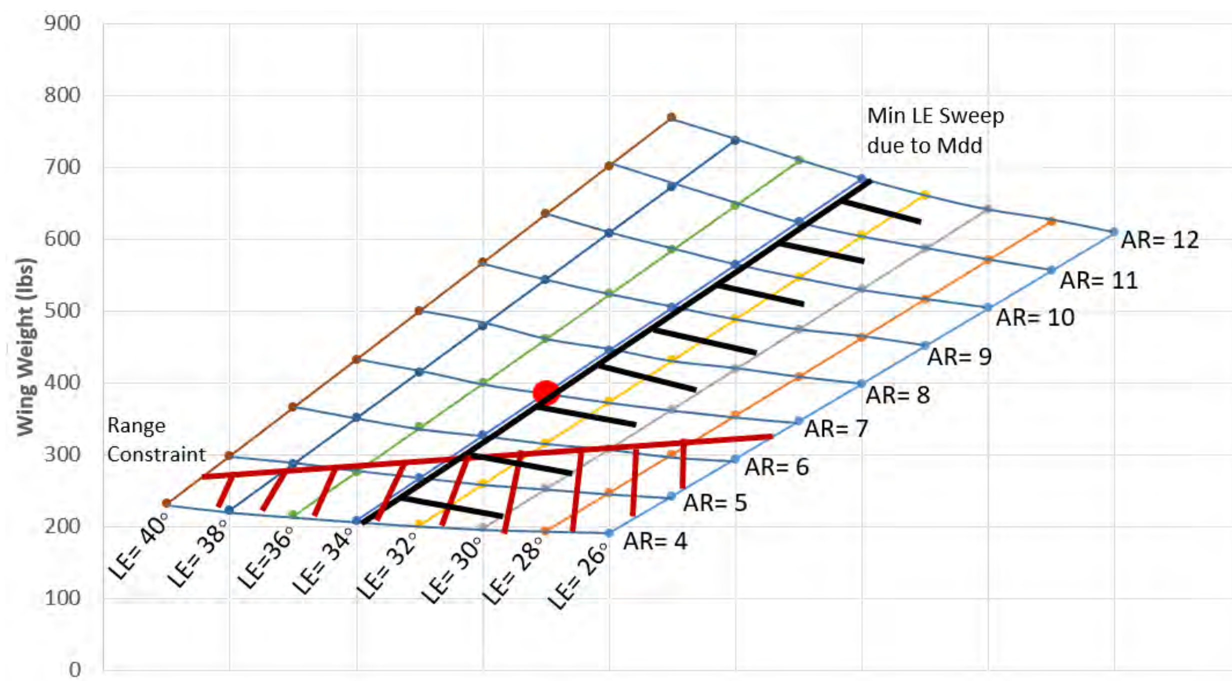

Figure 5.0-2: Effect of Leading Edge Sweep and Aspect Ratio on Wing Weight

5.1 Computational Fluid Dynamics

Computational Fluid Dynamics (CFD) was utilized to compare various design iterations of specific components of the aircraft. ANSYS FLUENT was the software chosen, and was used in determining the final taper ratio and winglet design. The main wing planform shapes were determined analytically, and some features were refined using CFD. The CFD code used in this design was validated using data from the National Aeronautics and Space Administration (NASA), on the Onera M6 wing. The results below show that the results from ANSYS FLUENT match the values that NASA had determined.

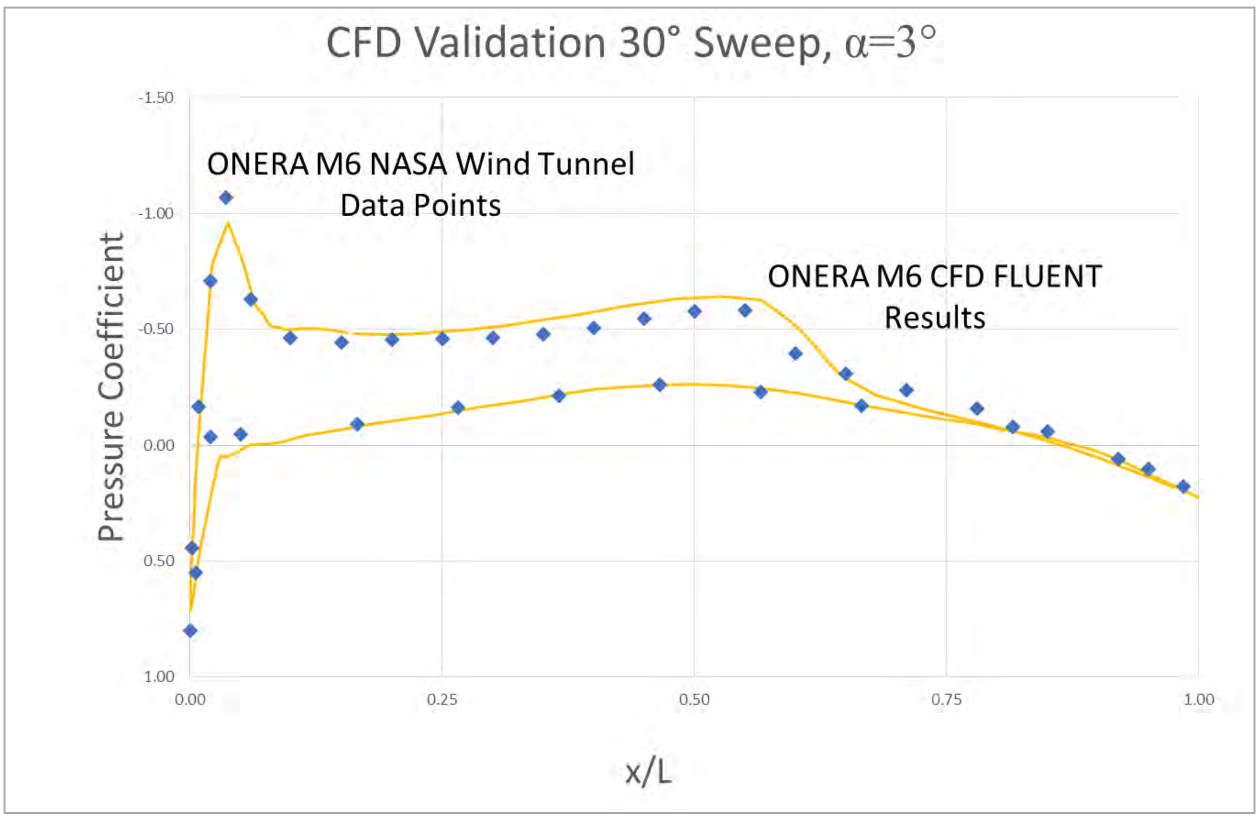

Figure 5.1-1: CFD Validation Curve

Moving forward, any feature that could not be determined analytically was CAD modeled in SolidWorks, and simulated using ANSYS FLUENT. This optimization method was more cost-effective than wind tunnel testing and allowed for a higher number of iterations. CFD allows designers to iterate at higher speeds and at full-scale. While the purpose was not to find definitive values, resulting trends drove optimization, providing a balance between physically possible and cost effective.

5.2 Wing Planform

Once the aspect ratio was finalized, the wing parameters were found. A taper ratio of 0.45 was initially assumed by performing some research and reading Reference [9]. Per Reference [9], taper ratios for business jets ranged from 0.4 to 0.6 which helped in choosing an initial point. For accurate results, three taper ratios were selected: 0.35, 0.40, 0.45 and the wing parameters were found for each taper ratio. Using these three taper ratios, a simulation was performed in ANSYS FLUENT to observe which taper ratio was giving the best L/D. A taper ratio of 0.40 had the best L/D for the wing. Table 5.1-1 shows the wing dimensions and Figure 5.1-1 shows the finalized wing that will be used on the 6 and 8-passenger configurations respectively. The aerodynamic center of the wing is labeled with a round circle which can be seen in Figure 5.1-1. The high lifting devices are also shown in Figure 5.1-1, but is further explained in Section 5.3. The winglet was initially designed to run simulations in Computational Fluid Dynamics (CFD) to observe if it provided better aerodynamic performance. However, it did provide better performance because it reduced drag so the winglet was kept.

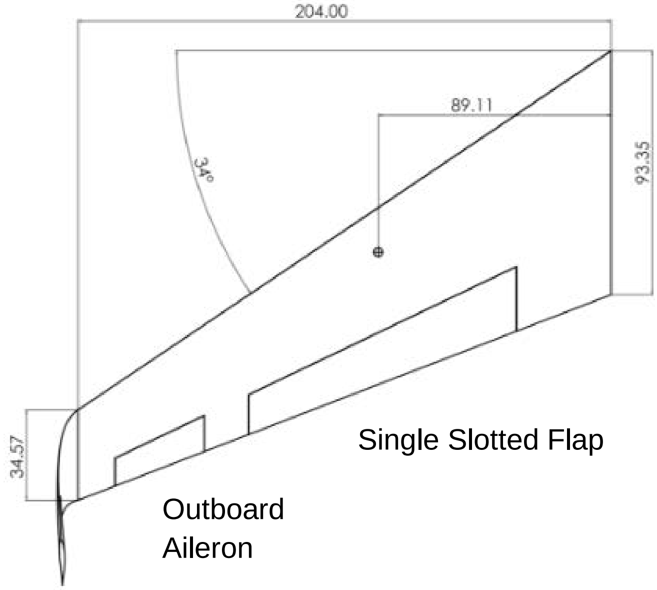

Table 5.2-1: Wing Parameters

Wing Area, S	165.15 ft^2
AR	7
Span, b	34.002 ft
Taper Ratio	0.4
LE Sweep	34 deg
MAC	5.155 ft
t/c	0.12

Figure 5.2-1: PFS-1000 Wing Planform (dimensions are in inches)

5.3 Airfoil

The airfoil chosen was the NACA 65-412. Several airfoils were compared, mainly using Reference [1]. The primary factors used to determine which wing to use were the max coefficient of lift, and the maximum Lift-to-Drag ratio. Additionally, some airfoils, specifically supercritical airfoils, due to limitations on control surface packaging. While supercritical airfoils perform well in the transonic regime, their thin trailing edges cause design constraints that would otherwise not exist.

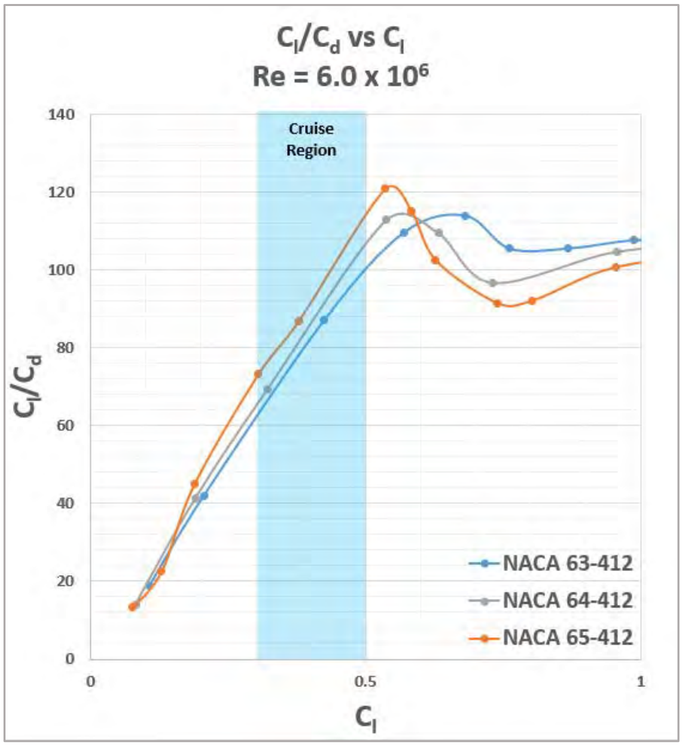

Figure 5.3-1: C_l / C_d vs. C_d Airfoil Comparison

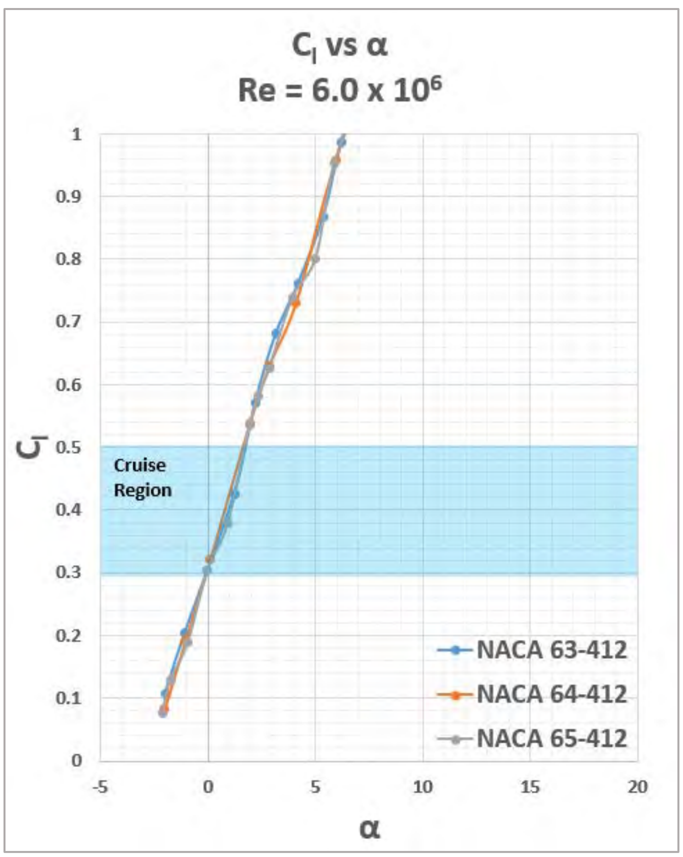

Figure 5.3-2: C_l vs. α Airfoil Comparison

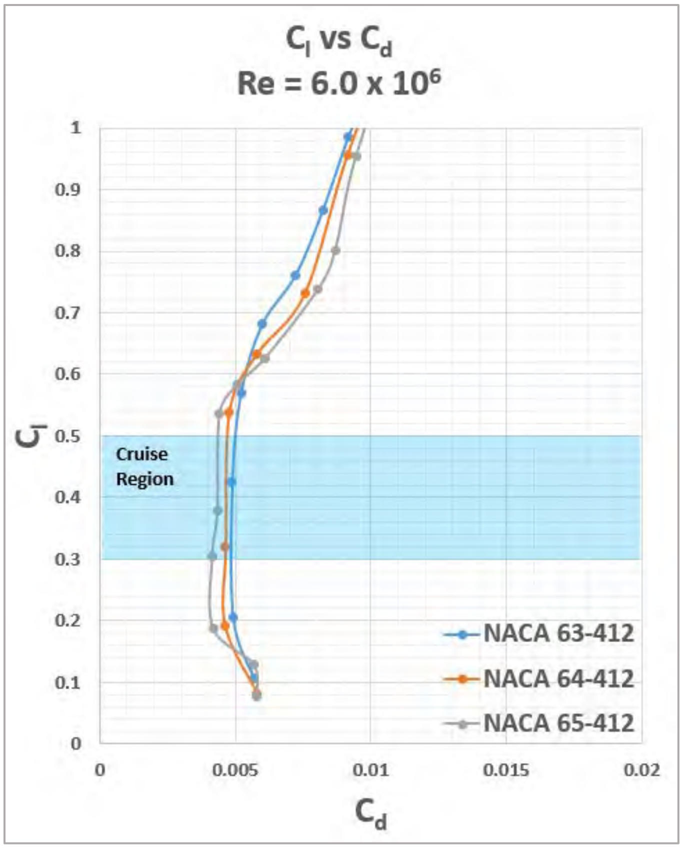

Figure 5.3-3: C_l vs. C_d Airfoil Comparison

Figure 5.3-4: NACA65-412 Airfoil Shape

5.4 High Lift Devices

The high lift devices in the wing design were calculated by the using Reference [5]. A single slotted flap was chosen from research and its better effectiveness when compared to a plain flap. Then a range of flap chord over chord, c_f/c, and deflection angle was compared to see which gave the best performance. The range of c_f/c was 0.15, 0.20, 0.25, 0.30, and 0.40 which was grouped with three deflection angles of 20, 30, and 40 degrees. The single slotted flap that had the best characteristics was a c_f/c of 0.3 and deflection angle of 40 degrees.

The single slotted flap was placed on the trailing edge, taking up 62.7% of the wing along the span. An outboard aileron took up 25% of the wing along the span. This wing design gave better results in lift and drag for takeoff, cruise, and landing conditions. Figure 5.3-1 below shows the increased lift coefficient for a flapped wing.

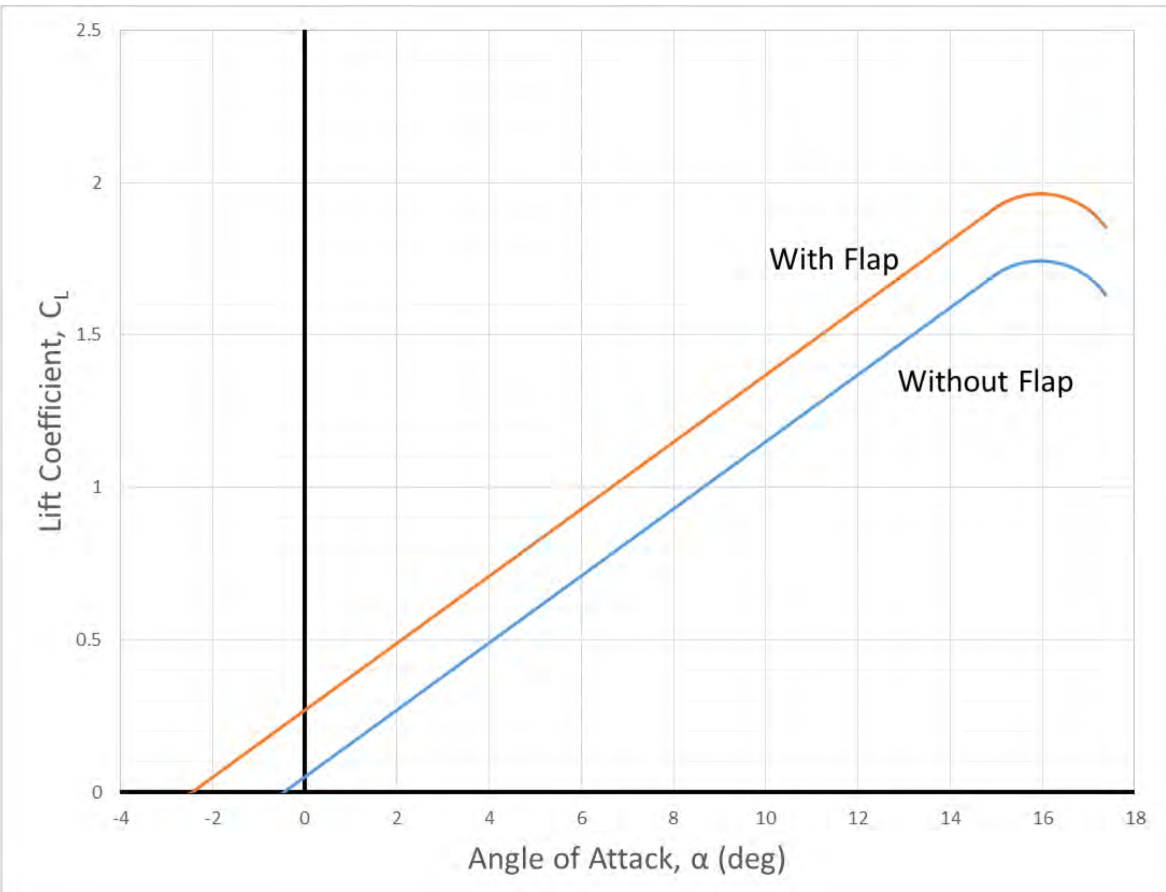

Figure 5.3-1: Lift Coefficient Comparison for Flapped and Non-Flapped Wing

6.0 Aerodynamic Performance

6.1 Drag (Parasite, Induced, Compressibility)

The drag for the PFS-1000 family was found by using the methods in Reference [5]. The drag found on the aircraft was for cruise condition only. Since the RFP stated, the aircraft must be able to cruise at M=0.85 at an altitude of 35,000 ft, this condition was what the drag was totaled for.

The total drag coefficient for the cruise condition was totaled from three drag coefficients: the parasite drag coefficient, C_{DP}, induced drag coefficient, C_{Di}, and the compressibility drag coefficient, C_{DC}. The parasite drag coefficient accounted for the drag for five parts: wing, fuselage, horizontal and vertical tail, and nacelle. The 6 passenger and 8 passenger had a slight difference in parasite drag because the 8 passenger has an 8 feet longer fuselage. The induced drag was based off the lift coefficient, Aspect Ratio, and Oswald efficiency factor. The Oswald efficiency factor was determined after thorough research from Reference [5]. The compressibility drag was determined from Figure 12.10 in Reference [9]. The drag divergence Mach number, M_{dd}, was needed to find the compressibility drag coefficient. The Korn equation was used to calculate an estimated Drag divergence Mach number. The total drag coefficient values for the aircraft are in Table 6.1-1.

Table 6.1-1: Drag Coefficient Values for M=0.85 @ 35,000 ft

Drag Type	6 Passenger Drag Coefficient Values	8 Passenger Drag Coefficient Values
C_{DP}	0.0255	0.0265
C_{Di}	0.0040	0.0040
C_{DC}	0.000825	0.000825
Total C_D	0.0304	0.0313

6.2 L/D and Other Performances

The drag polar, shown Figure 6.2-1 was calculated for the 6-passenger and 8-passenger to observe the max L/D. The drag polar was made up of the total drag which included the parasite, induced, and compressibility drag coefficient. Equation 6.2-1 was used to find the value of C_D by ranging the value of C_L from 0 to 1.5.

$$C_D = C_{DO} + (K * (C_L - C_{L0})^2 + C_{DC} \quad \text{(Eqn. 6.2-1)}$$

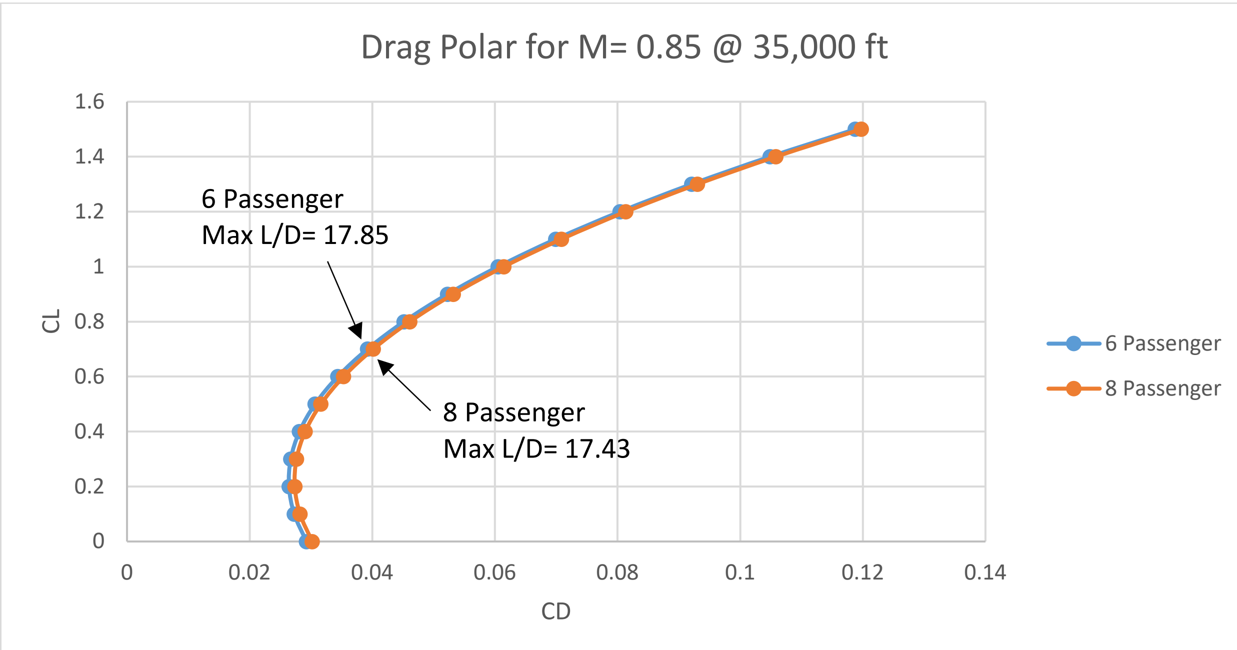

Figure 6.2-1: Drag Polar for PFS-1000 Family

As seen from the graph, the 6-passenger and 8-passenger share very similar drag polar graphs because the aircraft are very common. The only difference is the length of fuselage as mentioned in Section 6.1. From Figure 6.2-1, it can be seen that the slight difference in fuselage length plays a minimal effect on the max L/D.

7.0 Stability and Control

7.1 Vertical Tail

Initially, the vertical tail was sized by selecting a horizontal tail volume coefficient that was similar to other model of business jets. The value selected from [9] was C_{VT} = 0.09. The geometry of the aircraft was then used to determine S_{VT} from C_{VT}. This area was used in the initial weight and sizing of the aircraft. Stability analysis during one engine inoperable was done to allow the aircraft to fly and land in the case that one engine fails.

The vertical tail must be large enough to counteract the yawing moment that the one engine creates. This analysis was done assuming a flight altitude of 35,000 ft and a flight speed of $1.2V_{stall}$ to allow for safe control during flight and landing. A table of the vertical tail characteristics, geometry, and control surfaces are shown in Table 7.1-1. A drawing of the vertical tail can be seen in Figure 7.1-1.

Table 7.1-1: Vertical Tail Parameters

Vertical Tail Area	31.05 ft^2	Airfoil	NACA 64-008
Aspect Ratio	1.1	High Lift Device	Plain Flap
Span	76.45 in	C_f/C	30%
Root Cord	75.36 in	S_f/S	70%
Tip Cord	49.32 in	Flap Deflection	30°
Leading Edge Sweep	39°	C_L with flaps	1.02

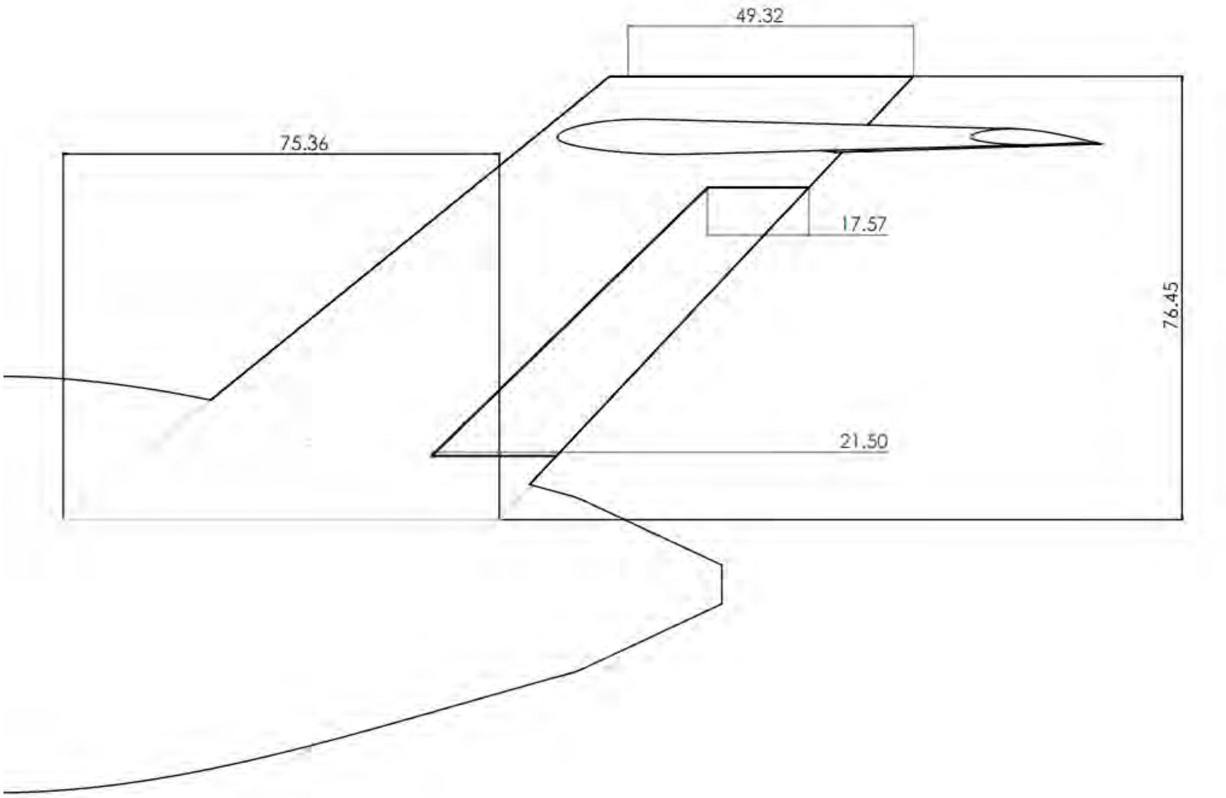

Figure 7.1-1: Vertical Tail Side View

7.2 Horizontal Tail

The sizing of the horizontal tail is dependent on three conditions: nose wheel liftoff, rear stability limit, and pitch control with flaps. Each of these conditions change with the CG of the aircraft. Figure 7.2-1 shows a notch diagram and how each control condition changes with CG location. The CG travel for the 6 passenger from section 10.2 was then placed into the highest "notch" between the condition lines. The height of the CG travel line determined the horizontal tail volume coefficient. In this case $C_{HT} = 0.86$. Table 7.2-1 shows some horizontal tail parameters and Figure 7.2-2 shows a drawing of the horizontal tail.

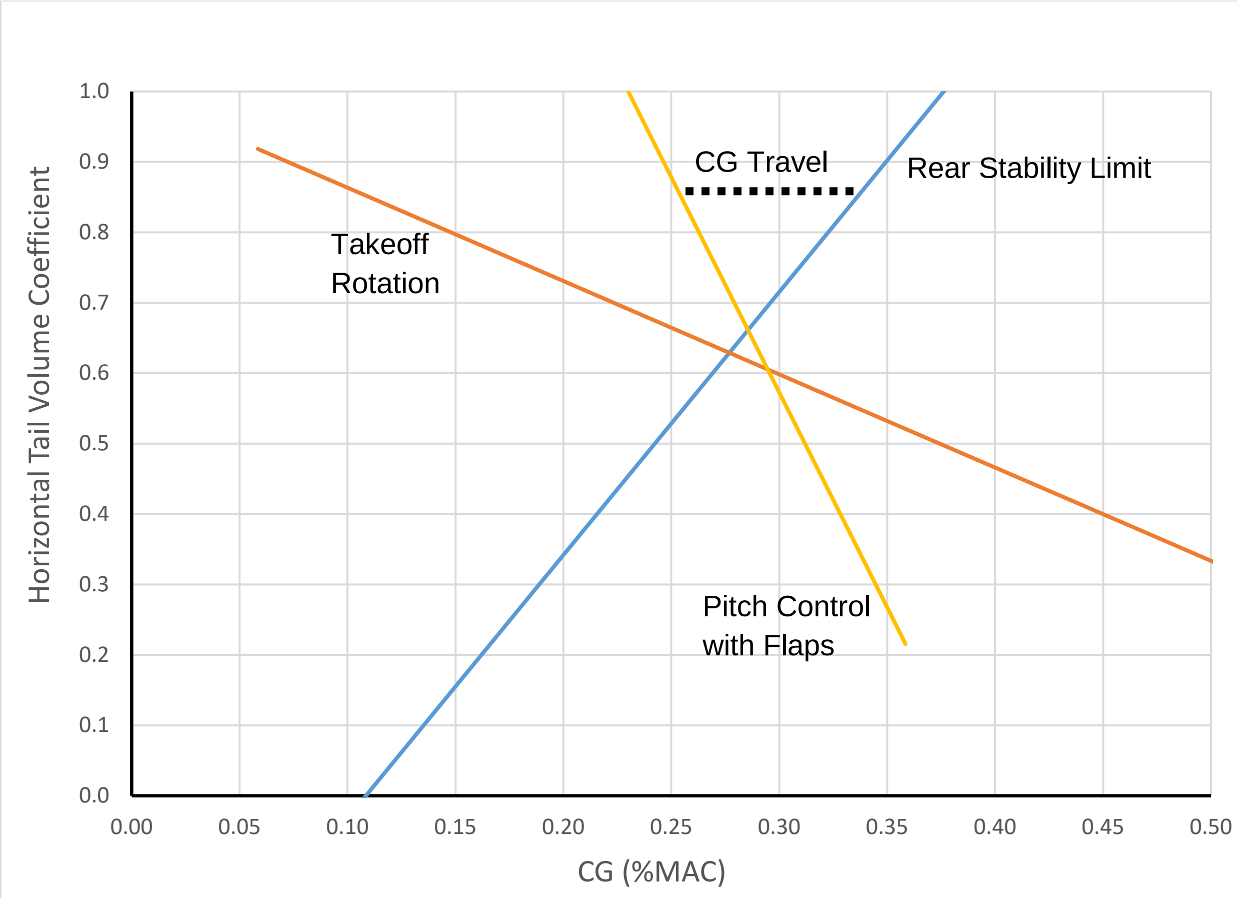

Figure 7.2-1: Notch Diagram for 6 Passenger Horizontal Tail

Table 7.2-1: Horizontal Tail Parameters

Tail Area	46.18 ft^2	Airfoil	NACA 64-008
Aspect Ratio	5	High Lift Device	Plain Flap
Span/2	91.15 in	C_f/C	30%
Root Cord	49.31 in	S_f/S	70%
Tip Cord	22.63 in	Flap Deflection	30°
Leading Edge Sweep	39°	$C_{L\alpha}$	3.38

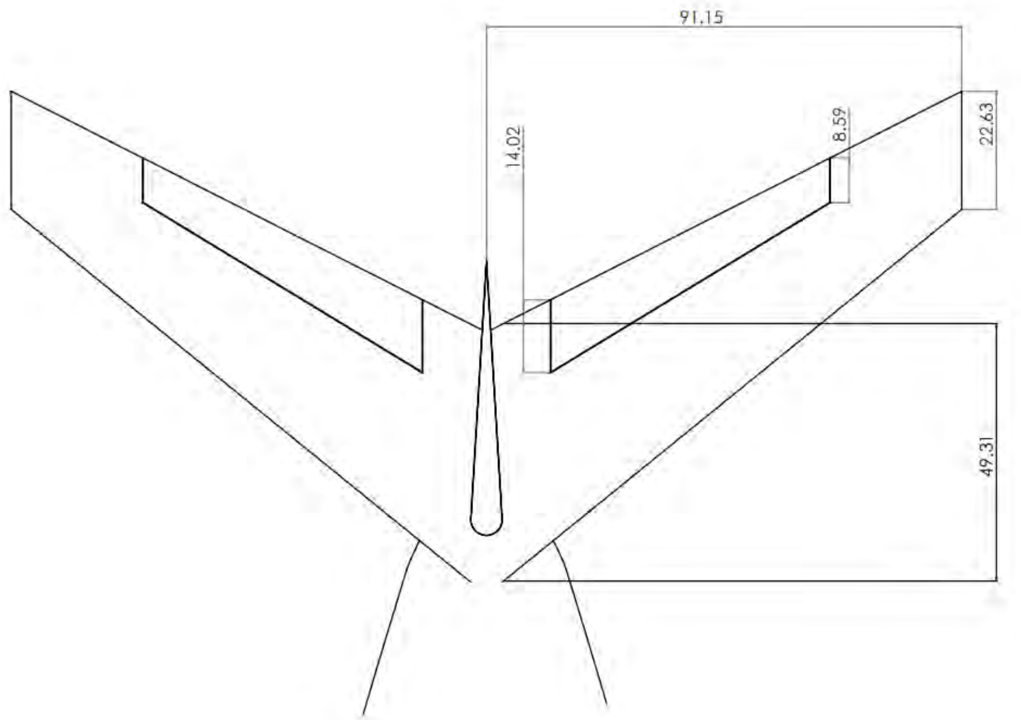

Figure 7.2-2: Horizontal Tail Top View

8.0 Propulsion System

For an airplane of this size and that can travel at Mach 0.85, a turbofan engine is the best option, this is because a turbojet is generally too loud for a business jet passengers and a propeller engine will not be able to meet the speed requirements.

The next step in selecting engines for the aircraft was to find the required thrust since it was already decided best to utilize a turbofan engine. It is desirable to use the same engine for both the 6 and 8-passenger configurations to help minimize engine acquisition costs. The required thrust was at least 4600 lb based on the 8-passenger takeoff weight of 11,959 pounds, and a desired thrust to weight ratio of 0.38. This thrust to weight ratio was selected based on the initial sizing and most constraining requirements as seen in the constraint diagram of Figure 4.0-1. Based on the required thrust and TSFC several engines would fit the requirements. These engines were the Williams FJ44-3A, the Pratt & Whitney JT15D-4B, and the Pratt & Whitney PW535. The graphs which compare static sea level thrust and the static sea level TSFC's are shown below in figures 8.0-1 & 8.0-2.

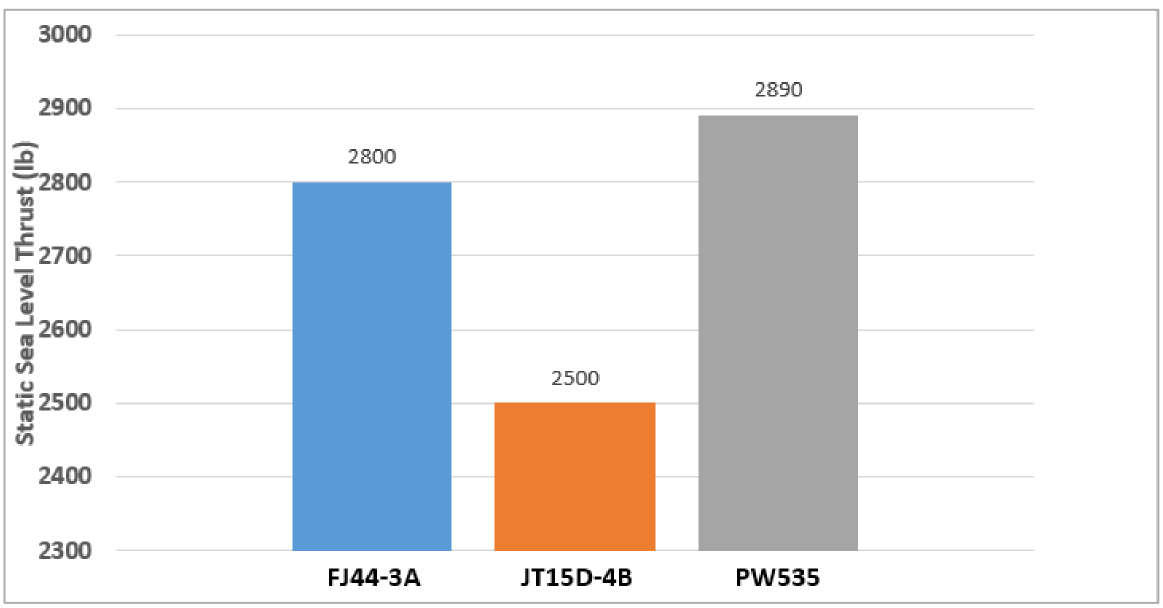

Figure 8.0-1: Comparing Engine Thrusts

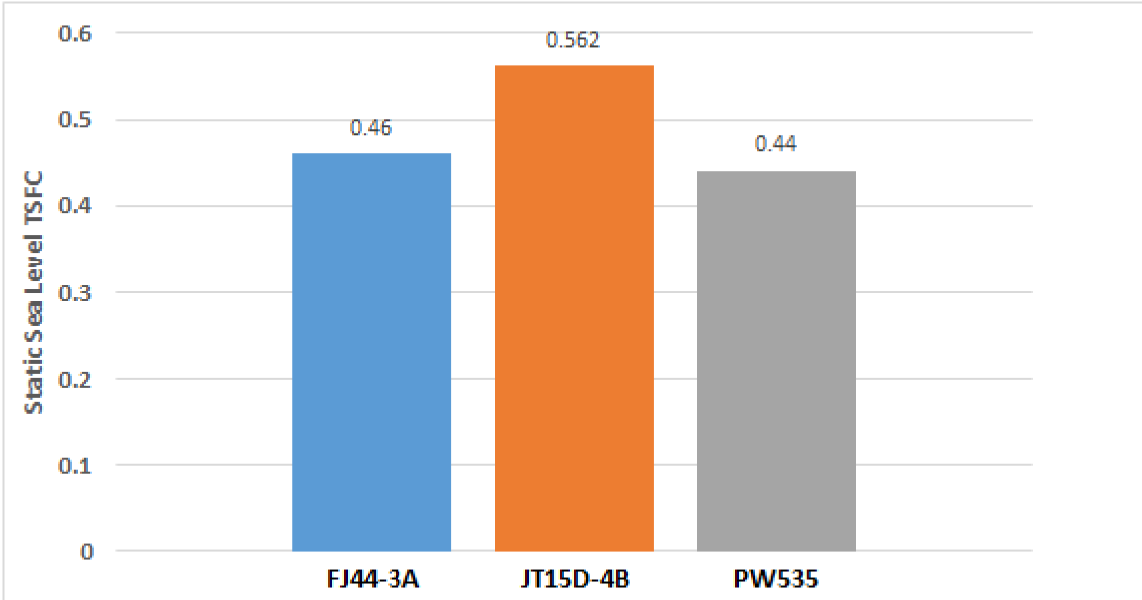

Figure 8.0-2: Comparing Engine TSFC

The Williams FJ44-3A engine was chosen because it meets the minimum required thrust and gives the best fuel efficiency of other engines in this class while still meeting the size requirements set forth for the design. The Pratt & Whitney PW535 gives slightly more thrust ~90 lb_f and has a slightly lower TSFC but it was decided to be slightly oversized for this application. The chosen engine, FJ44-3A seen in Figure 8.0-3 produces 2,800 lb of thrust with a static sea level TSFC of 0.46.

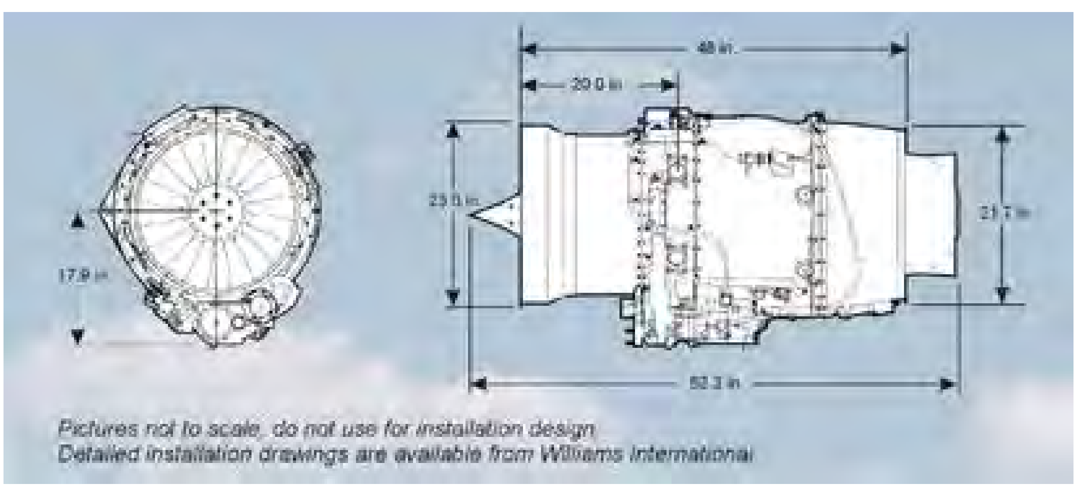

Figure 8.0-3: FJ44-3A Engine

The sea level static thrust for the FJ44-3A is the only TSFC available as common knowledge, so utilizing trends from Appendix J of Reference [5], the TSFC at 35,000 feet altitude was interpolated. This interpolation appears in Figure 8.0-4 below. This gives a cruise TSFC of around 0.775.

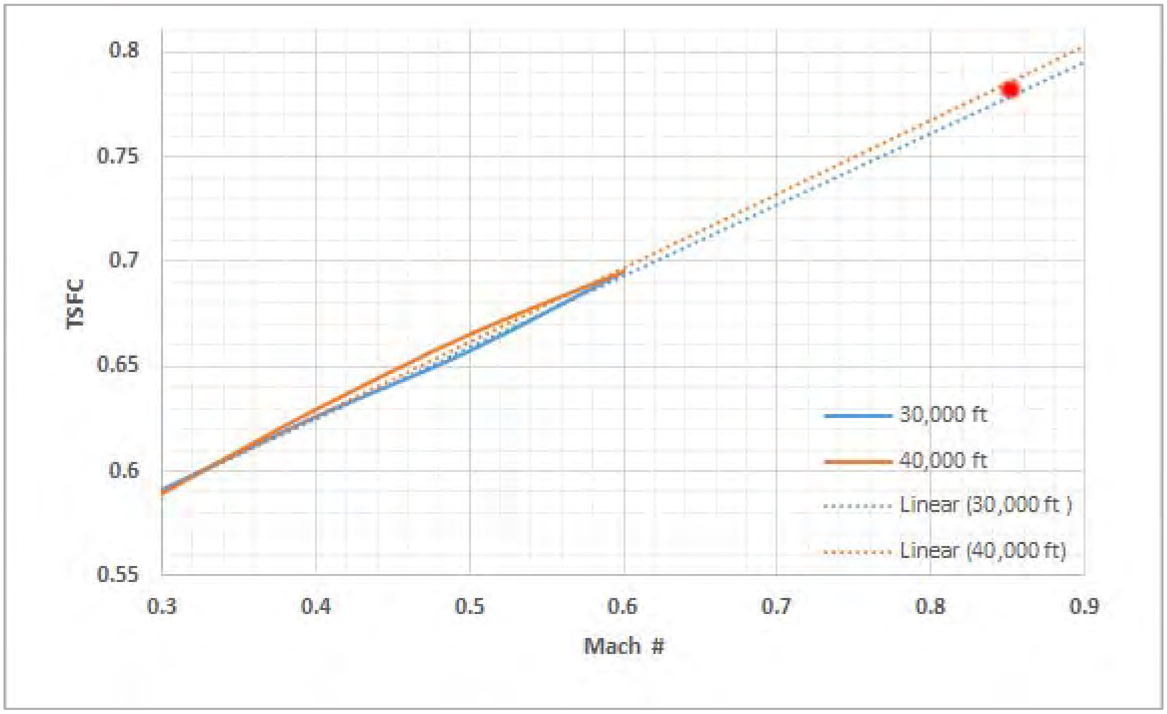

Figure 8.0-4: FJ44-3A TSFC vs. Mach @ Altitude

9.0 Aircraft Performance

9.1 Payload Range Calculations

The starting point for the 6-passenger payload-range curve is max payload of 1900 lb while the starting point for the 8-passenger payload-range curve is max payload of 3000 lb which consists of both passengers and their luggage. Both configurations must be able to carry their respective maximum payload at least 2500 nmi with the option for a 100 nmi alternate. Although there was no ferry range requirement stated by the RFP, it can be seen from the payload range diagrams that at a sacrificed payload both the 6 and 8-passenger configurations can fly much further distances than required in the RFP, even transatlantic if needed. The Payload-Range Diagrams which show the range performances of each aircraft can be seen below in figures 9.1-1 and 9.1-2 and these figures are based on the calculation involving the Breguet Range equation.

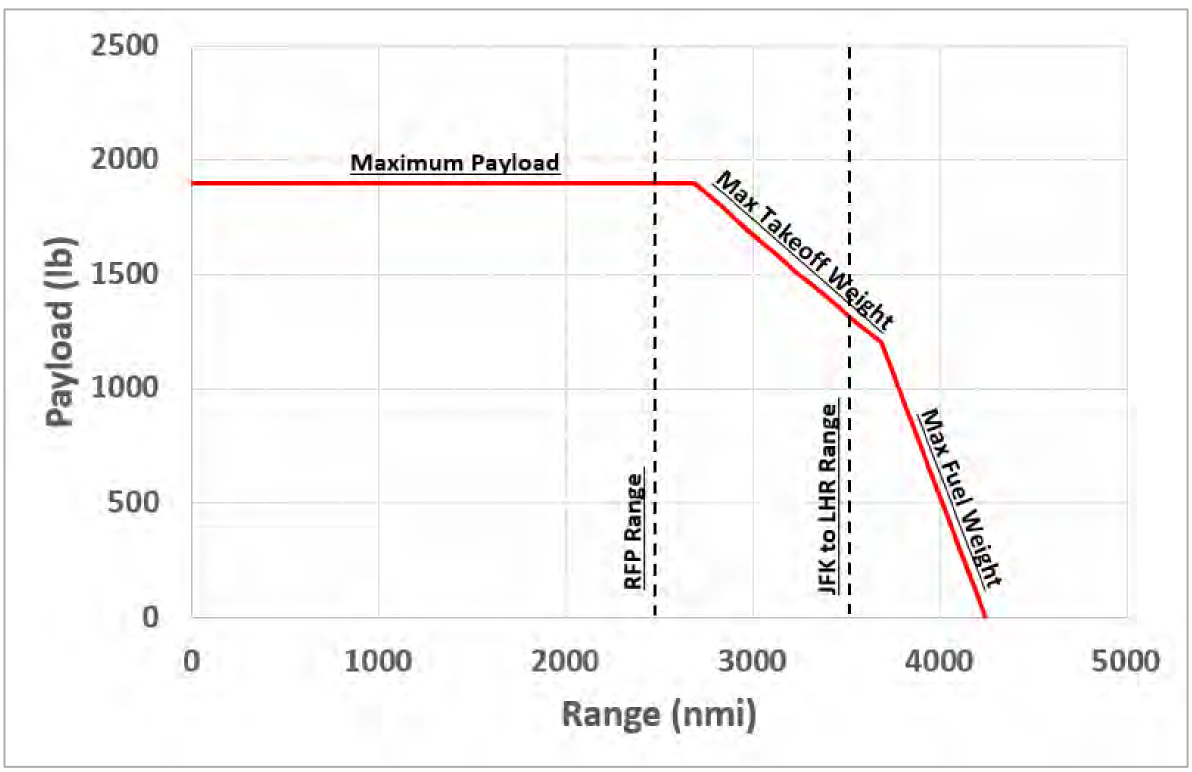

Figure 9.1-1: 6-Passenger Payload Range Curve

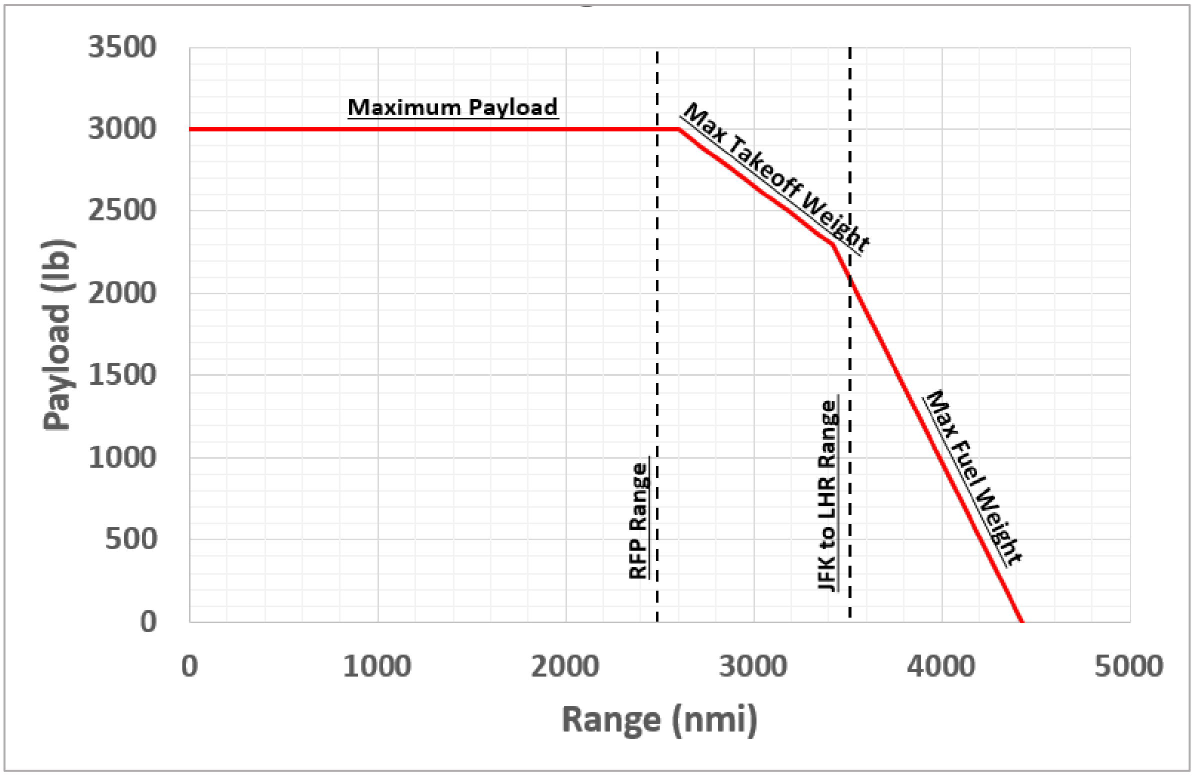

Figure 9.1-2: 8-Passenger Payload Range Curve

9.2 Take-off/ Landing Performance

Requirements state that both aircraft must have a balanced field length of 4000 ft and a landing field length of 3600 ft. There are two cases to be considered when determining balanced field length. The first is while accelerating, one engine becomes inoperable and the aircraft continues to take off. The second is when one engine becomes inoperable the aircraft brakes to a stop. The velocity where the distance of both cases are equal is V_1, and if the aircraft becomes inoperable after this velocity the aircraft must take off. The distance to take off with engine failures at V_1 is the balanced field length. Figure 9.2-1 and Figure 9.2-2 shows the balanced field lengths of the 6 and 8 passenger models respectively. Table 9.2-1 shows the distances for landing and takeoff for each model.

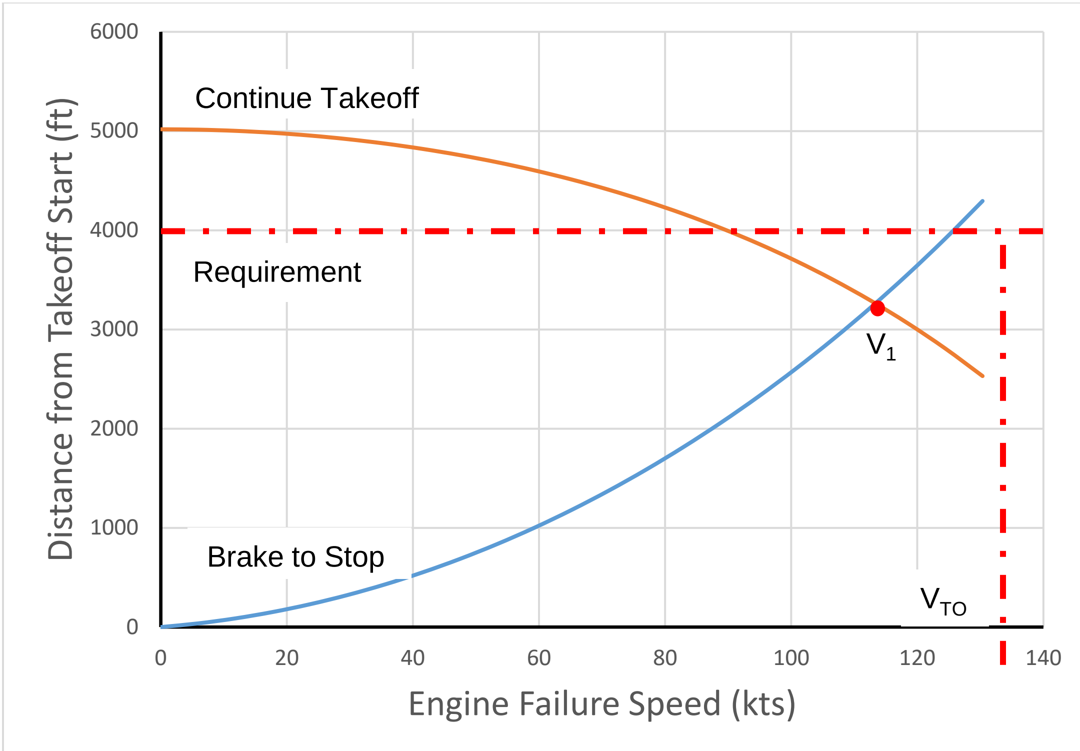

Figure 9.2-1: Balanced Field Length for 6 Passenger

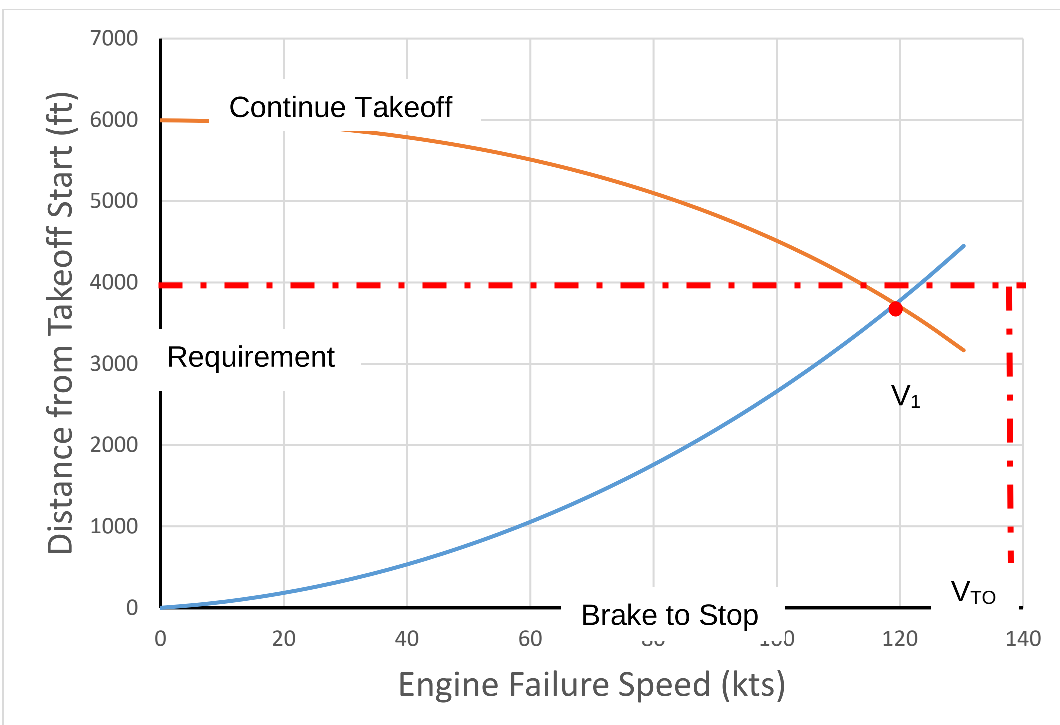

Figure 9.2-2: Balanced Field Length for 8-Passenger

Table 9.2-1: Landing and Takeoff Distances

	6 Passenger	8 Passenger
Takeoff Field Length	3241 ft	3789 ft
Balanced Field Length	3291 ft	3771 ft
Critical Velocity	112.6 kts	118.5 kts
Landing Field Length	3345 ft	3529 ft

9.3 Operational Envelope

An operational envelope was created for the 6 and 8 passenger PFS-1000 aircraft to show what the aircraft is capable of during flight. The operational envelope is made up of three boundaries which can be seen in Figure 9.3-1 for the 6-passenger aircraft and Figure 9.3-1 for the 8-passenger aircraft. The first boundary is the minimum speed or stall speed. The second boundary is the rate of climb where it displays the maximum ceiling. The third boundary is the maximum speed where the thrust equals the drag. The red line is the service ceiling requirement as stated in the RFP at 45,000 ft, which can successfully be reached. The max cruise point that was chosen is at Mach 0.85 at 35,000 ft which lands within the constraints of the operational envelope for both aircraft.

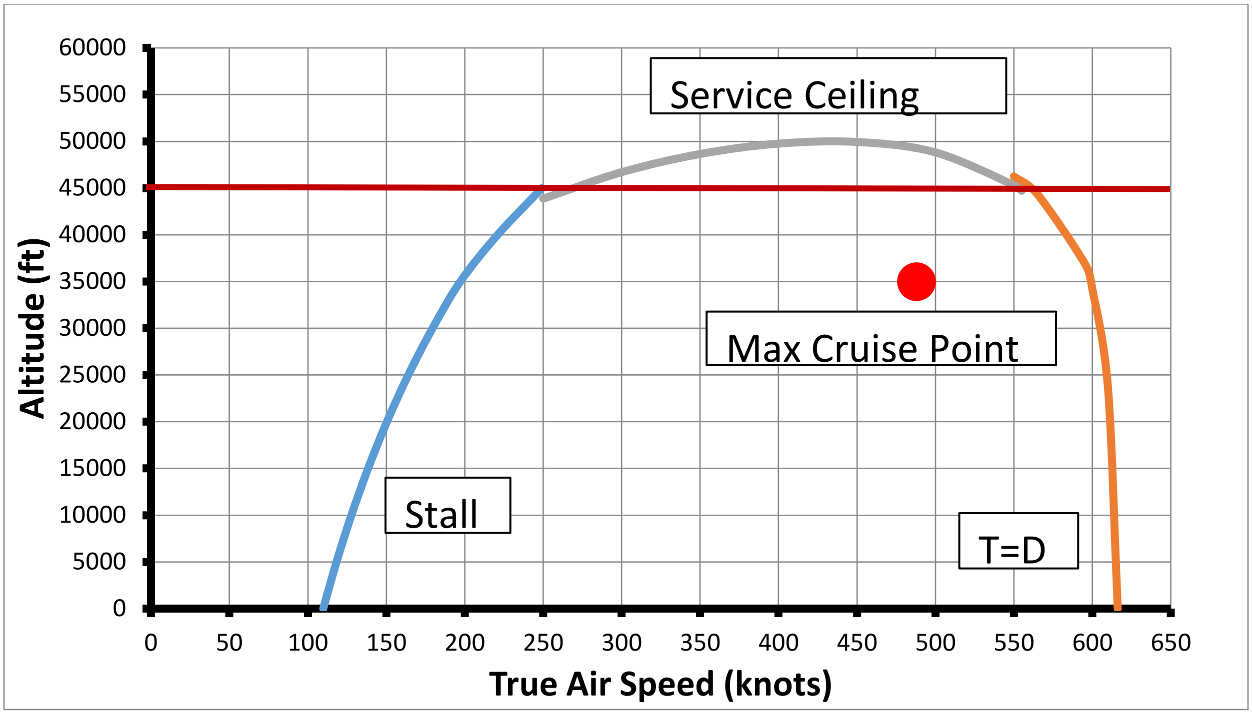

Figure 9.3-1: Operational Envelope for 6-Passenger

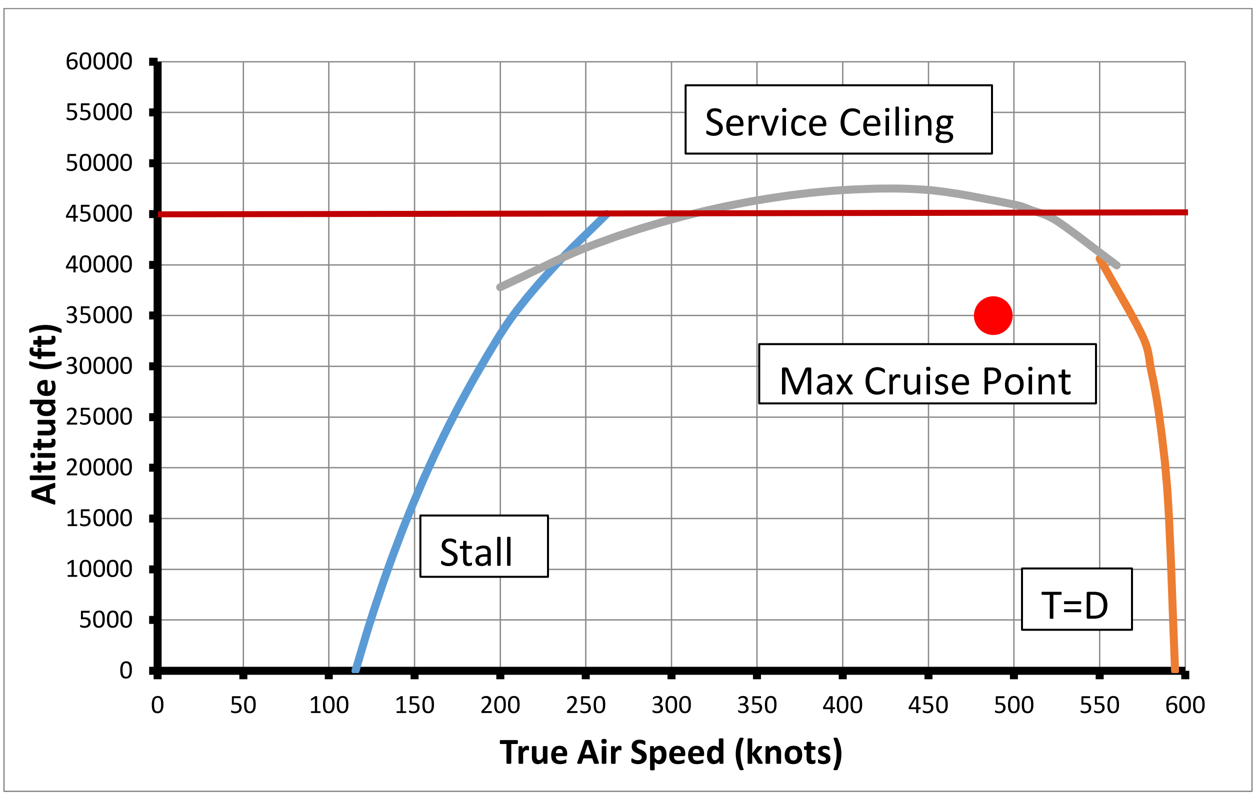

Figure 9.3-2: Operational Envelope for 8-Passenger

9.4 Rate of Climb

The RFP states the PFS-1000 family shall be able to climb at 3500 fpm at sea level. An excel spreadsheet including the rate of climb equation, Equation 9.4-1, was used to determine at what velocities the rate of climb would need to take place. By inputting altitudes, velocities, and the rate of climb needed, the *goal seek* function was used to find the boundaries for velocity that would fulfill the rate of climb requirement. The velocity needed to start the climb was 101.47 kt and could accelerate to a velocity of 563.56 kt before experiencing problems.

$$\dot{h} = \frac{(T-D)}{W} * V \quad \text{(Eqn. 9.4-1)}$$

10.0 Weights

10.1 Weight Breakdown

Completing a detailed weight breakdown of the aircraft into all its components allows for accurate weighing and balance calculations. To get accurate estimates, the method of Reference [5] was used along with gathering estimates of parts through online research and averaging them out. Tables 10.1-1 and 10.1-2 have the dry weight values as well as the additional entries for fuel, payload and crew. The tables show the percentages of dry weight that the components have.

Table 10.1-1 Weights: 6 and 8 *Passenger*

	Weight(lb)	Weight(%)
Propulsion System	1200.0	19.1
Wing/Tail	997.0	15.9
Empennage	243.0	3.9
Fuselage	777.0	12.4
Nacelle	176.0	2.8
Landing Gear	450.0	7.2
Fuel System	213.0	3.4
Avionics	235.0	3.7
Surface Controls	231.7	3.7
Hydraulic System	105.0	1.7
Electrical System	471.5	7.5
ECS	274.5	4.4
Anti Icing	130.0	2.1
Cabin Amenities	784.0	12.5
Aircraft Dry Weight	6287.7	100.0
Fuel	1921	
Payload	1700	
Crew	400	
Aircraft Total Weight	10308.7	

	Weight(lb)	Weight(%)
Propulsion System	1200.0	18.0
Wing/Tail	997.0	15.0
Empennage	243.0	3.6
Fuselage	934.0	14.0
Nacelle	176.0	2.6
Landing Gear	450.0	6.8
Fuel System	250.0	3.8
Avionics	235.0	3.5
Surface Controls	231.7	3.5
Hydraulic System	115.0	1.7
Electrical System	480.5	7.2
ECS	280.0	4.2
Anti Icing	130.0	2.0
Cabin Amenities	944.0	14.2
Aircraft Dry Weight	6666.2	100.0
Fuel	2969.0	
Payload	2600.0	
Crew	400.0	
Aircraft Total Weight	12635.2	

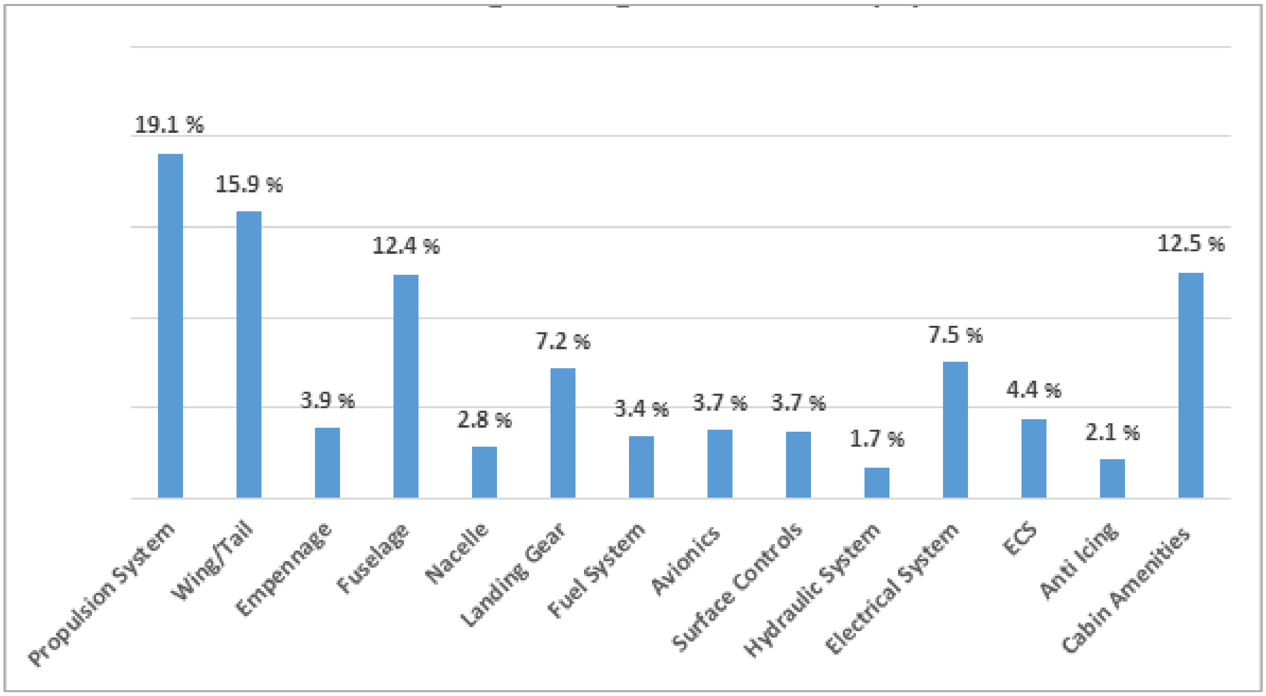

Figure 10.1-1 Weight Percentage Breakdown: 6 Passenger

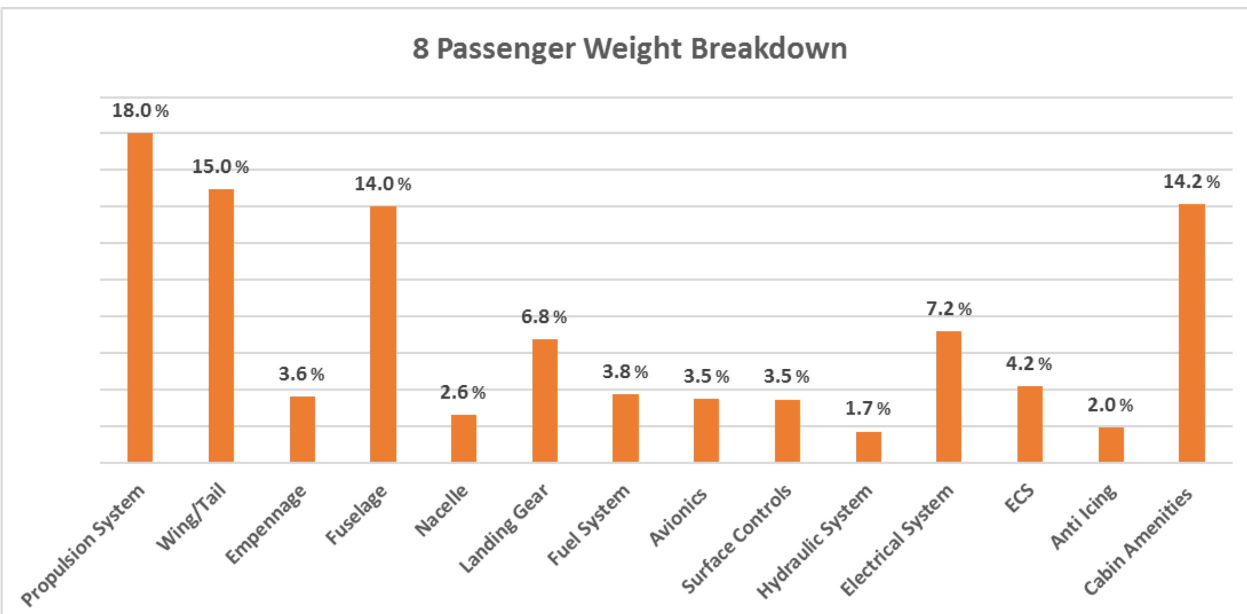

Figure 10.1-2 Weight Percentage Breakdown: 8 Passenger

10.2 CG Travel

The center of gravity is determined by summing the moments of the aircraft as it is divided into pieces and components, and then dividing it by its total weight. The C.G. will move as it is loaded and unloaded. The various conditions of C.G. location can be seen in Figure 10.2-3 and Figure 10.2-4 for the 6 and 8-passenger respectively. The C.G. can be seen relative to the aircraft's neutral point. This distance, static margin, is used for determining the stability of the aircraft. Figure 10.2-1 and Figure 10.2-2 display the center of gravity location on the aircraft's side view while the aircraft is fully loaded.

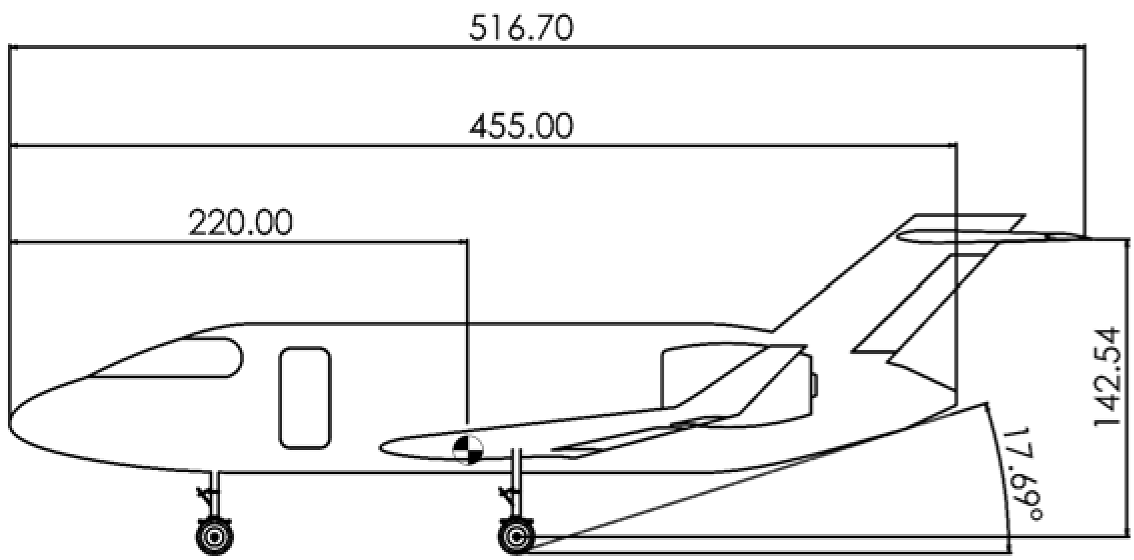

Figure 10.2-1 Center of Gravity Location: 6-Passenger

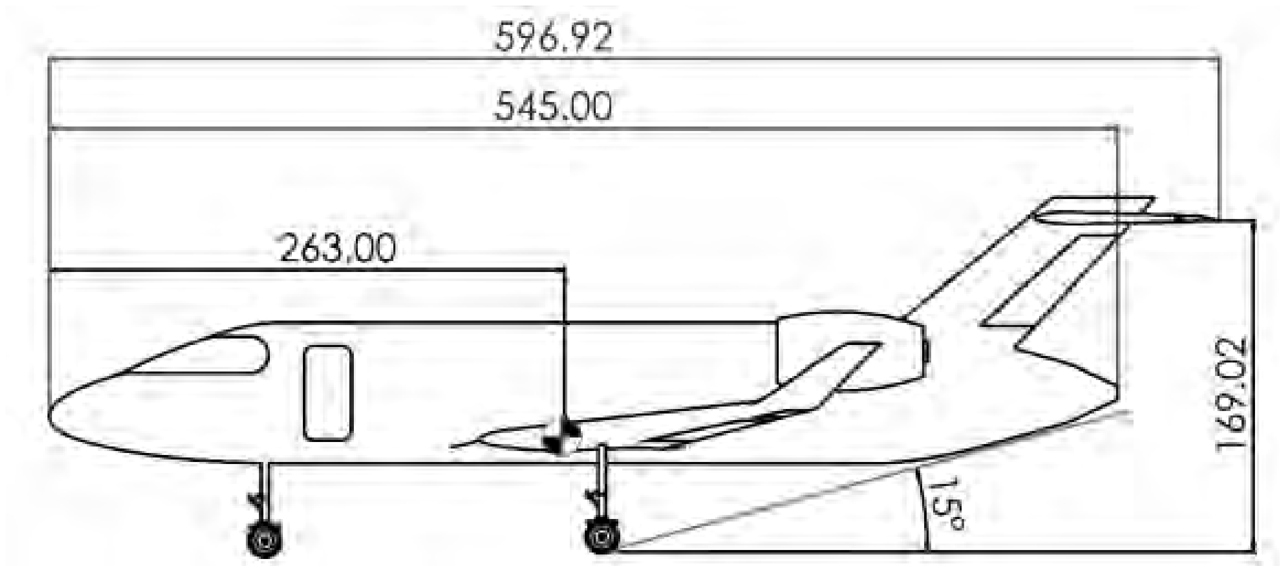

Figure 10.2-2 Center of Gravity Location: 8-Passenger

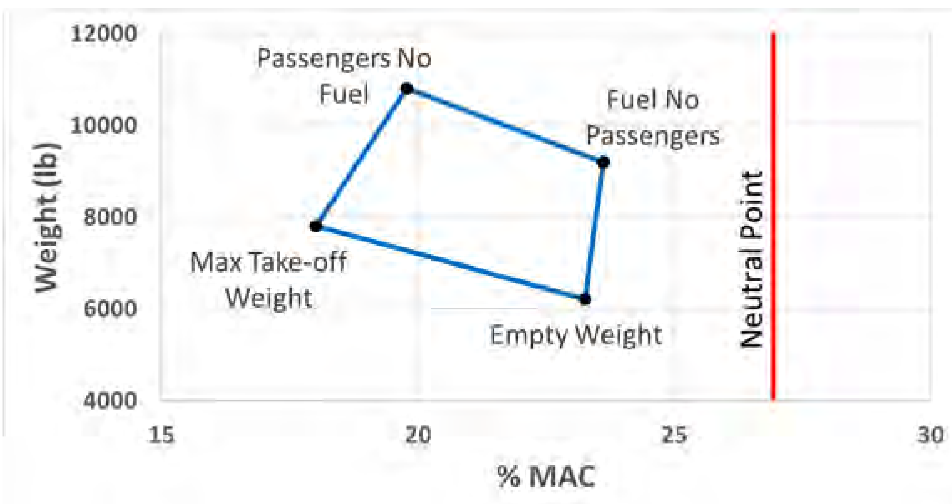

Figure 10.2-3 Center of Gravity Travel: 6 Passenger

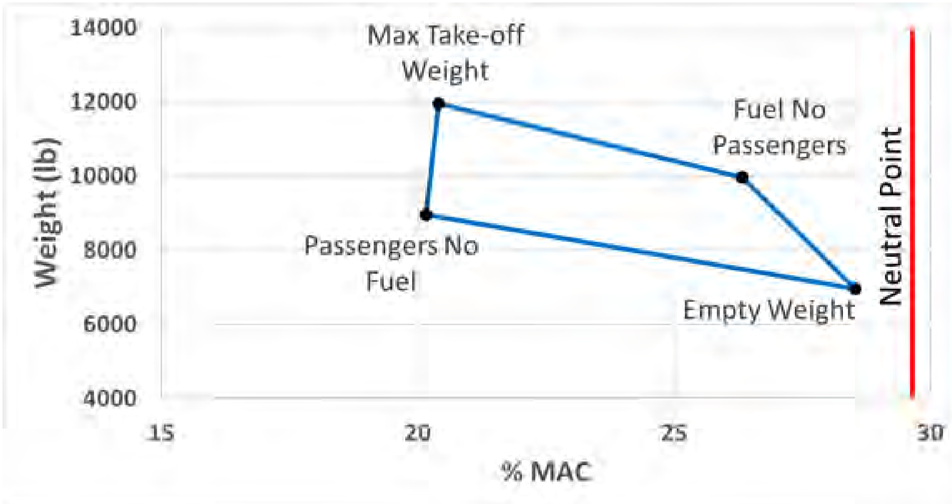

Figure 10.2-4 Center of Gravity Travel: 8 Passenger

11.0 Material Selection

During the initial conceptual design stages, the materials considered for the PFS-1000 were composite materials and conventional aerospace grade aluminum. The idea of composites lowering the Total Gross Takeoff Weight was very favorable in decreasing fly away costs. However, due to the complications of cost and time, composite materials were no longer in consideration and aerospace grade aluminum was the material selected. By choosing the conventional aerospace grade aluminum, the PFS-1000 will be cheap and reliable. The following section goes into which materials was used for the wing and fuselage structure.

12.0 Structural Analysis

12.1 V-n Diagram

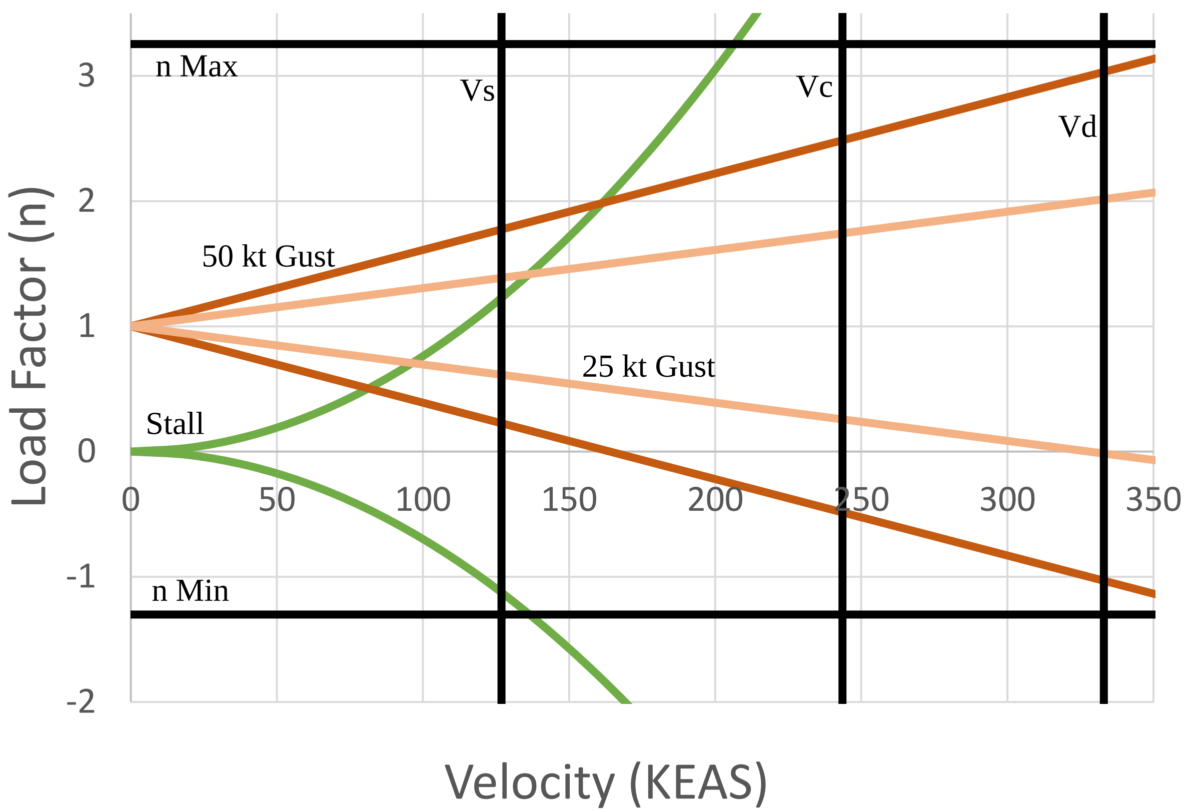

Figure 12.1-1 V-n Diagram for 6-Passenger Model

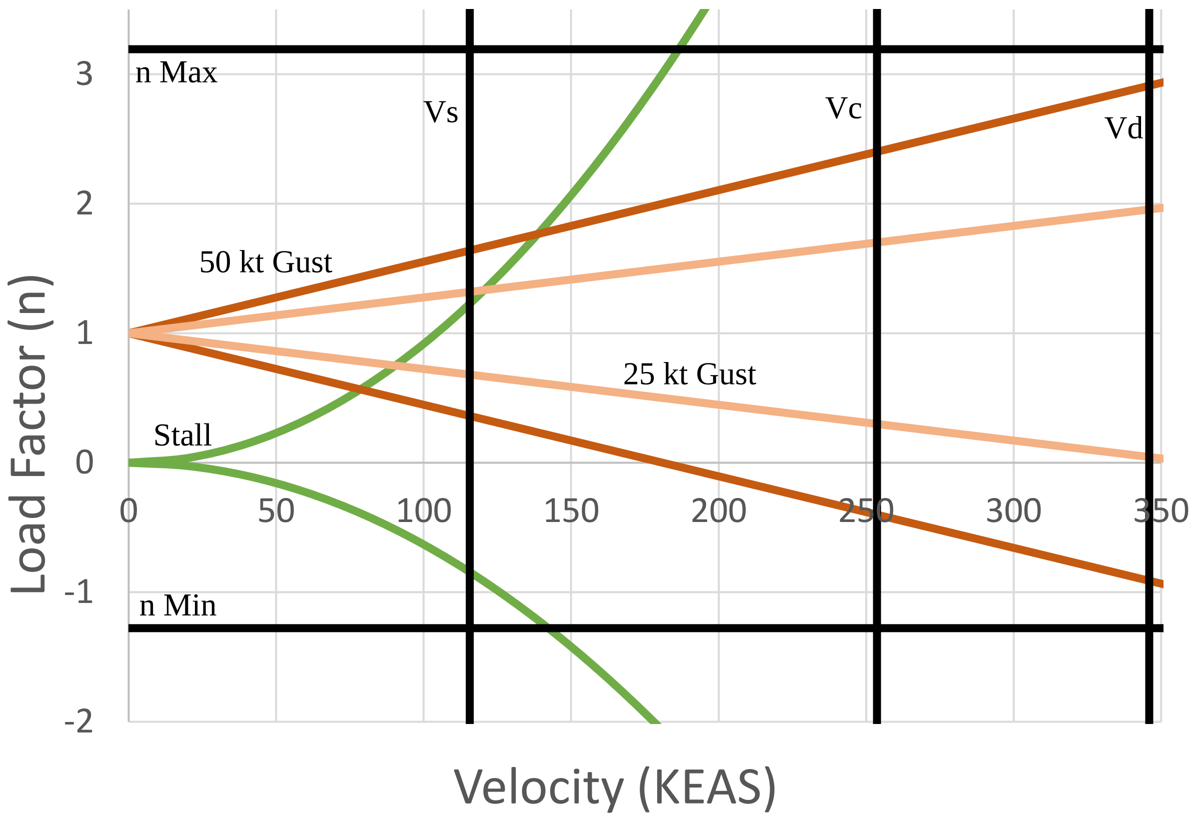

Figure 12.1-2 V-n Diagram for 8-Passenger Model

To begin the structural analysis of the PFS-1000, a V-n diagram was made. The Federal Aviation Regulation (FAR) Part 23 criteria was used for the 6-passenger variant. The FAR Part 25 criteria was used for the 8-passenger variant. The design speed for stall, cruise, dive, maximum gust intensity are shown in Figure 12.1-1 for the 6-passenger variant and shown in Figure 12.1-2 for the 8-passenger variant.

The maximum positive and negative load factor for the 6-passenger variant was 3.25 and -1.30, respectively. The maximum positive and negative load factor for the 8-passeneger variant was 3.19 and -1.28, respectively. Since the 6-passenger variant experiences a heavier load, the maximum positive load factor of 3.25 was used for the structural analysis of the wing. Note, this is a conservative approach on sizing both variants with the larger maximum positive load factor.

12.2 Wing

To accurately analyze the structure on the PFS-1000 wing, the span wise lift distribution was obtained using three methods. Two of the three methods were Schrenk's approximation of a span wise lift on a trapezoidal wing and on an elliptical wing. The last method used was the span wise lift on an elliptical wing from Reference [10]. The span wise lift was plotted against the span with Microsoft Excel and is shown in Figure 12.2-1. The average of all three methods was used to proceed with the shear and bending moment diagrams of the wing, which is shown in Figure 12.2-2.

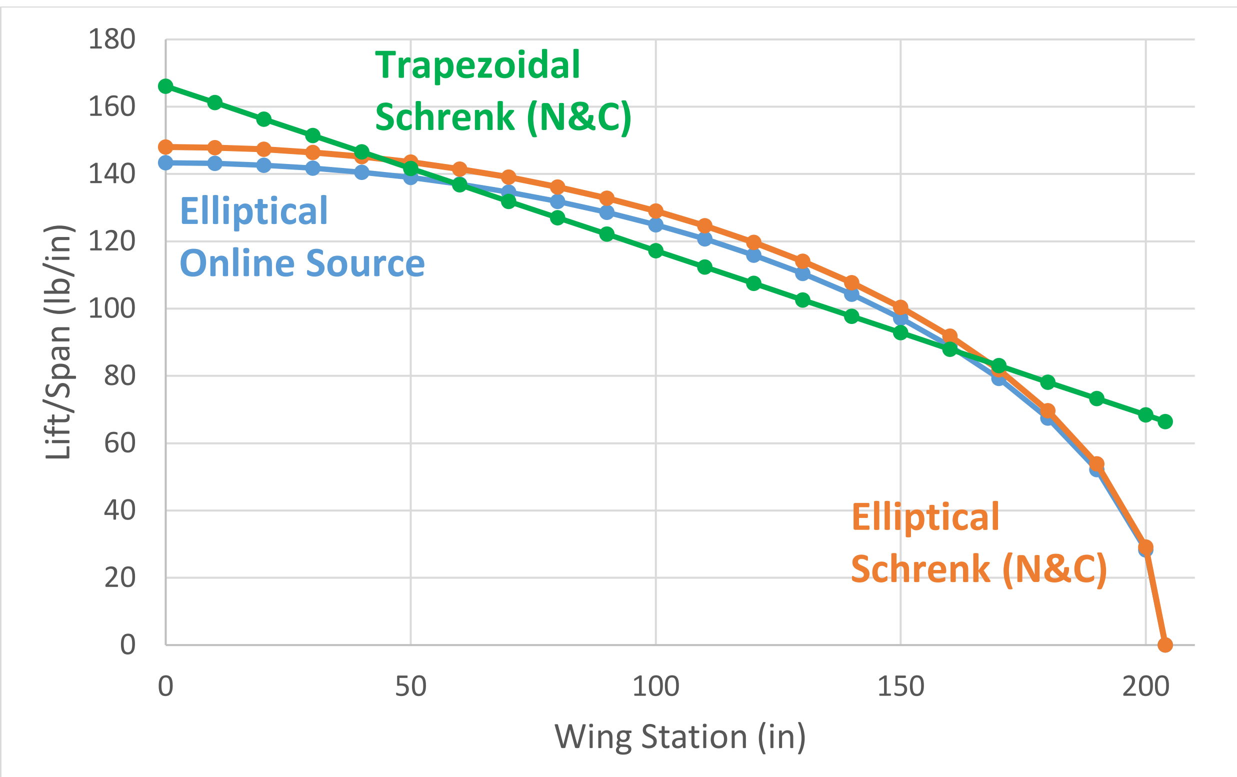

Figure 12.2-1: Various Lift Distribution

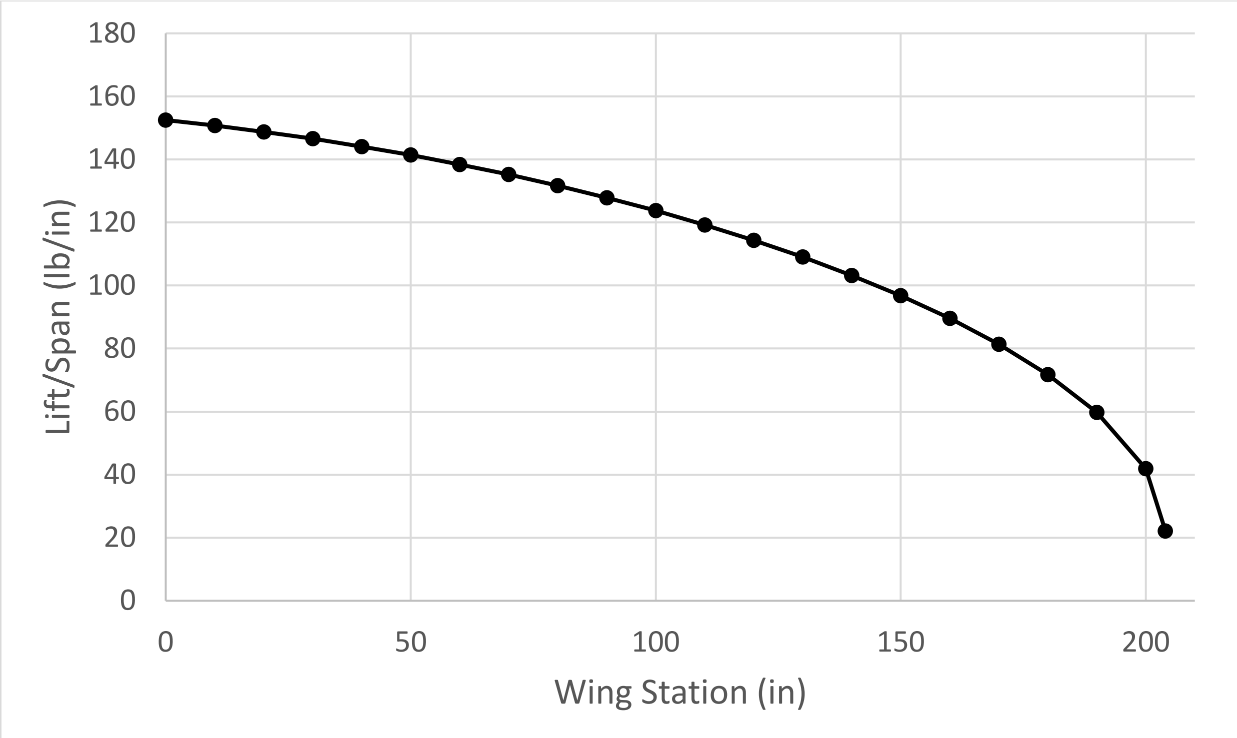

Figure 12.2-2: Average Lift Distribution

To proceed with the shear and bending moment, non-structural mass was included in the calculations. Since not all the fuel fit inside the wing box, the remaining 1000 pounds of fuel fit in the first 4 feet span from the root of the wing. Also, about 200 pounds of hydraulic system and fuel system weight was distributed across the entire span of the wing. By counteracting the approximated wing weight and the non-structural mass mentioned with the average span wise lift, the shear and bending moment diagrams were plotted and are shown in Figures 12.2-3 and 12.2-4, respectively.

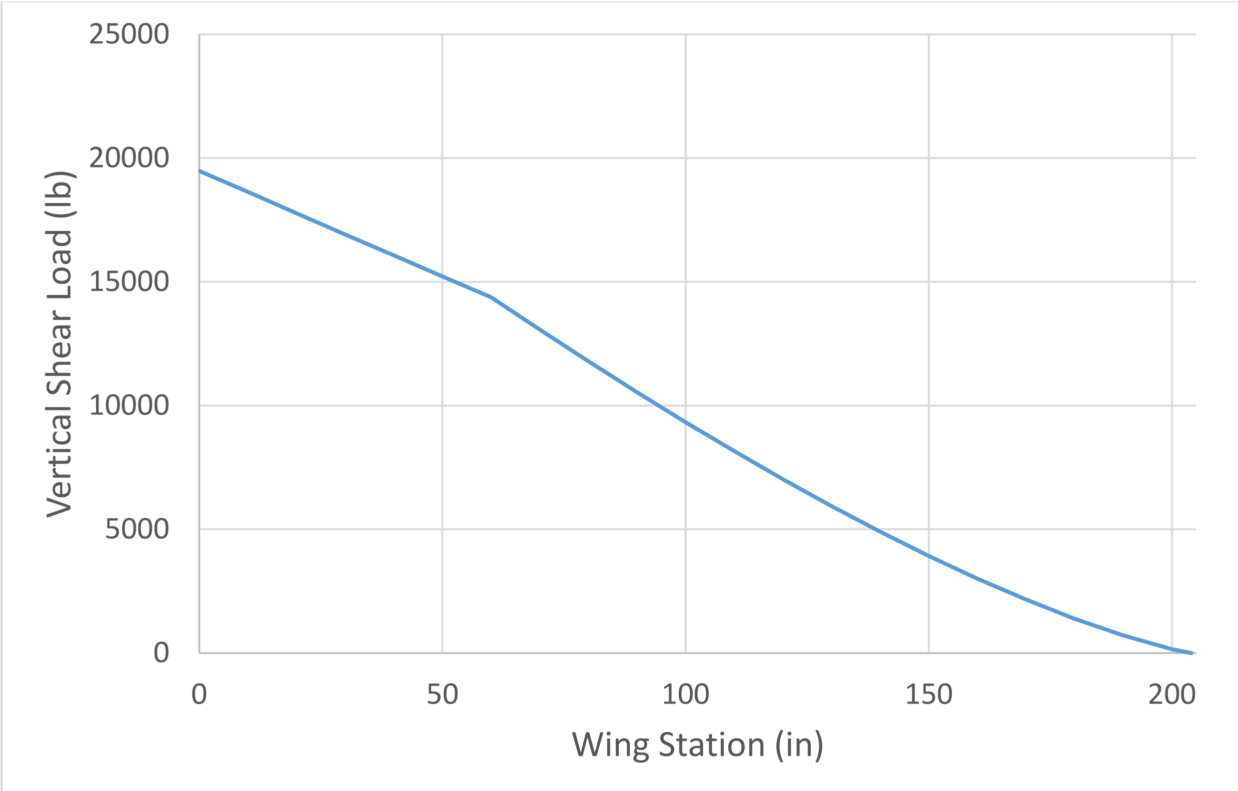

Figure 12.2-3: Spanwise Shear Loading of Wing

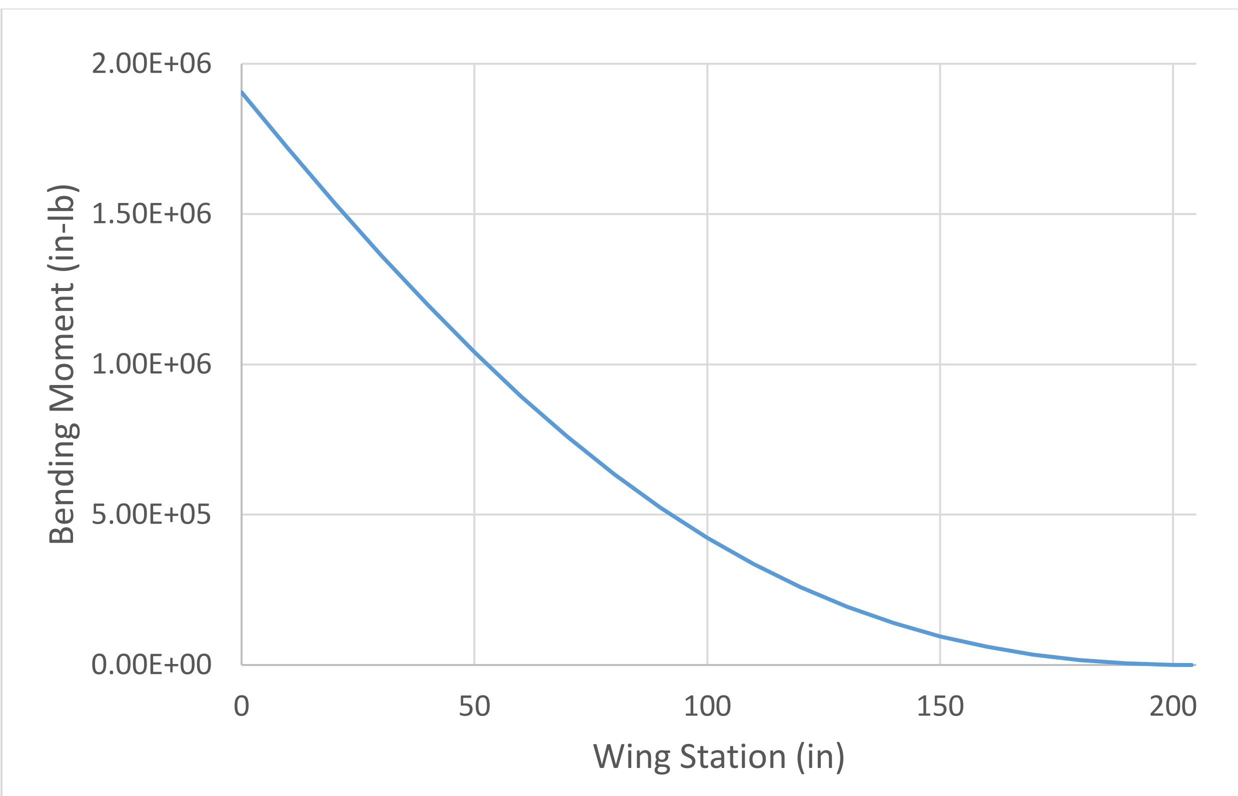

Figure 12.2-4: Bending Moment of Wing

By using the bending moment at the root of the wing, the spars of the wings were sized. The material used was Aluminum 7075-T6, which has an Ultimate Tension Allowable of 70 ksi, a Yield Compressive Allowable of 62 ksi, and a density of 0.102 lb/in^3. The load applied for the root of the wing for both spars was 190,654 pounds in both tension and compression. The factor of safety of 1.5 was used to solve for the ultimate load. This value was used to solve for the area of the top and bottom spar caps by dividing the ultimate load by the yield compression allowable and the ultimate tension allowable, respectively. The total area of the spars was found by adding the web area to the top and bottom spar caps areas, which was then used to find the total volume of both spars. The total volume was used to find the total weight of both spars. Table 12.2-1 displays the results of the procedure for spar sizing.

Table 12.2-1: Spar Dimensions

	Bottom Spar Cap Area (in^2)	**Top Spar Cap Area (in^2)**	**Web Area (in^2)**	**Total Area (in^2)**	**Total Volume (in^3)**	**Total Weight (lb)**
Front Spar	3.06	2.31	5.00	10.37	2114.76	215.71
Aft Spar	1.02	0.77	2.00	3.79	773.19	78.87

Note, this is a conservative estimate of the Total Weight of the spars. The taper of the wing was not accounted for in this procedure. Due to the taper of the wing, the total area of the spar will decrease as a function of span. However, in this procedure, the total area was approximated through the entire span of the wing, which make the spars oversized and overweight but easier and cheaper to manufacture.

The ribs of the wing were spaced at 2 feet apart and sized to be 0.75 inches thick. There was a total of 13 ribs modeled in the PFS-1000 wing to withstand any type of loading that the aircraft will experience. In Figure 12.2-5, the internal structure of the PFS-1000 wing is shown with the dimensions and spacing determined through the sizing procedure.

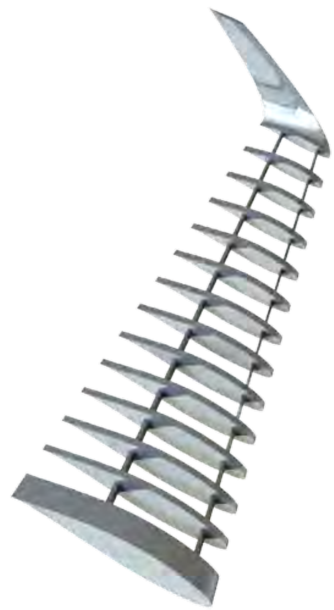

Figure 12.2-5: Internal Structure of Wing

12.3 Fuselage

The trade study between a fuselage with windows versus a fuselage with no windows was conducted by comparing the total weight of each panel with or without windows. The components of the fuselage that were modeled for this study were the skin, stiffeners (hat section), the frames, and the windows.

In Figure 12.3-1, the fuselage internal structure is shown with windows along with the cross section of a portion of the fuselage. The materials, thicknesses, and cross sectional area for each component is shown in Table 12.3-1.

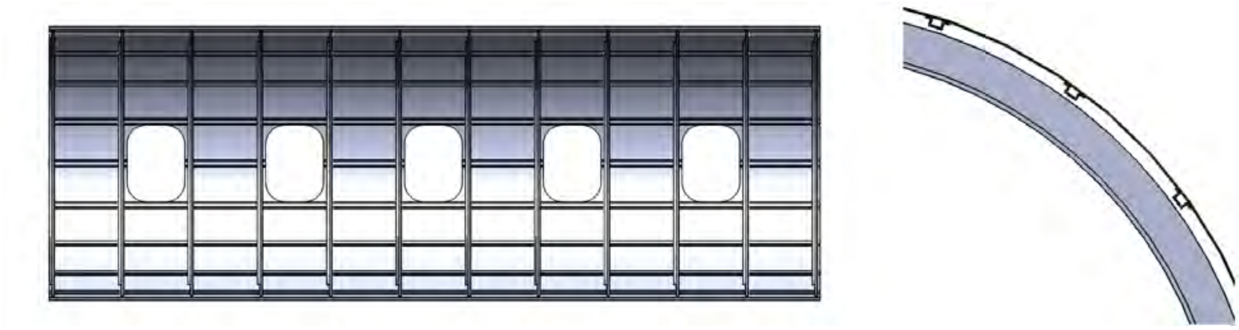

Figure 12.3-1: Internal Structure of Fuselage

Table 12.3-1: Fuselage Structure Component Characteristics

Structure	Material	Thickness	Cross Sectional Area
Skin	2024-T3 Al	0.063 in	--
Stiffener (Hat Section)	7075-T6 Al	0.1 in	0.28 in^2
Frame	7075-T6 Al	0.125 in	0.6 in^2
Window	Plexiglass	0.577 in	1.26 in^2

To account for the reinforcement of structure due to the stress concentration that the window carries, the components of the fuselage near the window were thicker in size or increased in area. Figure 12.3-2 displays the breakdown of sizing procedure and how it is going to be analyzed. The skin panel was three times thicker in the green region, two times thicker in the red region, and normal thickness in the blue region. Likewise, the stiffeners increased in area by three times in the green region, two times in the red region, and normal area in the blue region. Lastly, the cross-sectional area of the window was added to the area of the frame. By solving for the respective volumes, the total weight for the panel in between the two frames, highlighted in Figure 12.3-2, was estimated using the density of the respective materials and the additional weight for the window.

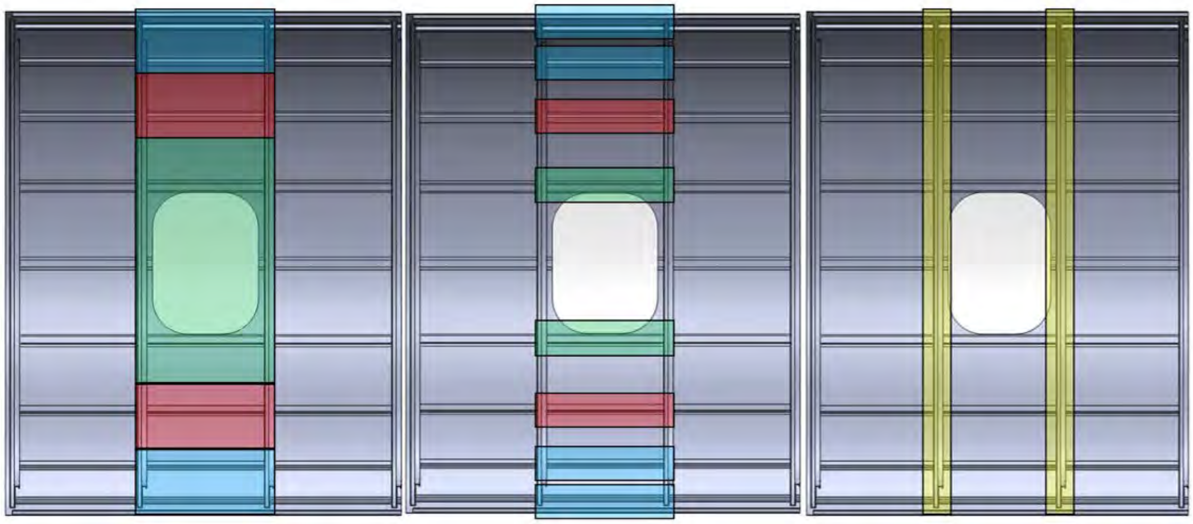

Figure 12.3-2: Breakdown of Fuselage for Analysis – Skin Panel, Stiffener, Frame

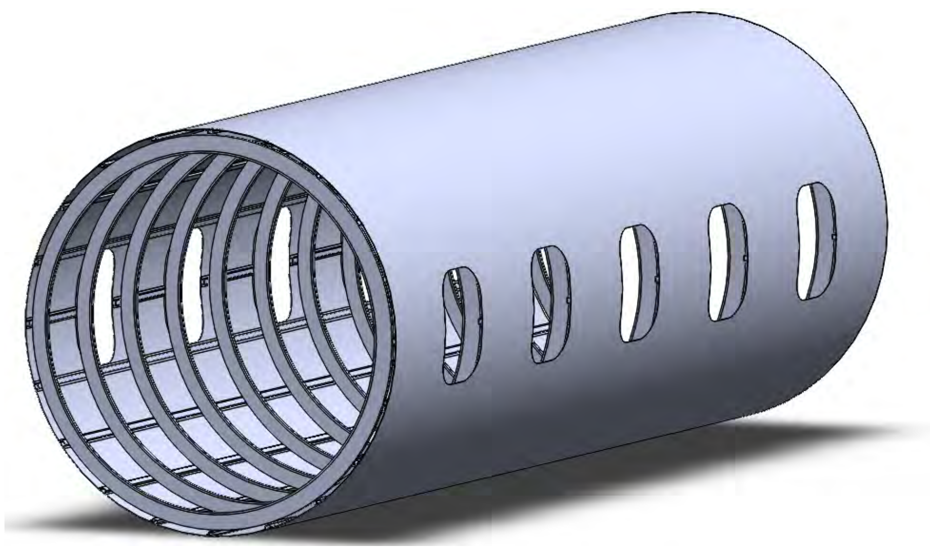

Figure 12.3-3: Fuselage with Windows

Due to the absence of windows in the window-less design, the weight calculation was straightforward and did not require an accounting for stress concentration. It was not necessary to reinforce the fuselage with additional structural weight. The normal dimensions, as provided in Table 12.3-1, were used to solve for the total weight of the area in between the two frames of the window-less fuselage. The weight of the TV, electronics, and camera were also added into the total weight of the panel of the window-less fuselage.

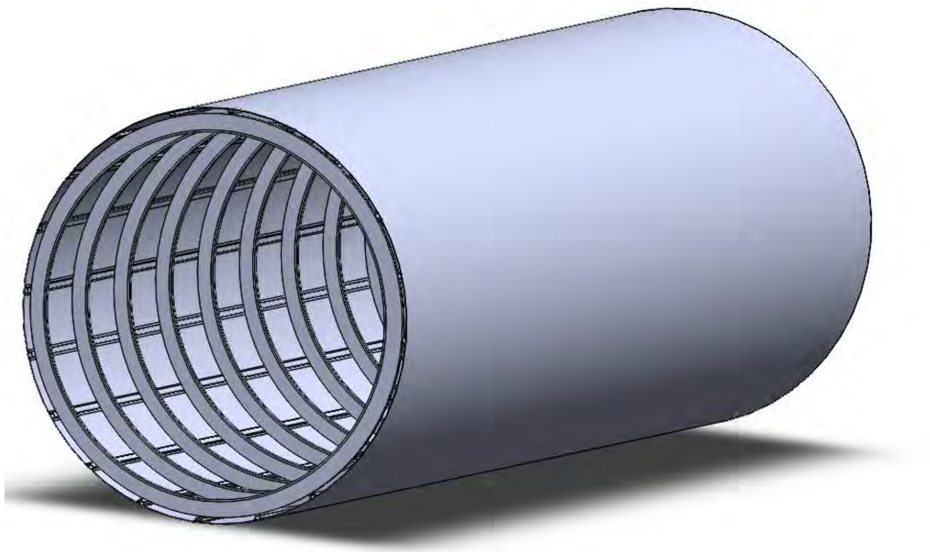

Figure 12.3-4: Fuselage without Windows

The weight differences of the panel of the fuselage is shown for both the 6-passenger and 8-passenger variant. The total weight savings for the 6-passenger and 8-passenger, switching from windows to window-less, is 169 pounds and 219 pounds, respectively. The percent drop in total weight of the panel in between the two frames was about 28% for both the variants. The results are shown in Table 12.3-2 and 12.3-3.

Table 12.3-2: 6-seater Total Weight Savings

6 – seater (10 windows)	Total Weight
Windows w/ reinforced structure	592 lb
Window-less with TV	423 lb
Weight Savings	169 lb
% drop	28.46%

Table 12.3-3: 8-seater Total Weight Savings

8 – seater (13 windows)	Total Weight
Windows w/ reinforced structure	769 lb
Window-less with TV	550 lb
Weight Savings	219 lb
% drop	28.46%

With this, the PFS-1000 will be able to fly away at a substantially lower weight, which provides a lower fuel consumption rate. This will attribute to a lower fly-away cost for the customer. Not only will the Virtual Skyline give customers the luxury of flying, it will also give the customer unique control of the look and feel of the interior cabin.

13.0 Landing Gear

The PFS-1000 family of aircraft adopted the tricycle landing gear configuration. This design features two landing gear housed in the wings with an additional landing gear under the nose. A plane is created from a point that sits on the ground, ten degrees behind the center of gravity in the longitudinal direction. In addition, the landing gear location was confirmed to allow the plane to tip back 15 ° during takeoff. To determine the lateral location of the rear landing ears, the design had to consider gust forces and forces experienced during taxi. In addition, packaging was considered when placing the landing gear, both along the wing and in the nose. An approximate angle for this on similar aircraft is 25 ° [13]. The PFS-1000 Aircraft exceed this and place the landing gear at 33 °, and allows for more efficient packaging for the landing gear and fuel systems.

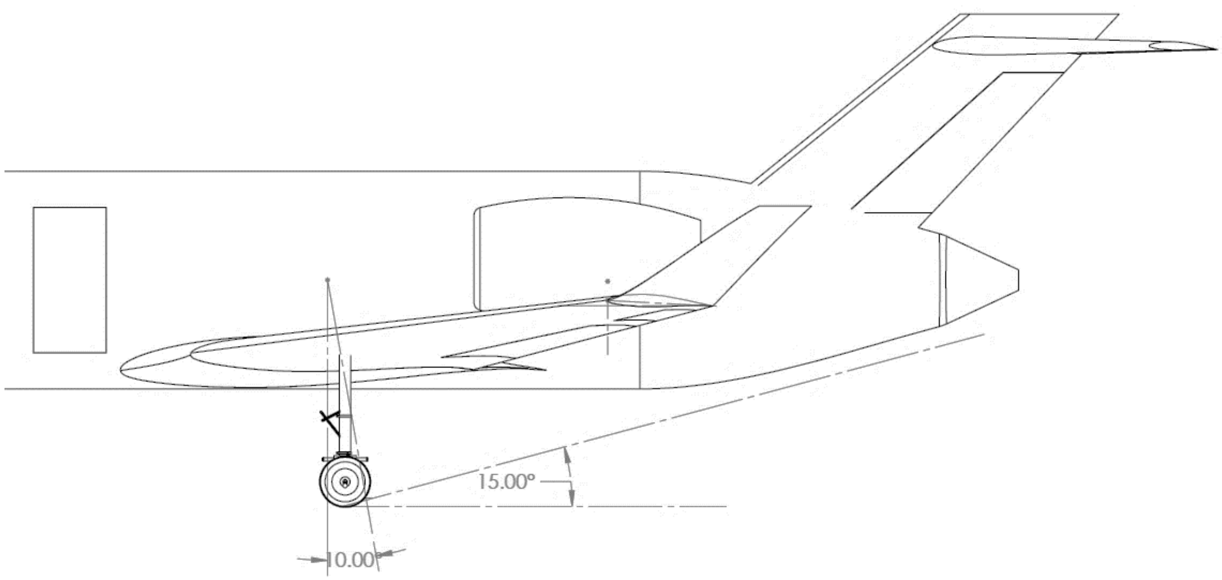

Figure 13.0-1 Landing Gear Placement and Tip-Back Angle

14.0 Fuselage Configurations

Due to the fuselage plug arrangement, both variants of the PFS-1000 family share identical fuselage cross sections. The fuselage has an outer diameter of 72 inches which is a size that offers a strong balance between passenger comfort and aircraft performance. The aisle width complies with the Federal Aviation Regulations and offers easy movement around the cabin.

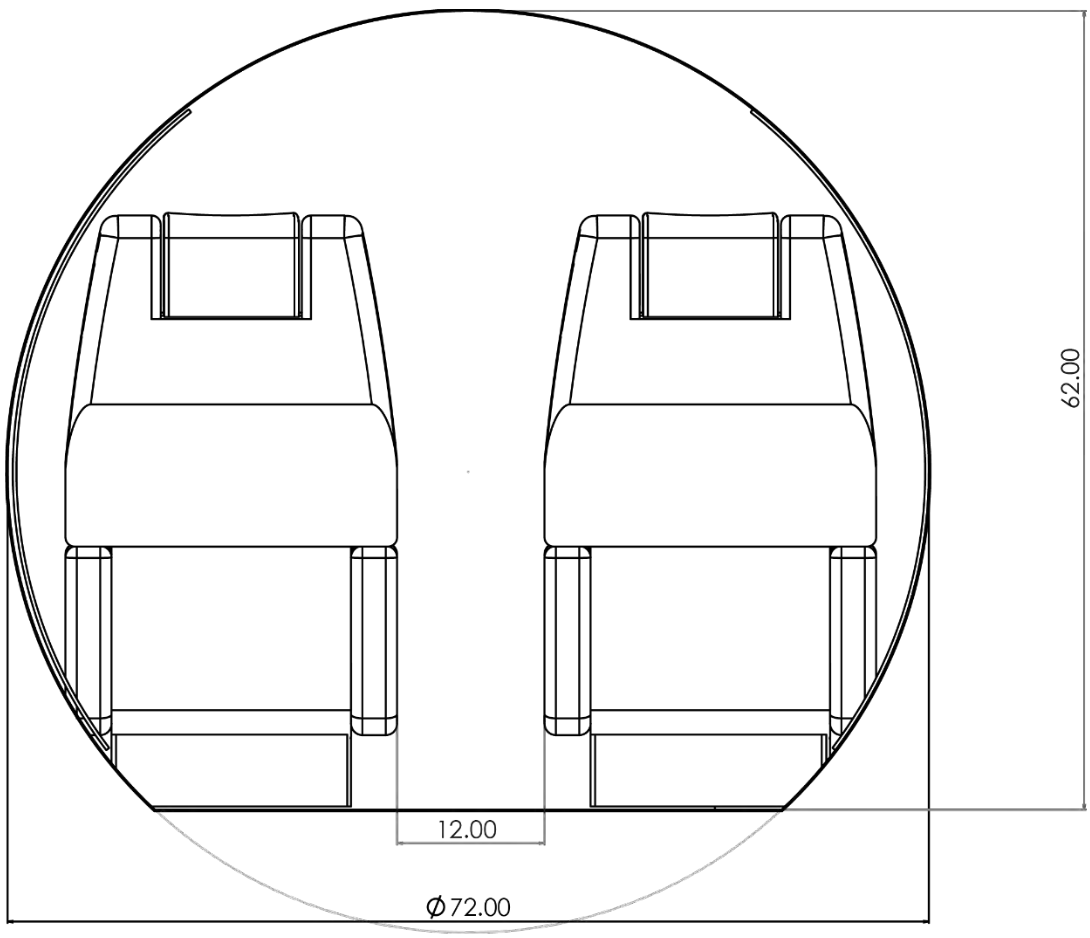

Figure 14.0-1 Fuselage layout and aisle view

14.1 Cabin Interior Layout

Premier Flight System's business jets are equipped with a luxurious interior that promotes productivity while in flight. Each passenger will have their own workstation and easy access to the virtual reality screens which line the inside of the aircraft's fuselage. Both the 6 and

8-passenger configurations contain 2 rows of comfortable seats which run along the length of the fuselage as well as a coffee maker, microwave, and toaster to keep sustain the passenger's productivity.

The 6-passenger aircraft has 1 row of aft facing seats, while the 8-passenger aircraft has all 4 rows of seats facing forward. An artist rendition of the cabin interiors of both the 6 and 8-passenger configurations with a mockup of the virtual reality skyline can be seen in Figures 14.1-1 and 14.1-3 respectively. A dimensioned interior layout for the 6 and 8-passenger layouts can be seen in Figures 14.1-2 and 14.1-4 respectively. All dimensions are in inches.

Figure 14.1-1: 6 Passenger Interior

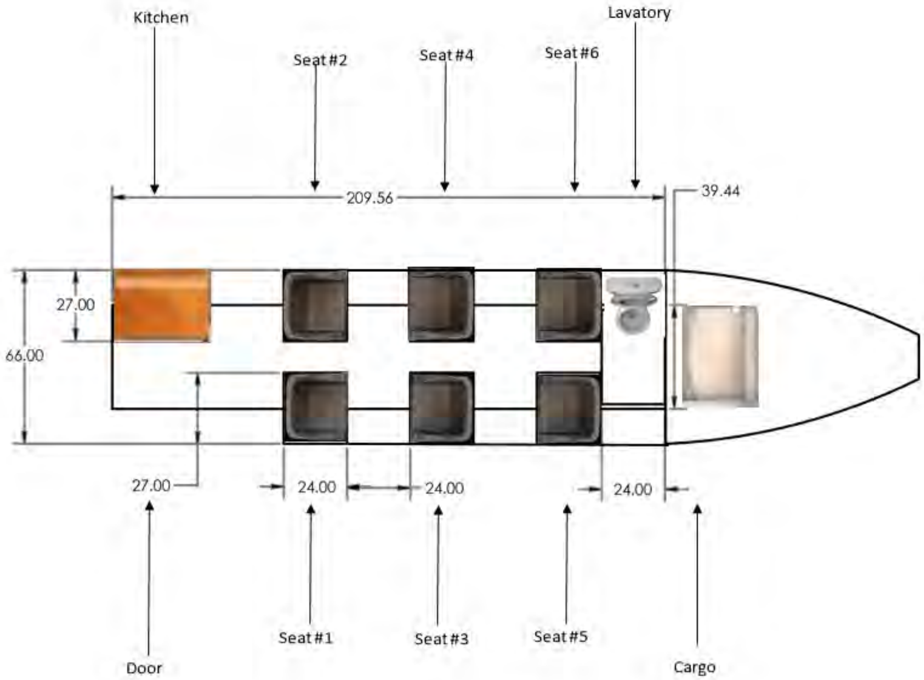

Figure 14.1-2: Dimensioned 6-Passenger Layout

Figure 14.2-3: 8 Passenger Interior

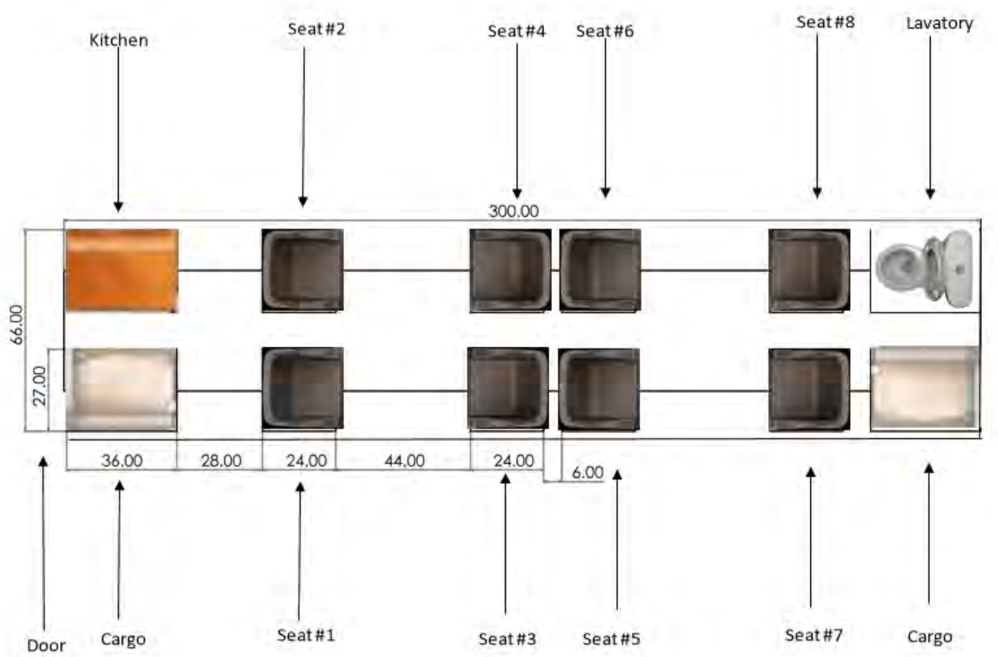

Figure 14.1-4: Dimensioned 8-Passenger Layout

14.3 TV's and Power

The virtual reality skyline configuration for the cabin interior will utilize several LG 65 in. OLED 4k televisions. These TVs are only 2.54 mm thick so they will not take up much space. For the 6-passenger configuration the TV weighs 84 lb; and the power draw is only 136-368 W based on the brightness settings. The TV's for the 6 Passenger will cost an additional $42,000 but this cost is offset due to the lack of bulkhead structure needed without windows. The weight of the 8-passenger TV's is 122 lb and the power draw is only 198-536 W based again on the brightness settings. Overall the TV cost per aircraft for the 8-passenger will be $61,200. These prices are expected to drop as technology advances and OLED 4k TV's become readily available in future years. A summary of the TV weights, power draw, and costs are presented in Table

14.3-1 and a visual representation of the Virtual reality skyline can be seen in figures 14.1-1 and 14.1-3.

Table 14.3: Virtual Skyline Equipment

	6 Passenger	8 Passenger
Weight	84 lb	122 lb
Power Required	136-368 W	198-536 W
Cost	$42,000	$61,200

15.0 Subsystems

15.1 Fuel

Utilizing the Breguet Range equation, the requirements with a 2500 nmi range at maximum payload (100 nmi alternate), yielded the required fuel weight for both the 6 and 8-passenger aircraft. Jet A-1 fuel has a density of .4838e-5 to .5244e-4, depending on altitude. The 6 and 8-passenger aircraft fuel weights and volumes can be seen in Table 15.1-1. Their respective tank locations, are found in Figure 15.1-1 and Figure 15.1-2. Tank 1 is the largest tank and is located in the wing box. Tanks 2 and three are in the port and starboard wing respectively. This tank is identified as "Tank 2-3" in the table. The 4th and 5th tanks are the furthest from the fuselage, and the smallest tanks.

Table 15.1-1 Fuel Sizing for 6 and 8 Passenger

6 Passenger

	Tank 1	**Tank 2-3**	**Tank 4-5**
Weight (lb)	982.66	299.65	149.83
Volume(ft^3)	20	6	3

8 Passenger

	Tank 1	**Tank 2-3**	**Tank 4-5**
Weight (lb)	982.66	599.31	399.54
Volume(ft^3)	20	12	8

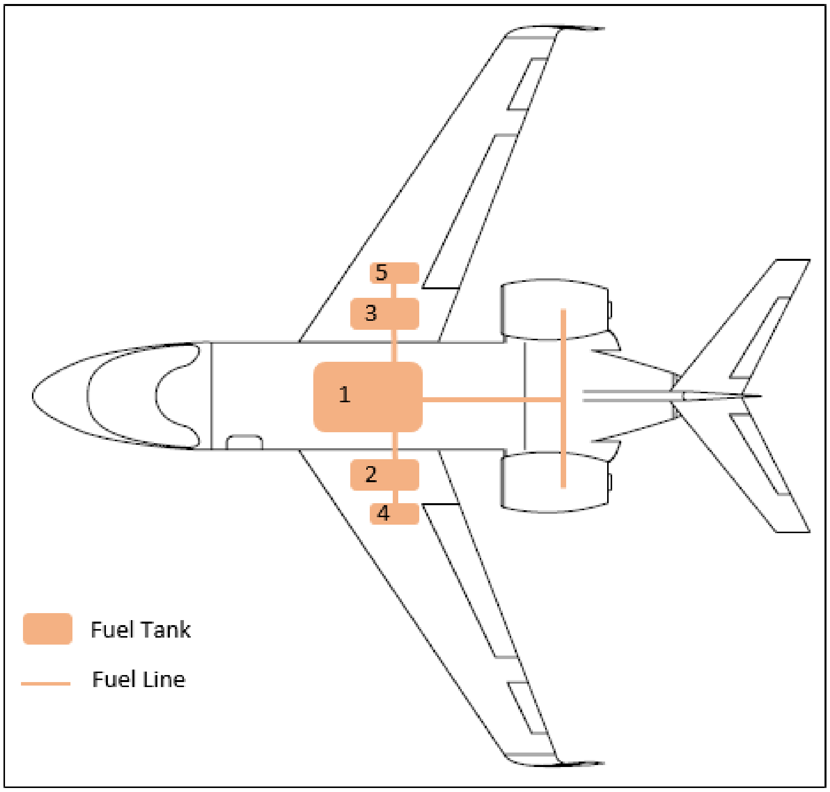

Figure 15.1-1 Fuel Tanks: 6 Passenger

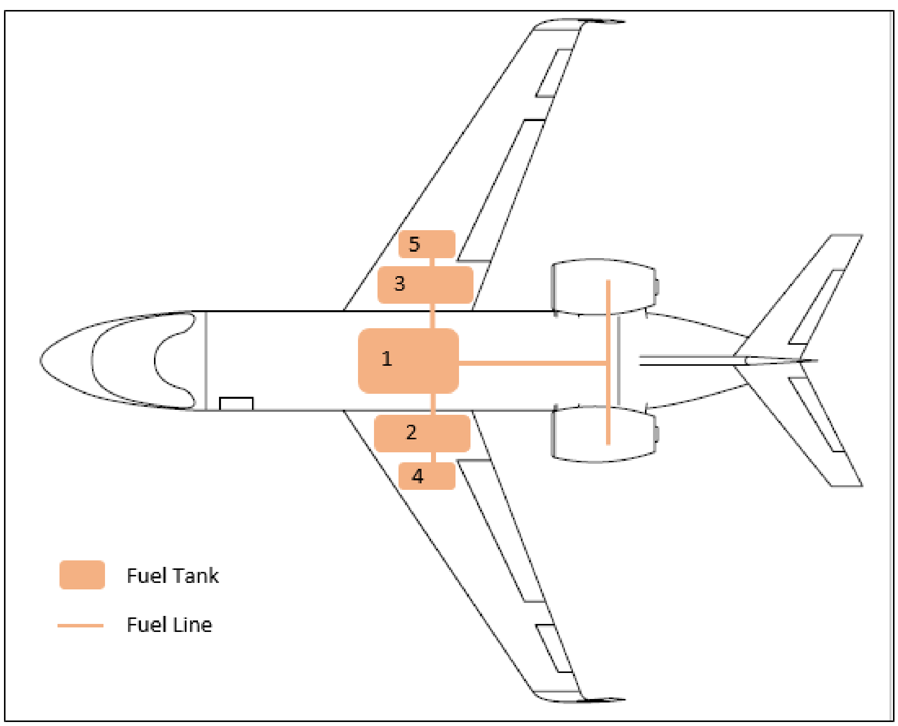

Figure 15.1-2 Fuel Tanks: 8 Passenger

15.2 Hydraulics

The hydraulic system layouts can be seen in Figure 15.2-1 and 15.2-2. The system was designed to provide hydraulic power to all necessary areas in the most weight effective manner. There are also redundancies built into the system. The two engines are connected to the main pumps for the system, with a redundant pump on the Auxiliary Power Unit (APU). The main reservoir is found in the aft of the aircraft, near the pumps, with two smaller tanks near the wings of the aircraft. Because of the commonality approach, all the control surfaces and landing gear are consistent for the two aircraft. So, the hydraulic system was sized for one of them, and stays consistent for the other. Therefore, the layouts for both aircraft are the same, with the lengths of the lines changing to make up for the added length in fuselage.

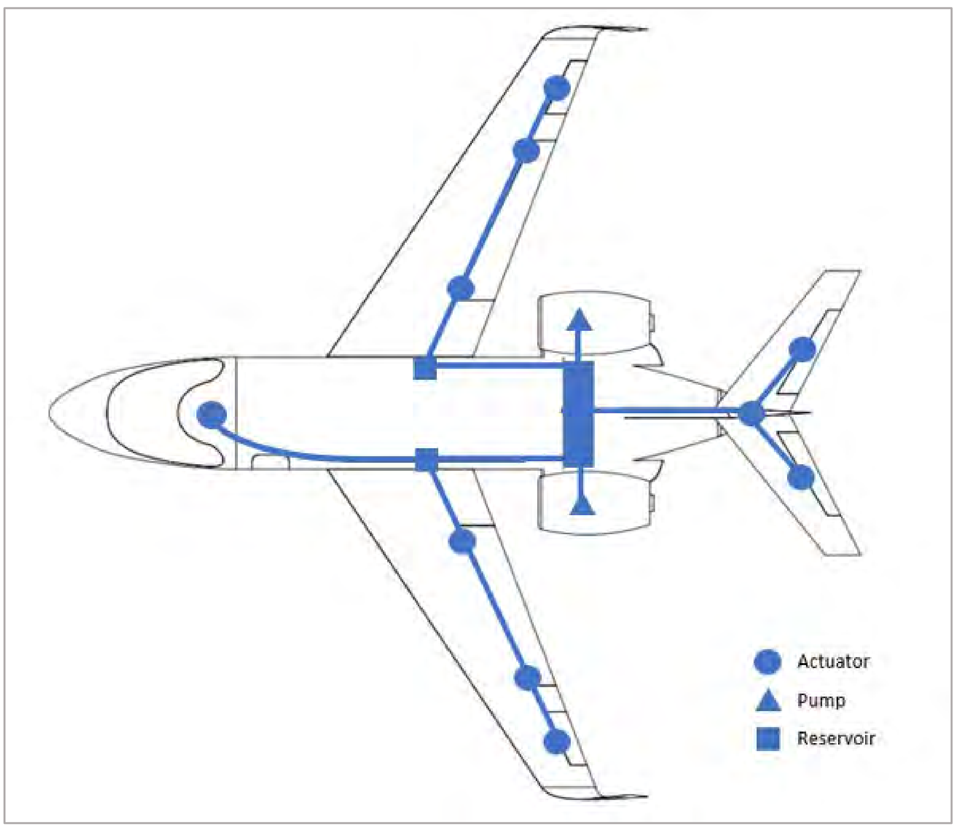

Figure 15.2-1 Hydraulic System 6-Passenger

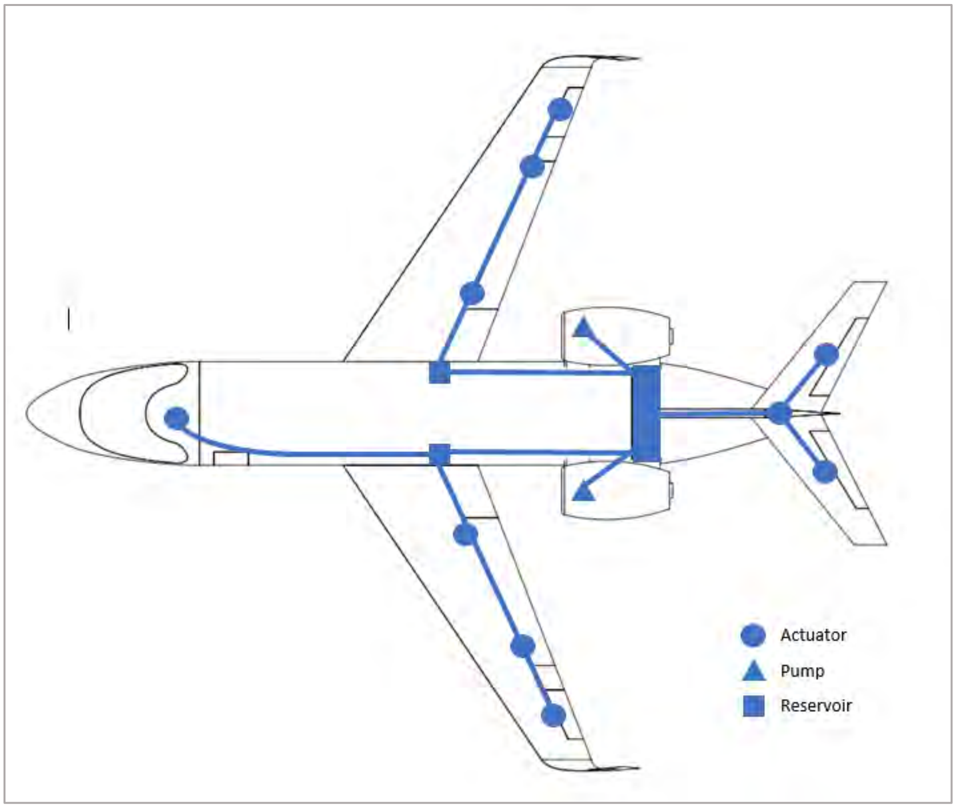

Figure 15.2-1 Hydraulic System 8-Passenger

15.3 Auxiliary Power Unit

The Auxiliary Power Unit that was selected to conform to FAA regulations as well as satisfy the requirements is the Honeywell HGT400. The driving requirement in the APU selection, besides conforming to regulations, is that it will be able to provide full utility power to the aircraft as it sits on the ground without use of the main engines. Utility power includes power to environmental control, cockpit operations, and full use of all cabin accessories while the aircraft is at rest. Therefore, the aircraft's cabin LCD screens will be fully powered as the passengers walk onto the aircraft. The aircraft will be a comfortable and a functioning workspace without requiring the main engines to run. Located towards the aft end of the aircraft for both the 6 and 8-passenger, the APU provides these mentioned capabilities as well as the engine starting.

15.4 Electrical Subsystem

The electrical schematic for the aircraft can be seen in Figure 15.4-1 below. The APU that was selected above in section will be located in the aft end of the fuselage. The rest of the electrical subsystems are comprised of a generator on each engine. The APU will allow the aircraft systems to be powered with the engines off while sitting on the tarmac.

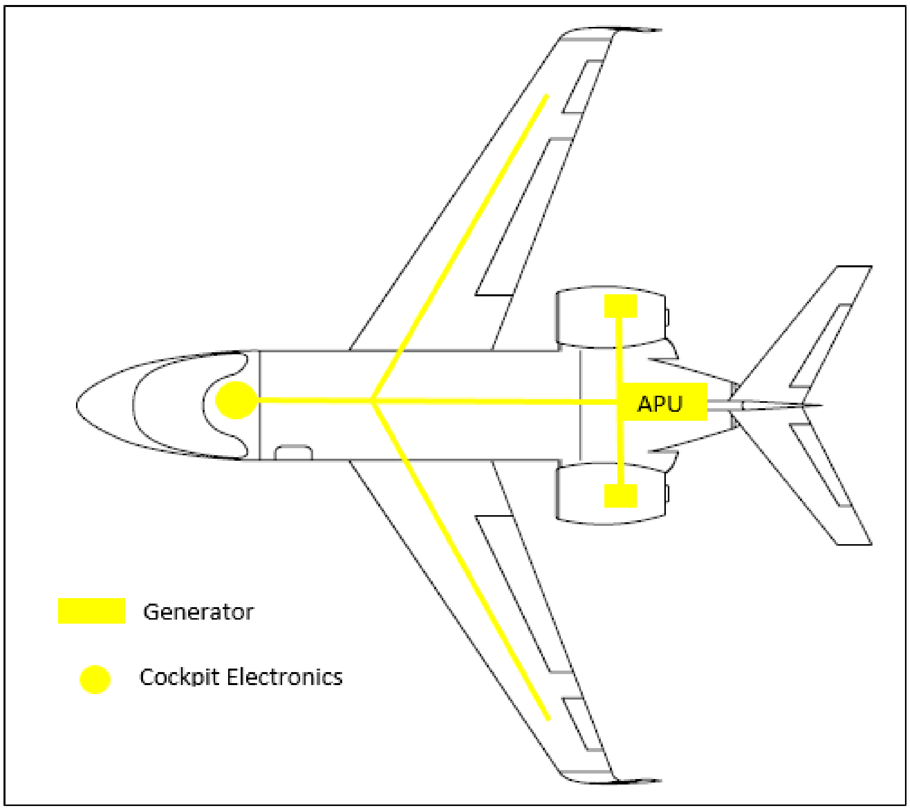

Figure 15.4-1: Electrical Schematic: 6 Passenger

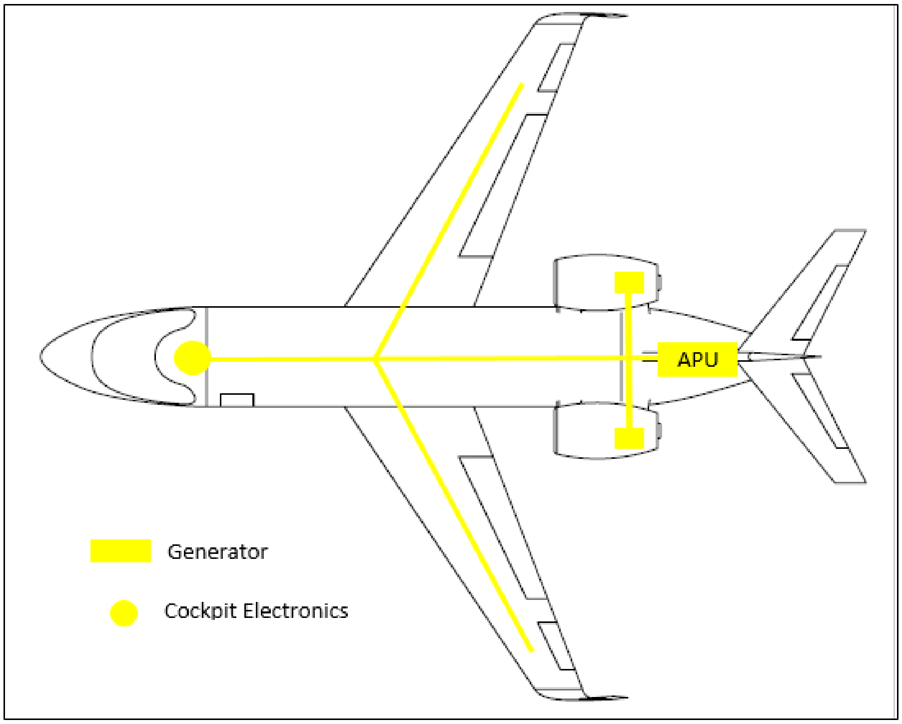

Figure 15.4-2: Electrical Schematic: 8 Passenger

15.5 Environmental Control Systems (ECS)

A very important feature of business jets is to have a comfortable cabin for the passengers, which requires the cabin to pressurized and air conditioned. In order to comply with the FAR regulation part 25§841, the cabin altitude will be held at 8,000 ft at the maximum cruise altitude of 35,000 ft, for the greatest passenger comfort. As a failsafe for cabin depressurization there will be an oxygen mask in the armrest of each seat, so each passenger will have their own supply of oxygen.

The ECS will also contains filters which will filter the air of any pollutants which may be harmful to the passengers as well as a dehumidifier to keep the cabin at a comfortable humidity level.

16.0 Commonality Analysis

Analysis on the commonality between the 6 and 8 passenger aircraft is a defined objective in the AIAA RFP requirements. The objective reads that the structure and components of the empty weight aircraft, not including engine, must be of 70% commonality by weight between the two variants. In the design philosophy, the requirement was exceeded. By increasing the commonality between the aircraft, the cost of design, manufacturing and maintenance was reduced significantly. To keep commonality as high as possible, a part would be designed so that it would work for both variants. This means that some parts were overdesigned, and the trade was a reduction in performance for the variant using a part not designed specifically for it. However, by finding a balance in these trades design teams were able to effectively design the aircraft and keep commonality high. Examples of these design trades can be seen in the larger components; wing design, engine selection (not included in commonality by RFP requirements), tail design, fuselage, and landing gear. The smaller components were easy to design for both aircraft. These larger components had to be designed for the more restraining aircraft, and so, were over designed for the less restraining aircraft. For example, the wings were sized for the larger heavier 8 passenger variant, and then the tail designed for the shorter moment arm on the 6 passenger variant. The engine, although not included in the commonality calculation, was selected for the 8 passenger variant. Thus making the 6 passenger more expensive because of “over engineered” wings and engine. So, the next trade that must be done is to make sure that this initial extra expense is worth what the commonality brings the company in manufacturing and maintenance. These trade conclusions lead design teams to accept these commonality trades, increasing the value in the commonality analysis. The table below shows the commonality, including some of the larger components to make such a high percentage possible.

Table 16.0-1 Commonality Analysis

	6 Passenger(lb)	8 Passenger(lb)	Difference(%)	
Propulsion System	1200.0	1200.0	0.0	
Wing/Tail	997.0	997.0	0.0	
Empennage	243.0	243.0	0.0	
Fuselage	777.0	934.0	16.8	
Nacelle	176.0	176.0	0.0	
Landing Gear	450.0	450.0	0.0	
Fuel System	213.0	250.0	14.8	
Avionics	235.0	235.0	0.0	
Surface Controls	231.7	231.7	0.0	
Hydraulic System	105.0	115.0	8.7	
Electrical System	471.5	480.5	1.9	
ECS	274.5	280.0	2.0	
Anti Icing	130.0	130.0	0.0	
Cabin Amenities	784.0	944.0	16.9	**Commonality**
Dry Weight	6287.7	6666.2	5.7	**94.3%**

17.0 Manufacturing

The overall manufacturing flow for the aircraft family is shown in Figure 17.0-1. The steps are simplified to utilize the ease of a bottom to top manufacturing process. The process brings the individual components together in smaller assemblies in process 1 and 2, then these assemblies are combined into the final product during process' 3 and 4. Processes 5 and 6 are to ensure that the aircraft are functioning 100% properly and meet stringent quality requirements. Along with the final system test and quality control check, there will be periodic QC inspections. Once the aircraft have been deemed of the highest quality they then are prepared for delivery and shipped to the final destinations.

Some assemblies will be produced by subcontractors which are highlighted below in gray boxes in Figure 17.0-1, will then be delivered to PFS-1000 for the final integration into the aircraft. The rest of the components will be manufactured in house to save on shipping costs, which in turn can be passed on to the customer.

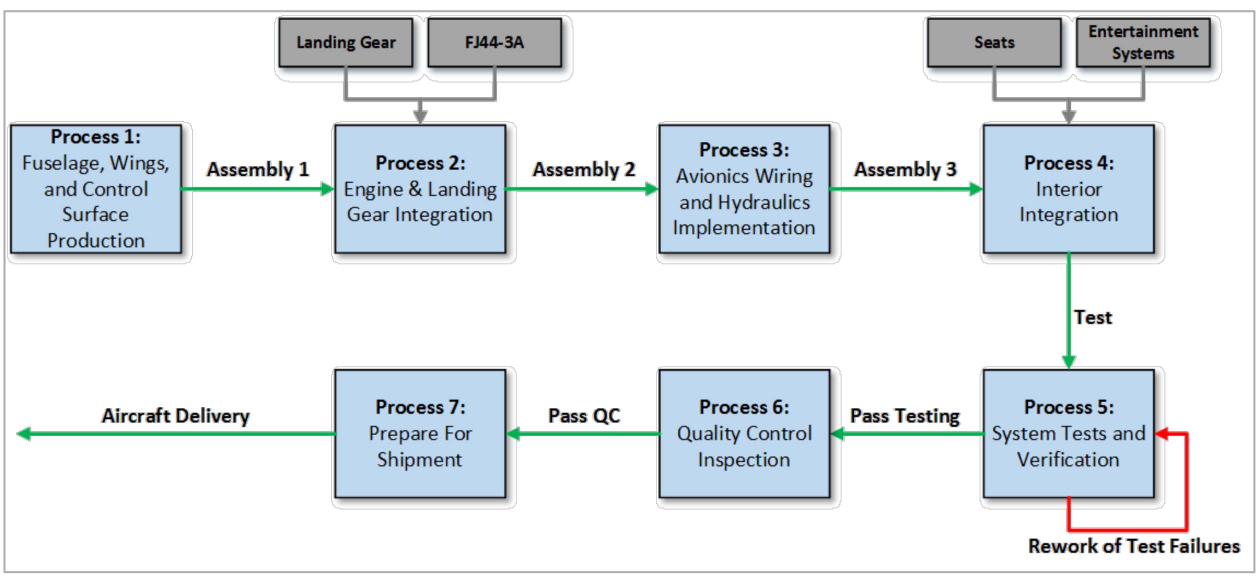

Figure 17.0-1: Manufacturing Process Flow

The initial program plan for manufacturing is to be able to manufacture 5 aircraft a month, alternating between the 6-passenger and 8-passenger configurations. At this rate PFS-

1000 plans to manufacture 360 aircraft in the first 6 years of production, 180 of each configuration.

18.0 Maintainability

The suggested maintenance schedule for all aircraft will follow the Material Steering Group MSG -3 schedule which consist of 4 maintenance check categories, and the MSG-3 program has been successful for many years in both civilian and military application. The MSG-3 program consists of A, B, C and D maintenance checks which are all conducted at different time intervals based on the number of flight hours. “A” checks are a light check which are carried out usually after every 20 flight cycles and consists of a brief inspection to ensure everything is functioning properly. A flight cycle is defined as a takeoff and landing. “B” Checks are another light check which is conducted every 3 months regardless of the aircraft’s flight cycles but B checks also include the replacing of worn out or broken parts that are visible. Both A and B checks are light inspection which does not require an in-depth tear down of crucial aircraft systems. “C” checks are a heavy maintenance check which is done every year, and requires a much more in depth inspection than either the A or B checks and puts the aircraft out of service for the duration. A “D” check is done approximately every 5 years of service and is even more in depth than the “C” checks. The D check essentially requires the aircraft to be torn down, inspected and overhauled.

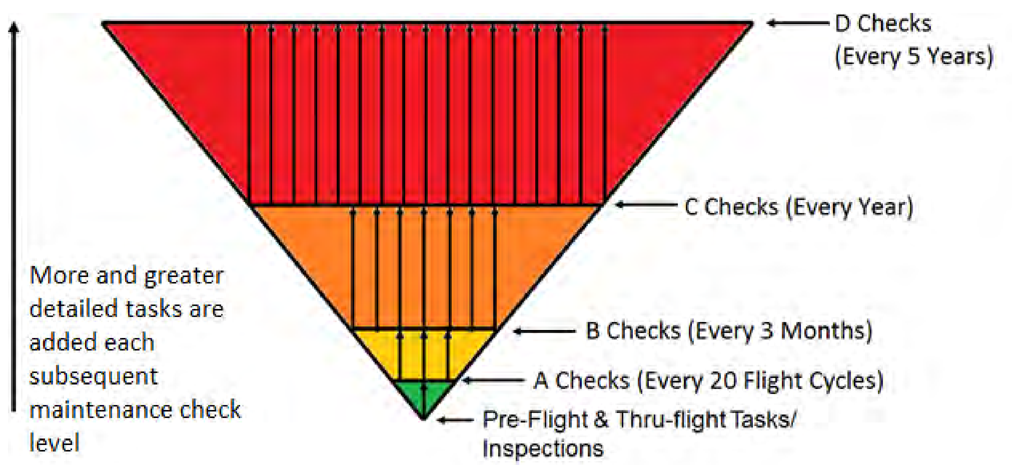

Figure 18.0-1: MSG-3 Visual Representation

19.0 Reliability

With a strict maintenance schedule, the PFS-1000 family will be examined on a frequent basis. The PFS-1000 aircraft, just like its competitors (SJ-30, Honda Jet, etc.) has the most up to date technology and also shares some similar parts. The engines used for the PFS-1000 family are two Williams FJ44-3A, which has proven itself as a reliable engine due to its usage on other aircraft. The SJ-30 also uses this engine due to its reliable performance.

20.0 Costs

20.1 PFS-1000 Program Costs

The research, development, test and evaluation cost for the 6-passenger and 8-passenger configuration was calculated utilizing the values of MTOW and the aircraft produced for the testing campaign which is 2 of each configuration. These aircraft designated for the test and evaluation phase of the program will be utilized to ensure flight safety and acquire FAA certifications.

The 6-passenger configuration R, D, T, & E costs will total $353.9 million dollars. This total is broken down into the 6 categories of airframe engineering ($159.16 million), the development support ($74.3 million), the flight test operations ($17.44 million), the manufacturing tooling will be the same as the 8-passenger, manufacturing labor ($32.81 million), and the quality control ($4.69 million). The 6-passenger research, development, test, and evaluation cost breakdown can be seen below in Figure 20.1-1.

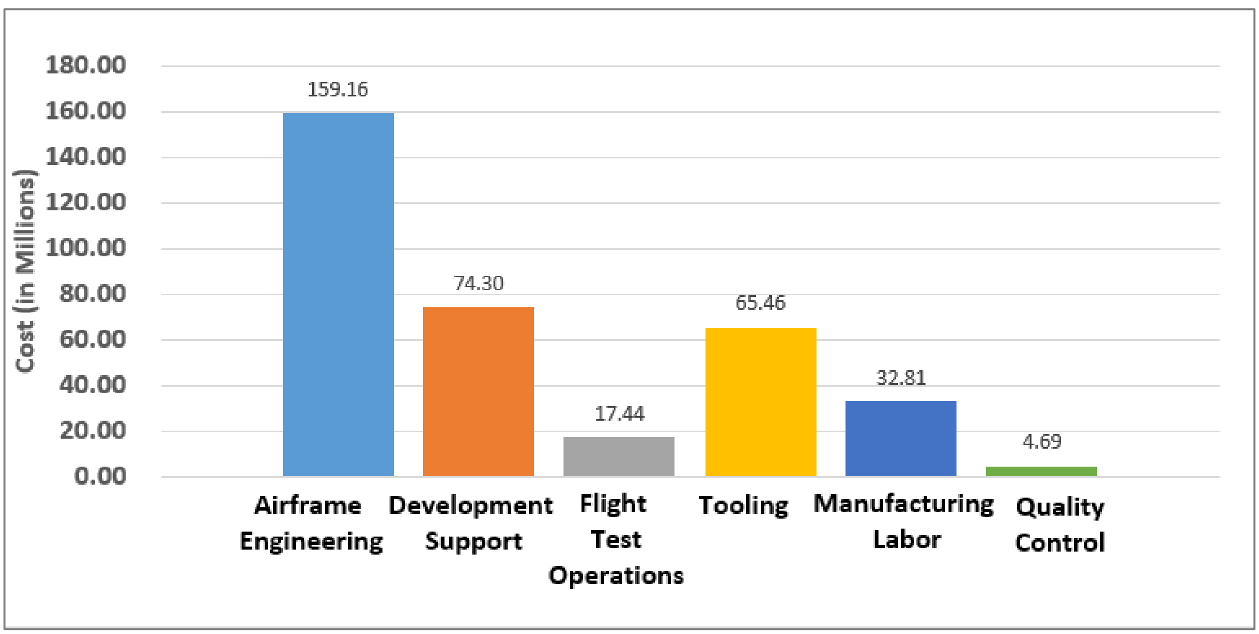

Figure 20.1-1: 6-Passenger R, D, T, & E Costs

The 8-passenger configuration R, D, T, & E costs will total $423.5 million dollars. This total is broken down into the 6 categories of airframe engineering ($174.12), the development support ($79.91 million), the flight test operations ($18.11 million), the manufacturing tooling ($65.46 million), Manufacturing labor ($32.81 million), and the quality control ($4.69 million). The 8-passenger research, development, test, and evaluation cost breakdown can be seen below in Figure 20.1-2. Much of the engineering development and manufacturing tooling costs can be shared between the 6 and 8-passenger configurations, since these configurations share greater than 70% structural commonality.

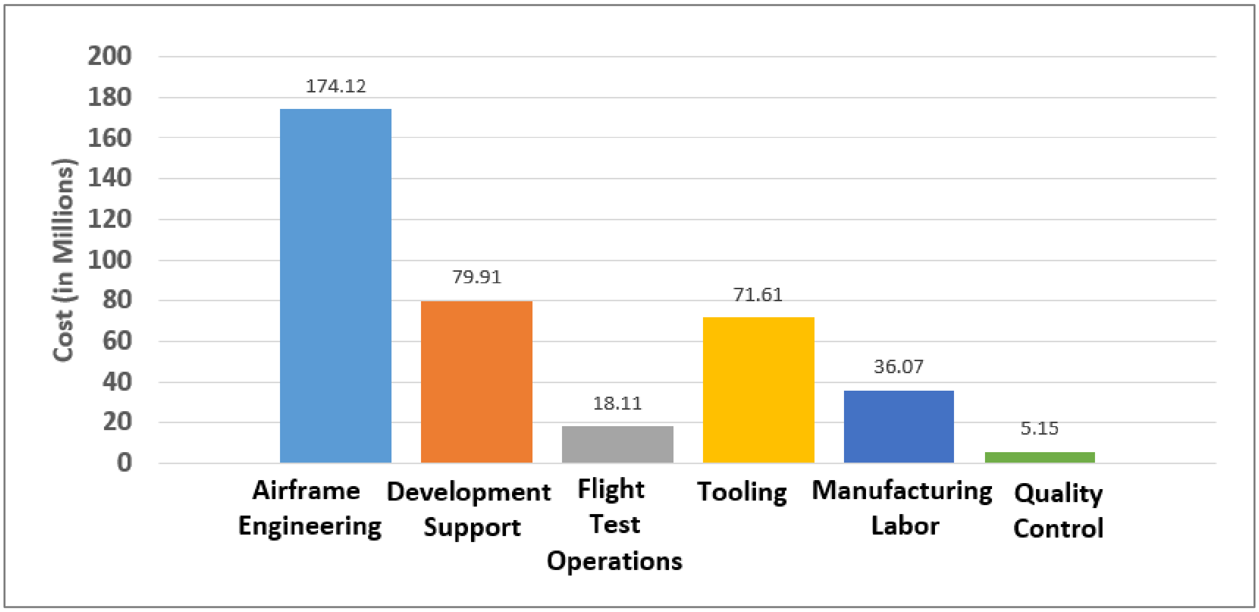

Figure 20.1-2: Program Costs (8 Passenger)

The unit costs of the PFS-1000 family will be $9.2 million for the 6-passenger and $9.6 million for the 8-passenger which will give 15% profit. These prices are slightly higher than similar aircraft available in the market today but those aircraft which are available will not meet the performance requirements of the RFP, and fall short of the PFS-1000 family capabilities. The PFS-1000 business jet family will give a greater range and max cruise speed than its competitors.

A comparison between several business jets available in the market today, their capabilities and unit cost can be seen in below in Table 20.1-1, their capabilities and unit cost can be seen in below in Table 20.1-1.

Table 20.1-1: Business Jet DOC Comparison

Aircraft	Passengers	Range (nmi)	Max Cruise (Kts)	Unit Cost (Millions)
PFS-1000 (6-PAX)	6	2,500	489	$9.2
PFS-1000 (8-PAX)	8	2,500	489	$9.6
Cessna Citation CJ4	7	2,165	454	$8.995
Embraer Phenom 300	7	2,268	444	$8.995
SyberJet SJ30	5	2,500	486	$8.31

With a 15% profit margin, it will take 375 aircraft for the entire light business jet program to break even. The cost-sale curves which highlight the breakeven point of the PFS-1000 aircraft program can be seen below for both the 6 and 8-passenger aircraft configurations.

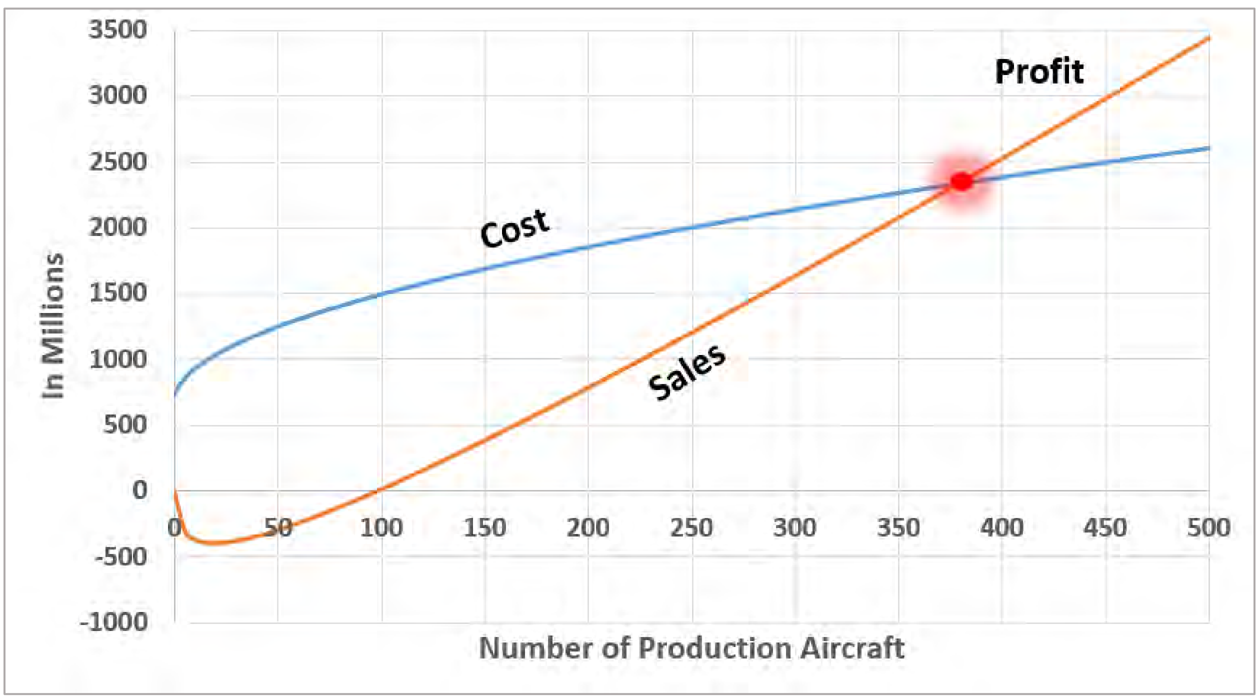

Figure 20.1-3: PFS-1000 Program Breakeven Point

20.2 Direct Operating Costs

The direct operating cost for each aircraft was calculated using the methods in chapter 5 of Reference [5]. The direct operating cost of the 6-passenger was calculated to be $715k a year or around $1,787 per operating hour while the direct operating cost of the 8-passenger was calculated to be $869k a year or around $2,170 per operating hour. The PFS-1000 aircraft family DOC's is made up of mostly flight crew's salary and fuel percentages being 37% and 32% respectively for the 6-passenger and costs being 30% and 40% respectively for the 8-passenger. The crew salary for the 8-passenger is about the same as the 6-passenger but the mission fuel required is more so the 8-passenger fuel percentage is greater than the 6-passenger. The percentage breakdown for both the 6-passenger and 8-passenger DOC's can be seen below in Figures 20.2-1 & 20.2-2.

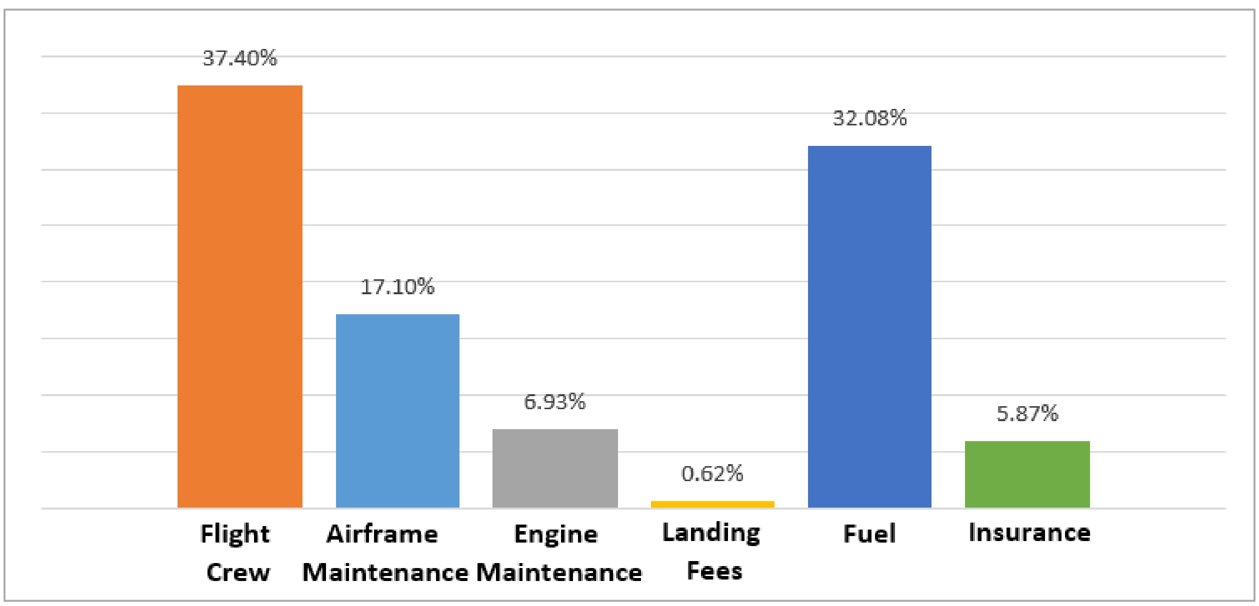

Figure 20.2-1: 6 Passenger Jet Direct Operating Costs

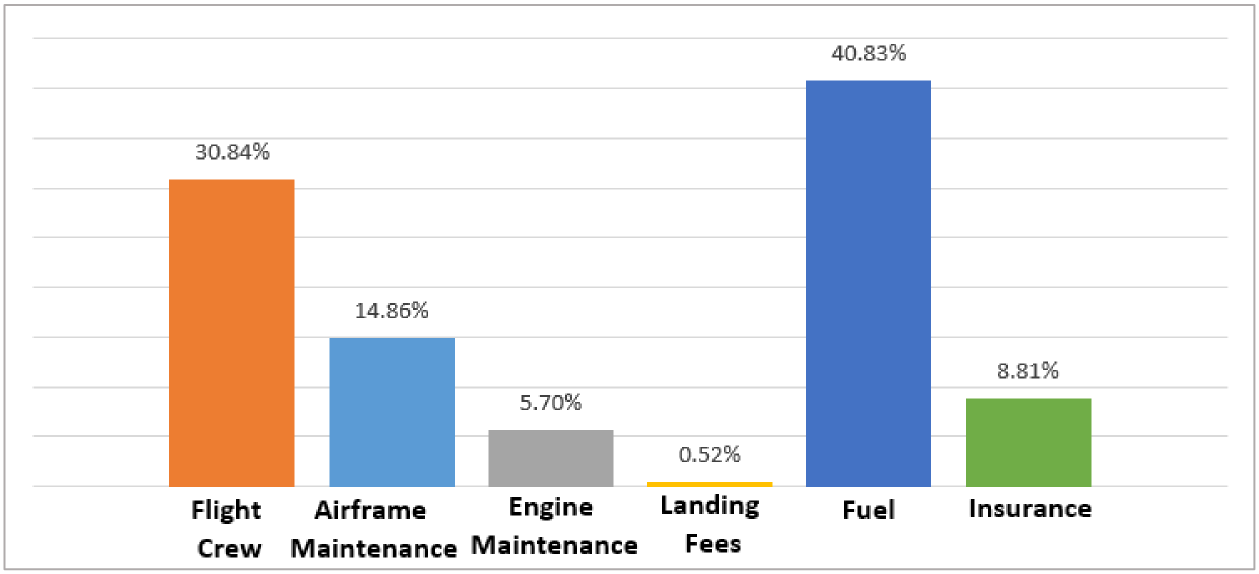

Figure 20.2-2: 8 Passenger Direct Operating Costs

The PFS-1000 business jet family direct operating costs are competitive with other business jets in the same class but the PFS-1000 family can achieve a greater range and a higher max cruise. The comparison between various light business jets' capabilities and hourly operating costs can be seen below in Table 20.2-1.

Table 20.2-1: Business Jet DOC Comparison

Aircraft	Passengers	Range (nmi)	Max Cruise (Kts)	Hourly Operating Cost
PFS-1000 (6-PAX)	6	2,500	489	$1,787.70
PFS-1000 (8-PAX)	8	2,500	489	$2,170.60
Cessna Citation CJ4	7	2,165	454	$1,970.20
Embraer Phenom 300	7	2,268	444	$1,757.50
SyberJet SJ30	5	2,500	486	$1,607.80

21.0 Conclusion

The PFS-1000 family of light business jets fulfills the requirements designated in the RFP created by AIAA. The design featured a 6 and 8 passenger model with the following capabilities: 2500 nmi range, max cruise speed of Mach 0.85 at 35,000 ft, balanced field length of 4,000 ft, landing field length of 3,600 ft, and a service ceiling of 45,000 ft. The commonality between the 6 and 8 passenger models is 94.3% resulting in a unit cost of $9.2 million and $9.6 million respectively. The PFS-1000 interior substitutes passenger windows with a virtual skyline to create a more memorable flight experience while saving structural weight to reduce flight costs. Premier Flight Systems presents the new standard in modern light business jets with comparable pricing to the current market with improved performance.

Appendix A: Compliance Matrix

Table A-1: Compliance Matrix

Requirement	Compliant (Yes/ No)	Proposal Section
Design Requirements		
2,500 nmi + 100 nmi alternative	Yes	9.1
Max Cruise of Mach 0.85 at 35,000 ft Altitude	Yes	9.3
Max 3,500 fpm Climb Rate	Yes	9.4
45,000 ft Service Ceiling	Yes	9.3
Takeoff Distance < 4,000 feet	Yes	9.2
Landing Distance < 3,600 feet	Yes	9.2
At least 70% Commonality	Yes	16
FAR 23/ 25 Compliant	Yes	ALL
6-Passenger Aircraft can hold 500lb/ 30 cubic feet of luggage	Yes	14.1
8-Passenger Aircraft can hold 1000lb/ 60 cubic feet of luggage	Yes	14.1

Appendix B: Reference List

[1] Abbott, Ira H., and Albert Edward Von. Doenhoff. *Theory of Wing Sections: Including a Summary of Airfoil Data*. New York: Dover, 2010. Print.

[2] Bruhn, E. F. *Analysis and Design of Flight Vehicle Structures*. Carmel, IN: Jacobs, 1973. Print.

[3] "Flight Requirements." *ECFR — Code of Federal Regulations*. FAA, n.d. Web. 09 May 2017.

[4] Liebeck, Robert H. *Advanced Subsonic Airplane Design & Economic Studies*. Cleveland, OH: National Aeronautics and Space Administration, Lewis Research Center, 1995. Print.

[5] Nicolai, Leland M., and Grant Carichner. *Fundamentals of Aircraft and Airship Design*. Reston, VA: AIAA, 2010. Print.

[6] Ogata, Katsuhiko. *Modern Control Engineering*. Boston: Prentice Hall, 2010. Print.

[7] Raymer, Daniel P. *Aircraft Design: A Conceptual Approach*. Reston, VA: American Institute of Aeronautics and Astronautics, 2012. Print.

[8] Sadraey, Mohammad H. *Aircraft Design: A Systems Engineering Approach*. Chichester: Wiley, 2013. Print.

[9] Schaufele, Roger D. *The Elements of Aircraft Preliminary Design*. Santa Ana, CA: Aries Publications, 2007. Print.

[10] Shevell, Richard S. Fundamentals of Flight. Upper Saddle River, NJ: Prentice-Hall, 1989. Print.